5.3.8.4 *Groet History Match*

The main issues in the GRT history match are:

- Overall volumetrics
- Contact behaviour

In the base case match we needed to multiply the overall volumes by 0.95 to get a pressure match overall (and to match the material balance analysis). The model has a quite good pressure match.

There is not as much quantitative evidence about GWC rise available for this study for GRT as in BGM, nevertheless it is clear that the contact has gone up by as much as 50m (several wells have watered out). A GWC measurement that came in during the progress of the study suggests as much as 80m at GRT1. This latter value we have not been able to match, but the 50m was quite achievable. To do this we needed to lower permeabilities in GRT from the static model (contrary to BGM). Significantly lower permeabilities in GRT are compatible with the observed possible transition zone. The transition zone was not modelled since it was judged that the extra effort was not warranted given that GRT is not the focus of the study. It should be noted that there was no GRT por/perm core plug data available for this study, and the por/perm transform used for the model (so also for GRT) was based on BGM data alone. Nevertheless, the results match well enough to conclude that the GRT contact behaviour does not appear incompatible with the assumption that the field has little or no aquifer. The contact rise mechanism is similar to BGM, related to the non-uniform well placement.

Examining the pressure match zoom-in (Figure 5-57), we again see that the structure of the model is simpler than in reality (although it is a bit obscured by noise in the points). And, like in BER, this situation can be fixed by introducing a baffling fault (Figure 5-58). Thus we have some indications for sub-seismic faults in all three fields studied.

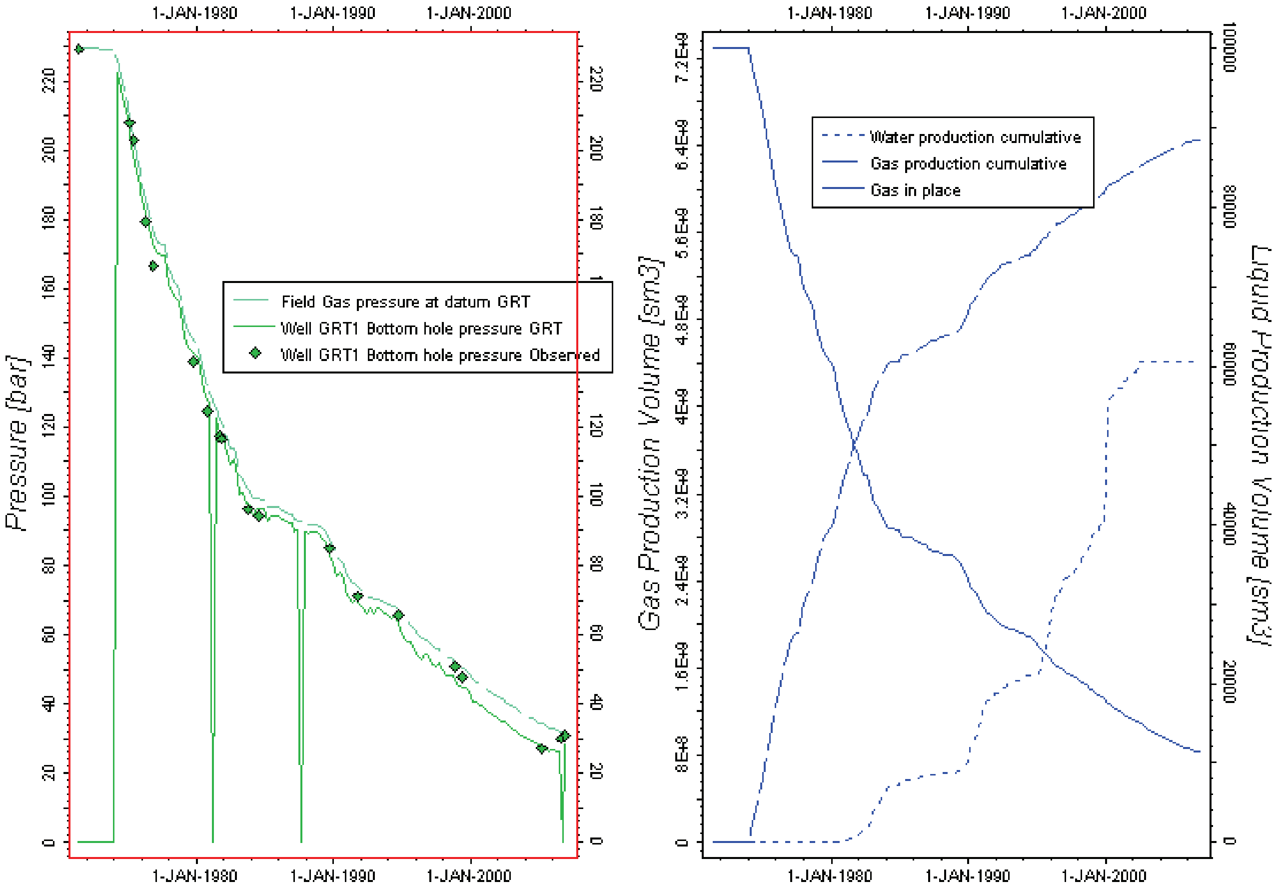

Figure 5-56 Base case GRT pressure match (left graph) and cumulatives and water production (right). The left plot shows both GRT1 BHP's and field average pressures (marked as 'pressure at datum' in the plot) to indicate the difference between the two (in GRT the permeabilities are lower), to be able to compare the pressure mismatch visually against model drawdowns.

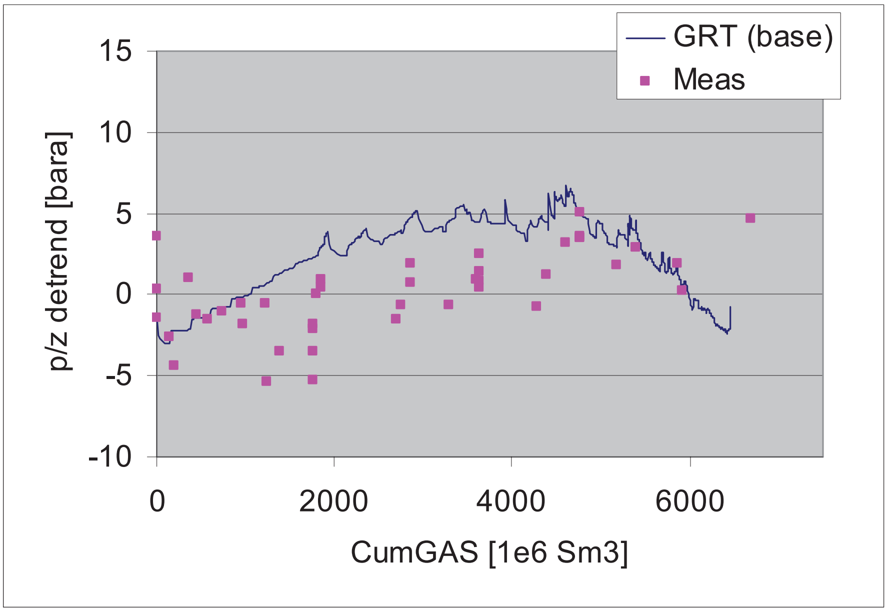

Figure 5-57 GRT pressure match, zoom-in by plotting detrended (cf. Figure 5-14) [This graph was taken from the 25 layer BGM+GRT model.]

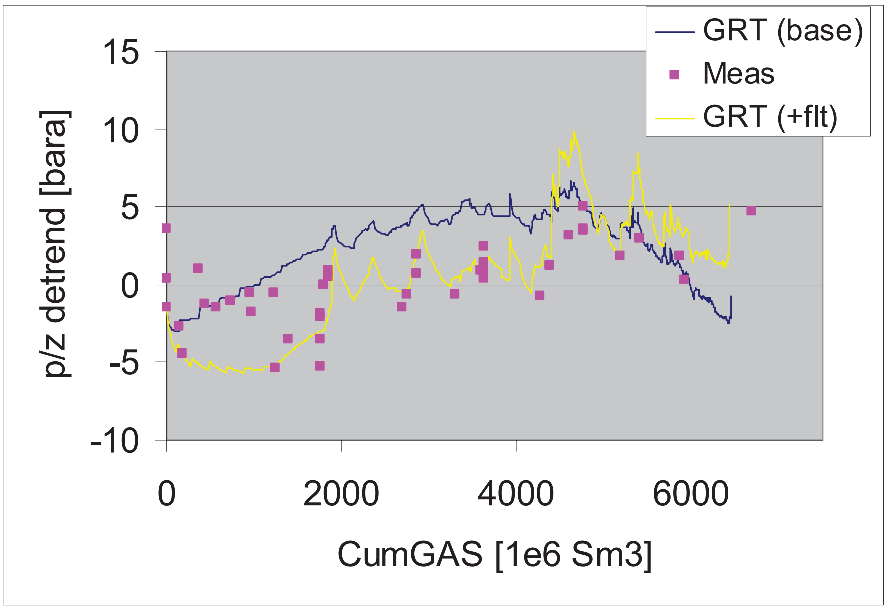

Figure 5-58 Faulted GRT pressure match, zoom-in by plotting detrended (cf. Figure 5-14). See Figure 5-59, and compare to the effect of an aquifer in Figure 5-67.

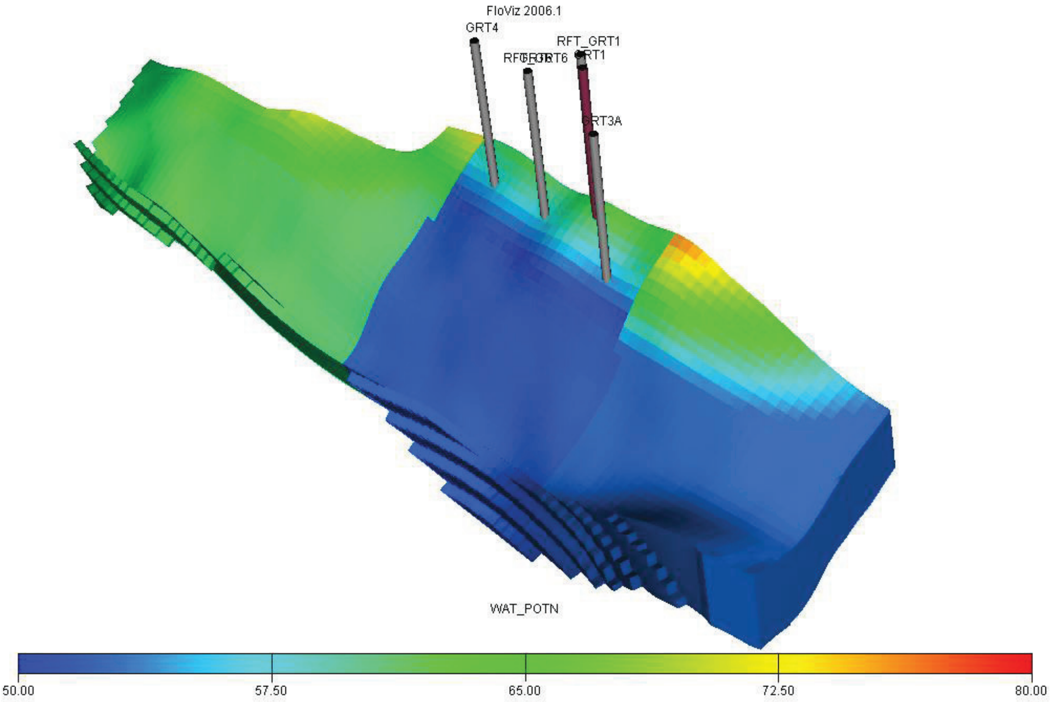

Figure 5-59 **Faulted GRT 2006 water potentials, indicating position of faults, as well as magnitude of pressure jump across them. Two faults are introduced; this is not meant to be realistic, just serves to create roughly right-sized compartments. [It should be noted that, like in BGM, the faults influence the contact dynamics. If the configuration is like this, i.e. an additional fault between the GRT wells and the spill point, this facilitates gas moving all the way down to there. However, no match could be achieved with a fault in GRT, with no fault at the spillpoint.]**

5.3.8.5 Combined BGM+GRT match

As discussed above, the BER field shows least potential evidence for a connection to its surroundings. Therefore, to study possible communication between BGM and the outside, we only ran sensitivities with the GRT field (cf. the recommendation in [18]). The area of interest (AOI) for these combined runs is plotted in Figure 5-34). Aquifer sensitivities (described later) have been run with some of the water blocks surrounding this area.

The key factor in such combined runs is the connection between the two fields. To be able to vary this an adhoc fault is introduced at the spillpoint. As argued in the geology section (chapter 4), the presence of additional faults in the area between GRT and BGM is likely. Moreover, there is an unambiguous indication for a sub-seismic baffling fault in BGM itself, and some indication (as just discussed) for such faults in BER as well as GRT.

What limits the transmissibility across such a fault? As we concluded from the material balance discussions, this will be the mid-history pressure match in GRT and the end-history match in BGM. This is illustrated by Figure 5-63. After matching, the conclusion is that we can get an acceptable match if we introduce a fault at the spill point that has a transmissibility multiplier of the same order as the one used between BGM and BGM7, i.e. 0.0002.

The consequence of this small value (note that, contrary to BGM←→BGM7 there is only water at the fault's location) is that the amount of fluids travelling across is reasonably small. The evolution of the gas contacts, even though they go down in some places, is not such that the two gas accumulations communicate in the historic period (Figure 5-61). [It should be noted that in some older versions of the model the contact descent in the north of BGM and the south of GRT was so large that this communication did *just* take place even with a properly baffling fault. No large gas volumes were exchanged in this case either, however.]

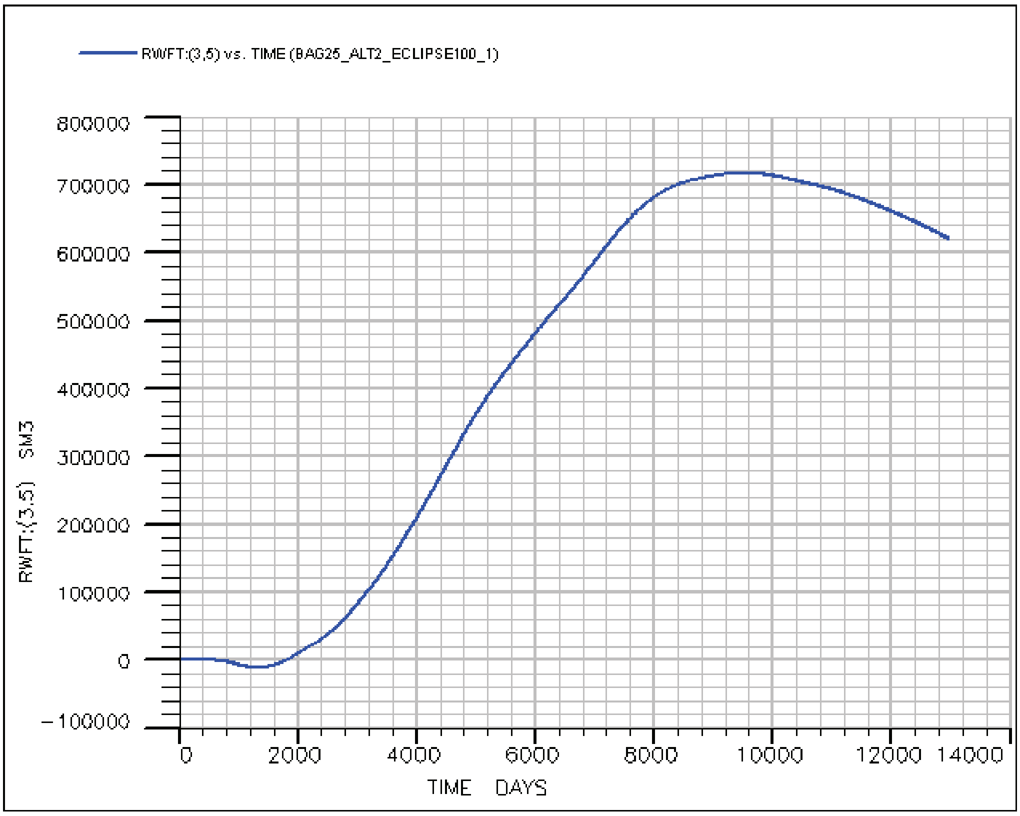

Figure 5-60 BGM→GRT water flow cumulative ('RWFT') across the spillpoint for matched BGM+GRT run (25 layers). Actual flow is the derivative of this curve. The sign convention is positive BGM→GRT. The amount of water moved is less that 1e6 sm3.

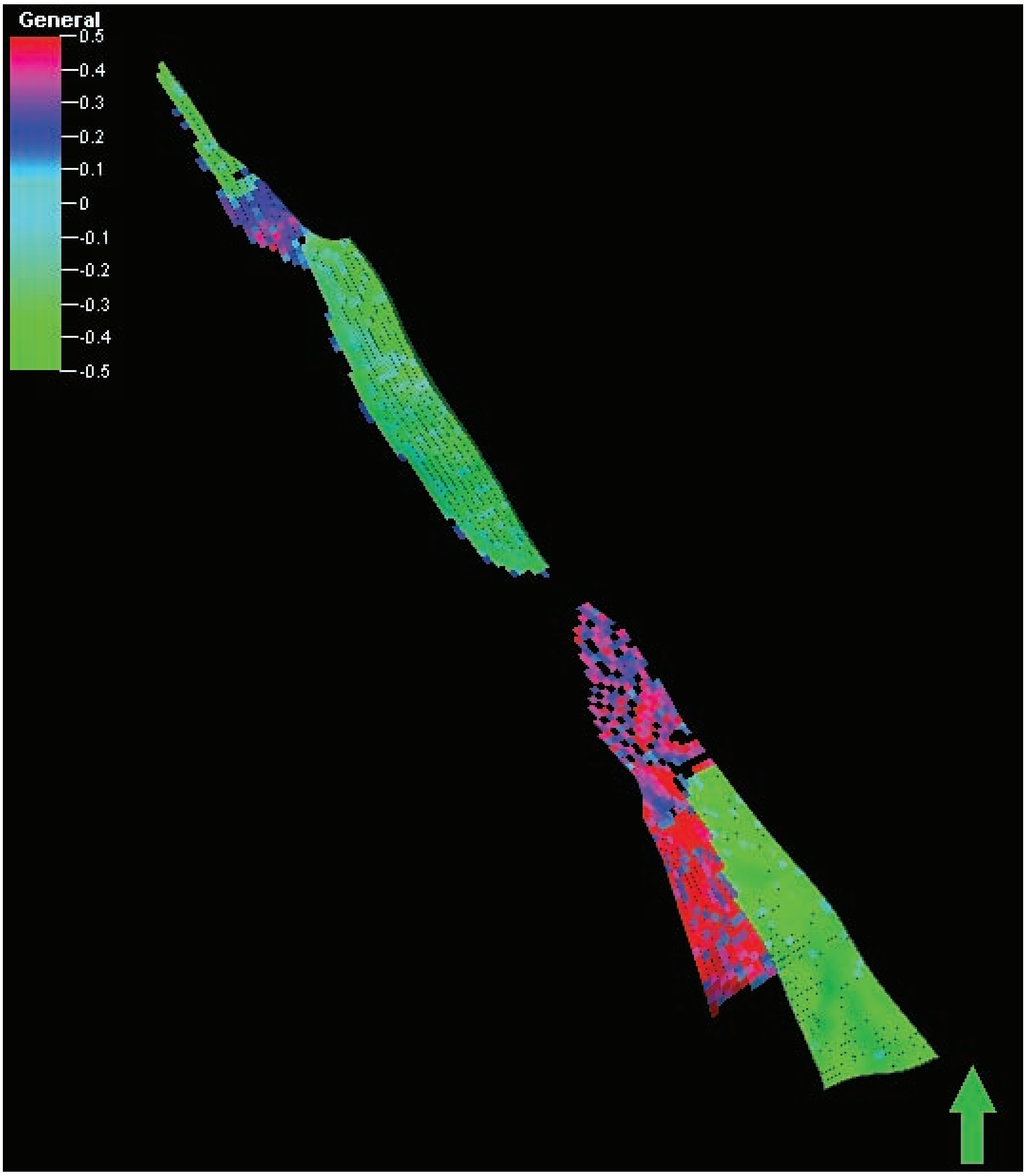

Figure 5-61 dSgas = Sgas[2006]-Sgas[1971] plotted for BGM and GRT (combined run).

5.3.9 Scenarios

5.3.9.1 Property scenarios

The static (property) scenarios discussed in chapter 4 have all been run. Since the main driver for the fields is volumetrics, the differences are small: different pore volume multipliers (MULTPV) were used to compensate for the different volumetrics of the scenarios (chapter 4). The matched runs will be carried forward into UGS forecasting to investigate if they have any impact on future behaviour.

As noted in chapter 4, the runs have somewhat different behaviour as regards larger-scale heterogeneities. The effect of this is most notable in the 'discontinuous' runs; cf. the discussion on the contact dynamics above.

Main parameters and key results can be found in Table 7-3 and beyond. The property variations are marked ‘DISMID’, ‘MIDLOW’, ‘MIDMID’ and ‘MIDHIGH’.

5.3.9.2 Structural scenarios

The static (structural) scenarios discussed in chapter 4 have all been run. Since the main driver for the fields is volumetrics, the differences are small: different pore volume multipliers (MULTPV) were used to compensate for the different volumetrics of the scenarios (chapter 4). The matched runs will be carried forward into UGS forecasting to see if they have any impact on future behaviour.

Main parameters and key results can be found in Table 7-3 and beyond. The structural variations are marked ‘SHIGH’ and ‘SLOW’. A probably significant result is that, as can be seen, the ‘SHIGH’ scenario has significantly higher base GIIP (i.e. needs much lower MULTPV). This could indicate that, for BGM, the real structure is higher than the base case structure. This observation, however, does of course not really offer a clue as to *where* the difference should be located.

A specific structural sensitivity has been run in which only the BGM7 block was partially uplifted. This is marked ‘SUP7’. The purpose was to investigate if the BGM7 volume could be brought in line with the material balance results. However, this is only possible to a very limited extent.

5.3.9.3 Connection sensitivities

5.3.9.3.1 Connectivity BGM ←→GRT

To be able to have a ‘worst case’ connection scenario, a case was prepared with higher GRT←→BGM transmissibility. As can be expected, the mismatch on GRT in particular is clear (Figure 5-63), indicating that this is certainly an overestimate of connectivity. Still, we will take this case forward into FC as a ‘worst case’ run.

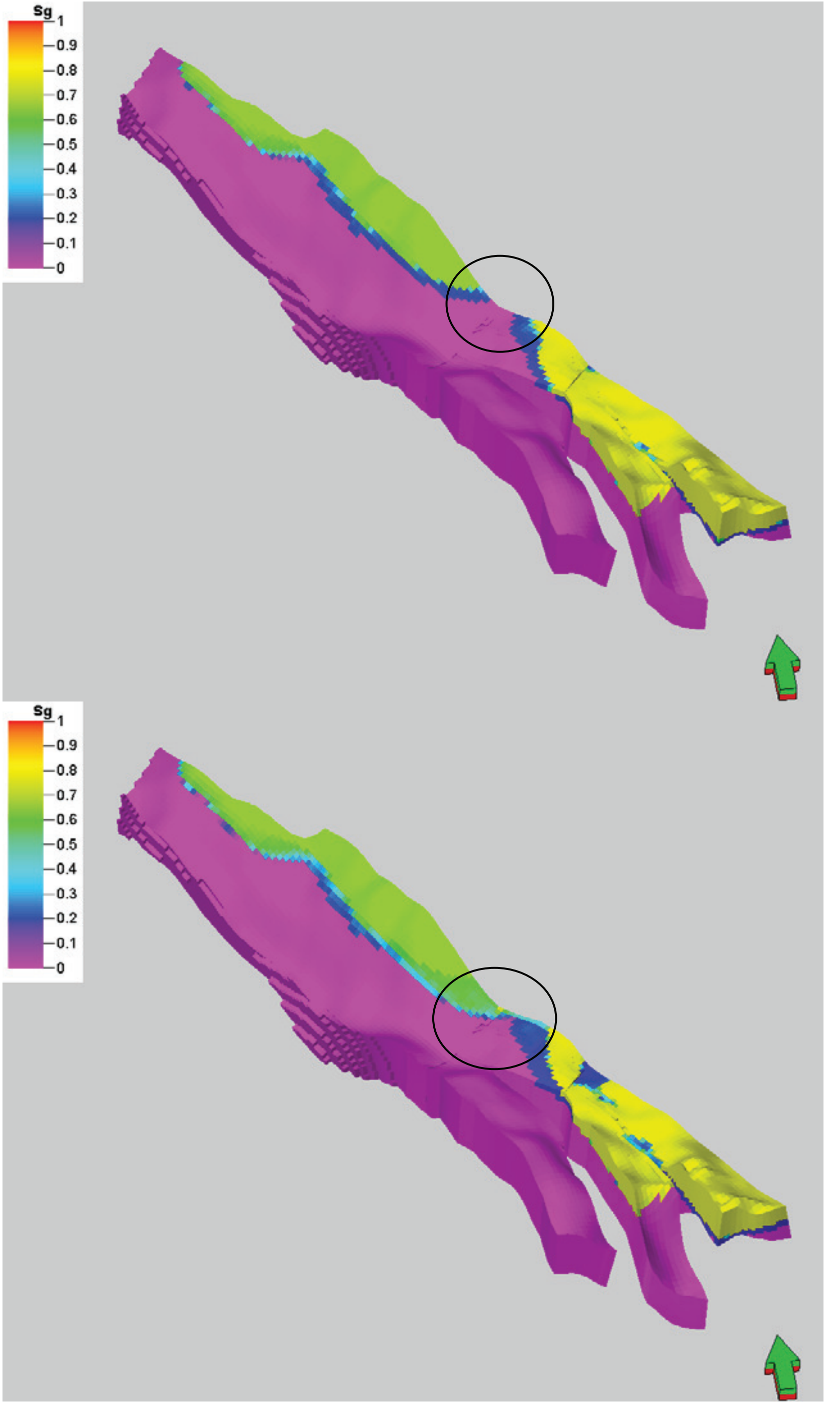

Figure 5-62 Sg distribution at Dec-2005 if the adhoc fault at the spillpoint is more open than in the base case (right; the fault transmissibility multiplier MULTFLT is 100 times higher, 0.02) vs. the base case (left). Extension of fault2 is westward in these runs (i.e. GRT is connected to BGM-main). In the base case run the GRT contact in the south of the field rises, whereas in the ’open’ run the contact goes down due to the BGM pressure sink; the two gas accumulations just make contact.

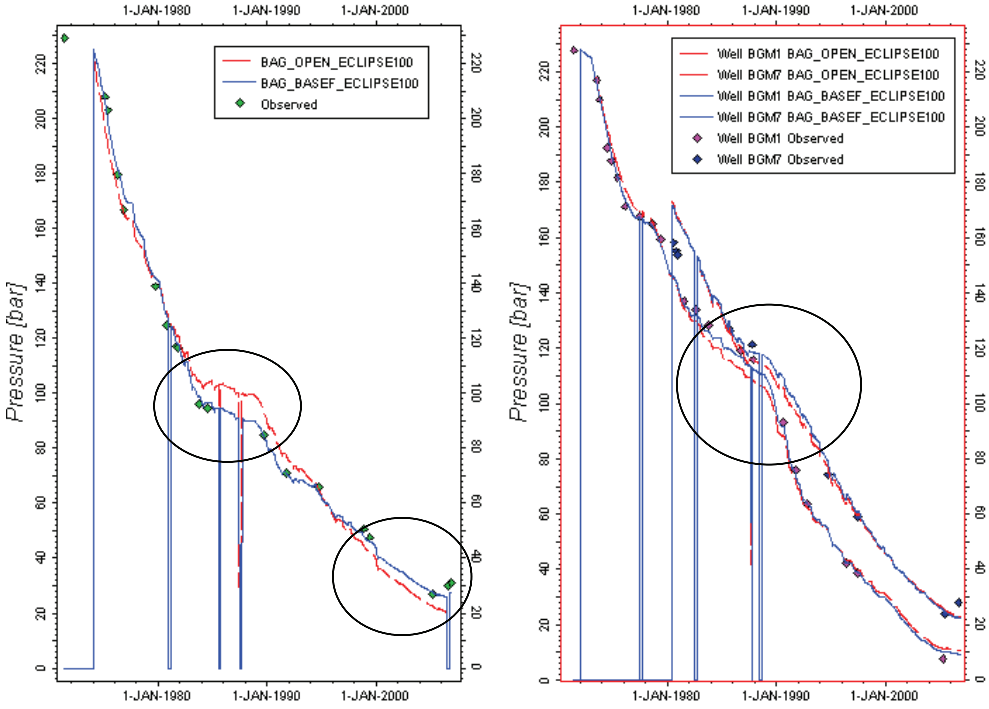

Figure 5-63 **Comparison of base BGM+GRT simulation (blue) with sensitivity with more open spillpoint-fault (red). Cf. the field pressure differences in Figure 5-17. The left plot shows GRT pressures, the right BGM-main and BGM7 pressures. The circles indicate the points of mismatch: overpressure in GRT mid-history with associated under-pressure in BGM mid-history, and under-pressure in GRT end-history. Since GRT is smaller than BGM, the effect on GRT is larger than the effect on BGM.**

5.3.9.4 Aquifer sensitivities

Several sensitivities have been run with an aquifer attached to GRT and BGM. Considering where to connect the aquifer to the flow simulation model, the bottom seems implausible, because the Carboniferous is extremely tight. Also we know that the saddle area of the field is likely poorly permeable. Many faults along the reservoir sides have throws larger than the Rotliegend thickness (a.o the E bounding fault, and the fault to the BGM4 block). For GRT that means that the most likely aquifer attachment point is to the north. For BGM, the most likely attachment is the block to the west of the BGM7 block. Based on this, likely attachments were selected (Figure 5-64). A BGM sensitivity with a bottom aquifer (Figure 5-65) has been run nevertheless, and will be reported on later.

The aquifer type chosen is a Fetkovich aquifer, the recommended model for a small aquifer.

5.3.9.4.1 Aquifer to GRT

We attached a 'Fetkovich' aquifer model to the north (Figure 5-64) with the following properties to GRT:

- Vaq = 2e9 sm3
- Caq = 6e-5 /bar
- PI = 10 sm3/bar/day

The aquifer volume is related to the volume in the field itself (6e8 m^3, so the aquifer is several times larger); the compressibility is related to the rock & water compressibility, and the value of the aquifer performance index (PI) is tuned by the pressure match. From the match plots it can be seen that this really is somewhat too large to be realistic (Figure 5-66, Figure 5-67 indicate a clear mismatch in the mid-history, as well as at the end), even though the influx rates are quite low (Figure 5-76). Any actual aquifer will be less strong than this one. Nevertheless, we keep this scenario alive as a "worst case" possibility, aquifer-wise.

5.3.9.4.2 Aquifer to BGM-main

We attached a 'Fetkovich' aquifer model to BGM via the SW (Figure 5-64) with the following properties:

- Vaq = 2e9 sm3
- Caq = 6e-5 /bar
- PI = 3 sm3/bar/day

The aquifer parameters were set in the same way as for GRT (for the BGM blocks the water-in-place is 5e8 m^3), but in case of BGM we were, given the focus of the study, a bit more critical in the amount of mismatch tolerated when tuning the PI. As a result influx rates are lower than in GRT (Figure 5-76).

Because the 'fault2' scenario chosen here is 'West' ("alt1"), this aquifer will support the BGM-main block.

The pressure match (Figure 5-71) shows the aquifer is beyond the edge of what the data allows (although less so than the GRT case discussed above).

5.3.9.4.3 Aquifer to BGM7

We attached a 'Fetkovich' aquifer model to BGM via the SW (Figure 5-64) with the same properties as above, but this time with a 'fault2' scenario chosen as 'East' ("alt2", i.e. east), this aquifer will support the BGM7 block.

The pressure match (Figure 5-72) shows the aquifer is beyond the edge of what the data allows (although less so than the GRT case discussed above). Any real aquifer will be weaker than this. Nevertheless, we will keep the case alive as a 'worst case' scenario (aquifer wise) to use in forecast sensitivities.

5.3.9.4.4 Aquifer to bottom

A sensitivity was run in which the aquifer was attached to the bottom, rather than to the side. The model was a base model (i.e. with the ‘fault2’ extension westwards). As we can see the results differ somewhat from the “W-edge” aquifer run, in that the strength we can handle before problems occur is larger, and in that the effect on the pressure curve is a bit different (Figure 5-72). It should be noted, however, that the addition of the water blocks to the W of BGM7 increases the initial water content of the model from 5e8 m^3 to 1.6 m^3. (I.e. the addition of the blocks amounts in itself to increasing the aquifer size).

It should be noted that if we keep the blocks W of BGM in the model, and attach the aquifer to the whole bottom, the majority of the water/aquifer is still to the W, so that such a run will be almost indistinguishable from a W-edge-aquifer run as described above.

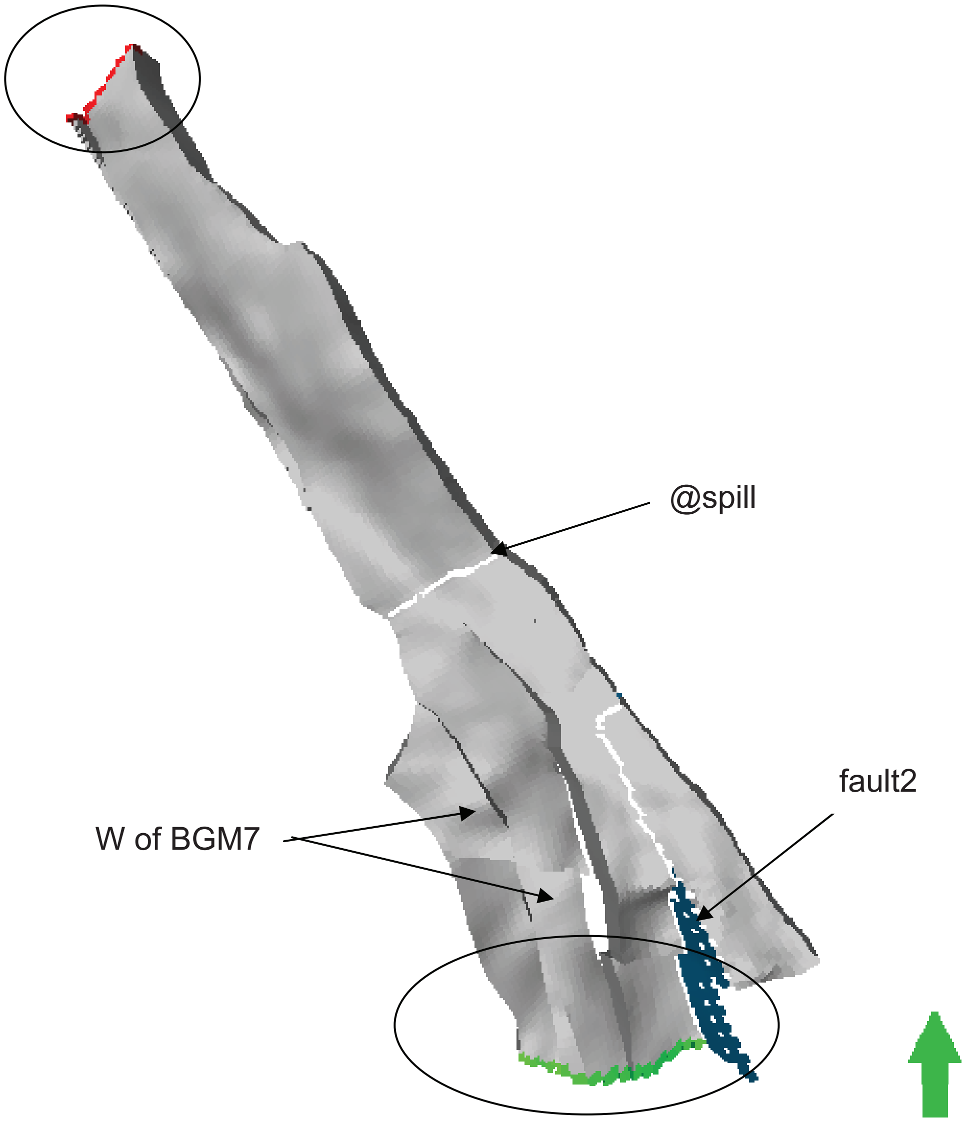

Figure 5-64 Attachment for GRT aquifer (red, top) and BGM aquifer (green, bottom). The spillpoint "fault" and "fault2" are indicated. For stand-alone BGM and GRT runs with an aquifer the part north and south of the spillpoint, respectively, are used. Hence for BGM+edge-aqf runs, we include the additional blocks W of BGM7 (but cf. Figure 5-65)

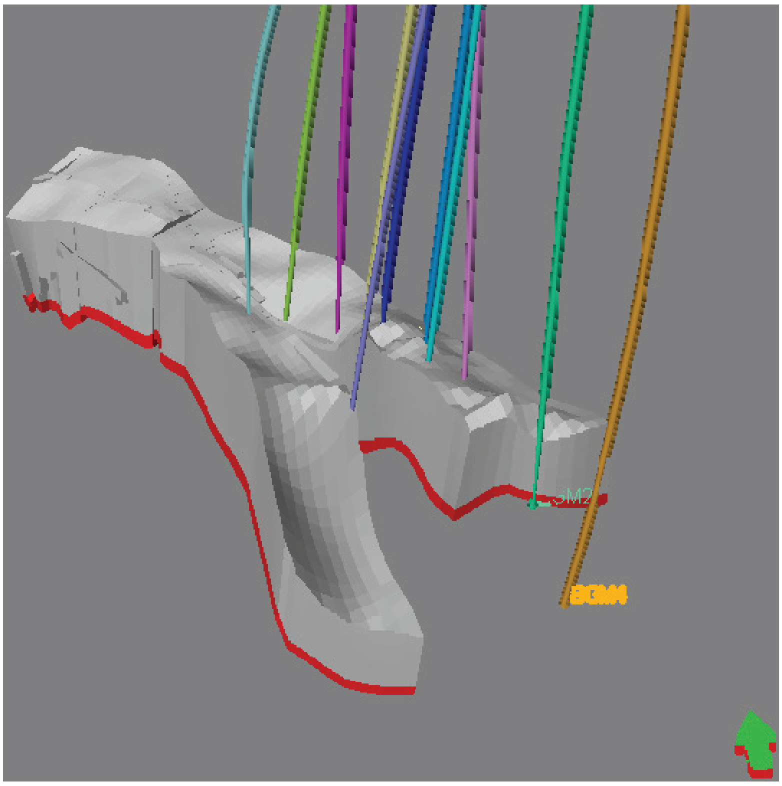

Figure 5-65 Indication of aquifer attachment in bottom aquifer sensitivity. Note that, in contrast to the side aquifer (Figure 5-64), the BGM run does not include the blocks W of BGM7.

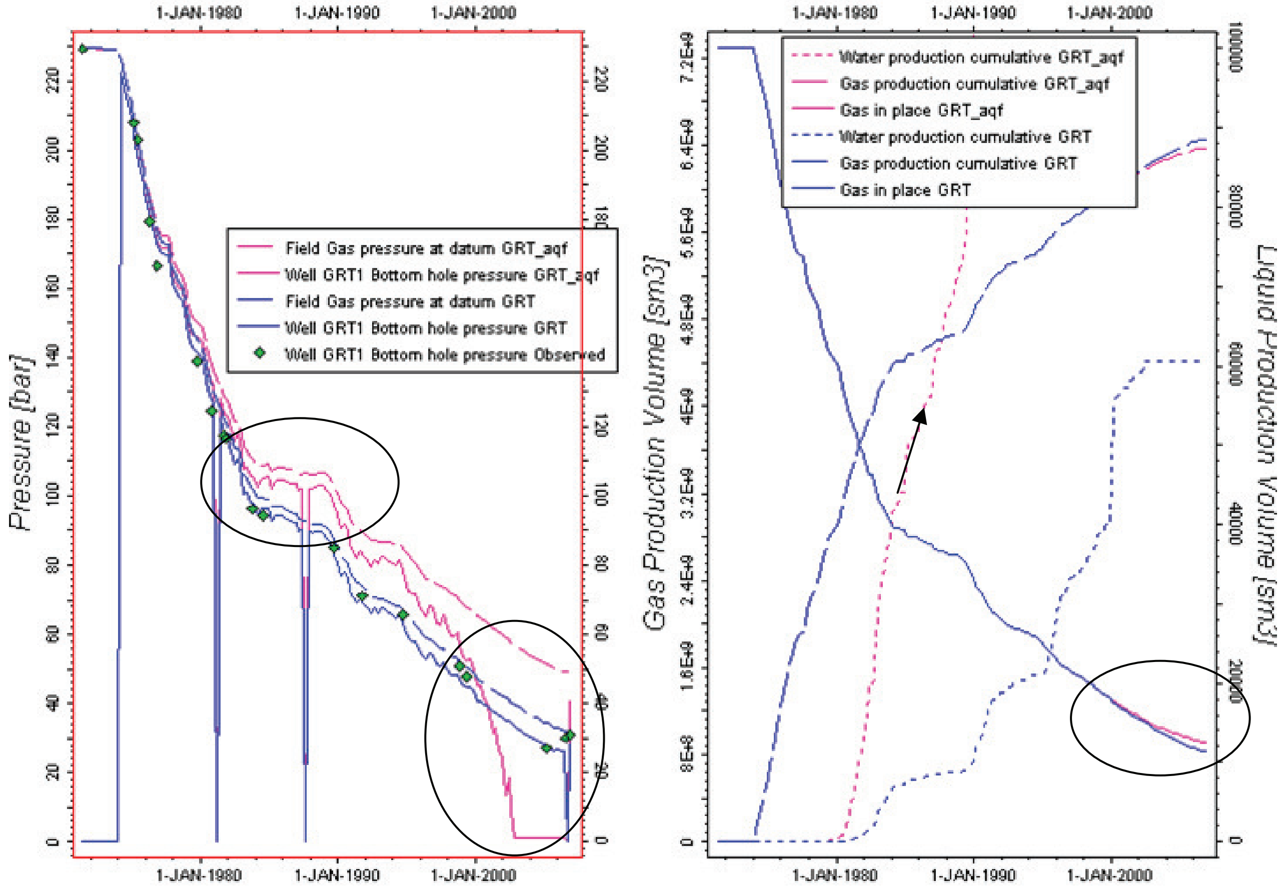

Figure 5-66 Comparison of base case GRT match (blue) with Fetkovich aquifer match (purple) with an aquifer PI of 10 Sm3/bar/day. The left plot shows the pressure match. Mid-history pressures are clearly too high; at the end of the field-life GRT1's bottom-hole pressure collapses due to water encroachment. The right plot shows water production cumulative (dotted lines); the aquifer run shows much more water production (purple dotted; marked by arrow) than the base case (blue dotted). The right plot also shows gas underproduction due to GRT1 failing at the end of the historic period. As discussed in the text, we keep this aquifer for forecasting purposes as a 'worst case', despite its mismatch.

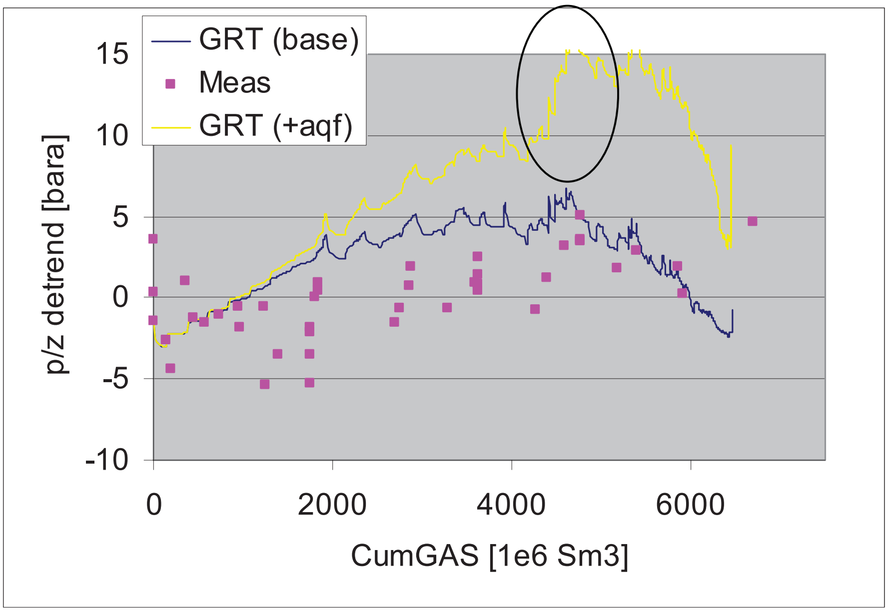

Figure 5-67 Effect of aquifer on GRT match [detrended p/z; both curves from 25 layer combined BGM+GRT run]. The marked large pressure increase around 4.8e9 Sm3 corresponds to the low rate period just before 1990; since the horizontal axis is cumulative production rather than time. (Compare with the effect of internal compartmentalization in Figure 5-58.)

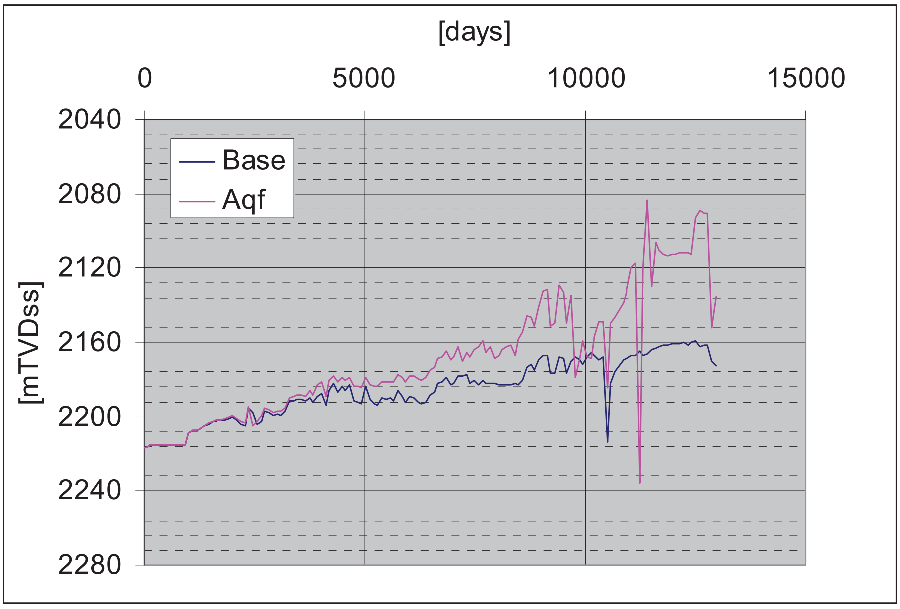

Figure 5-68 Impact of GRT aquifer on GRT1 contact rise: unsurprisingly adding an aquifer makes the contact go up.

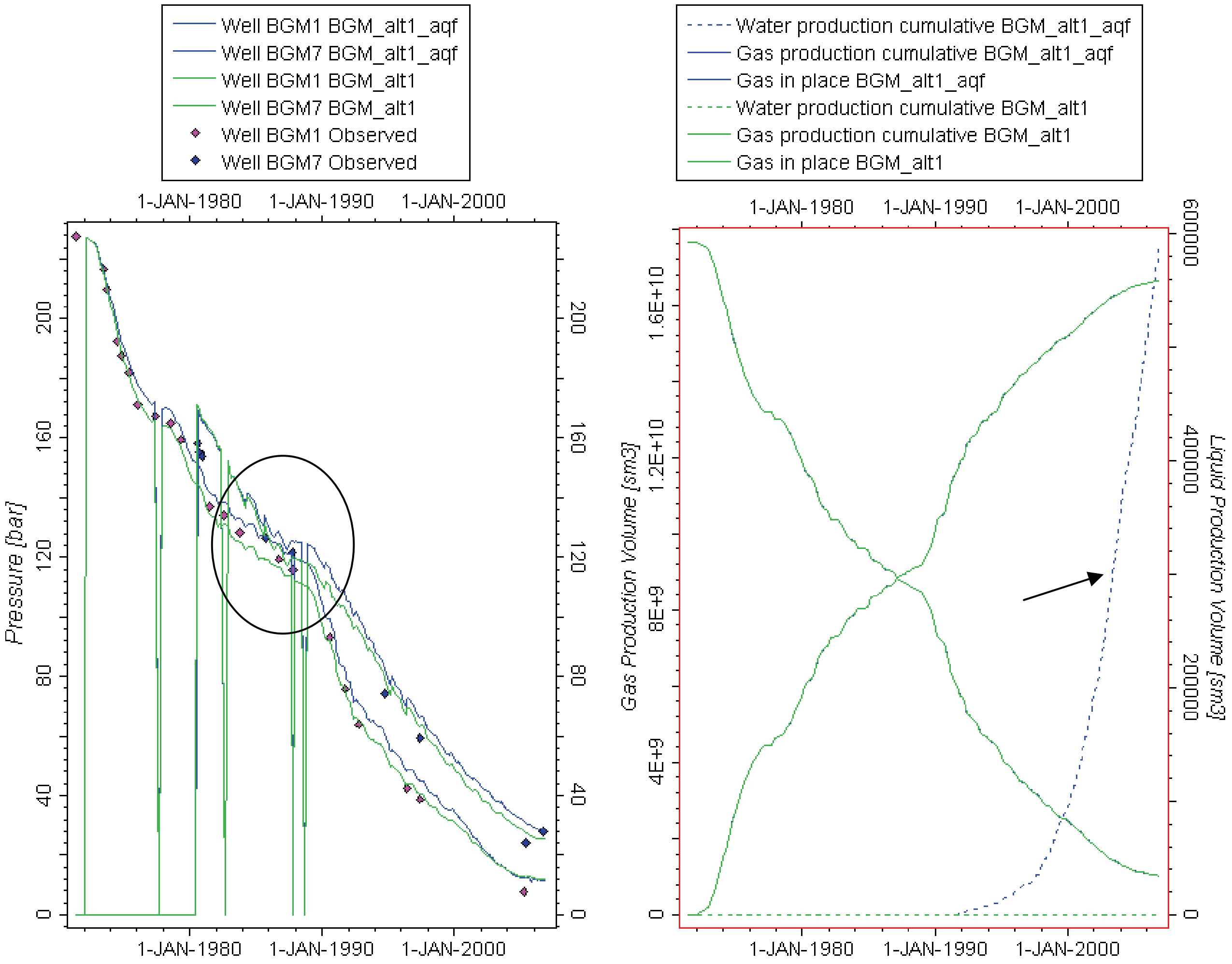

Figure 5-69 Aquifer attached to BGM, which in combination with a 'W' scenario for 'fault2', leads to the aquifer supporting BGM-main. The aquifer run in blue is compared to a green base run ("alt1": with W fault2 extension). The left plot shows the pressure match (like in GRT the main difference is at the low rate period in the late 80's). The right plot shows rates & cumulatives. The indicated blue curve is the water production cumulative resulting from enhanced contact rise in the aquifer run.

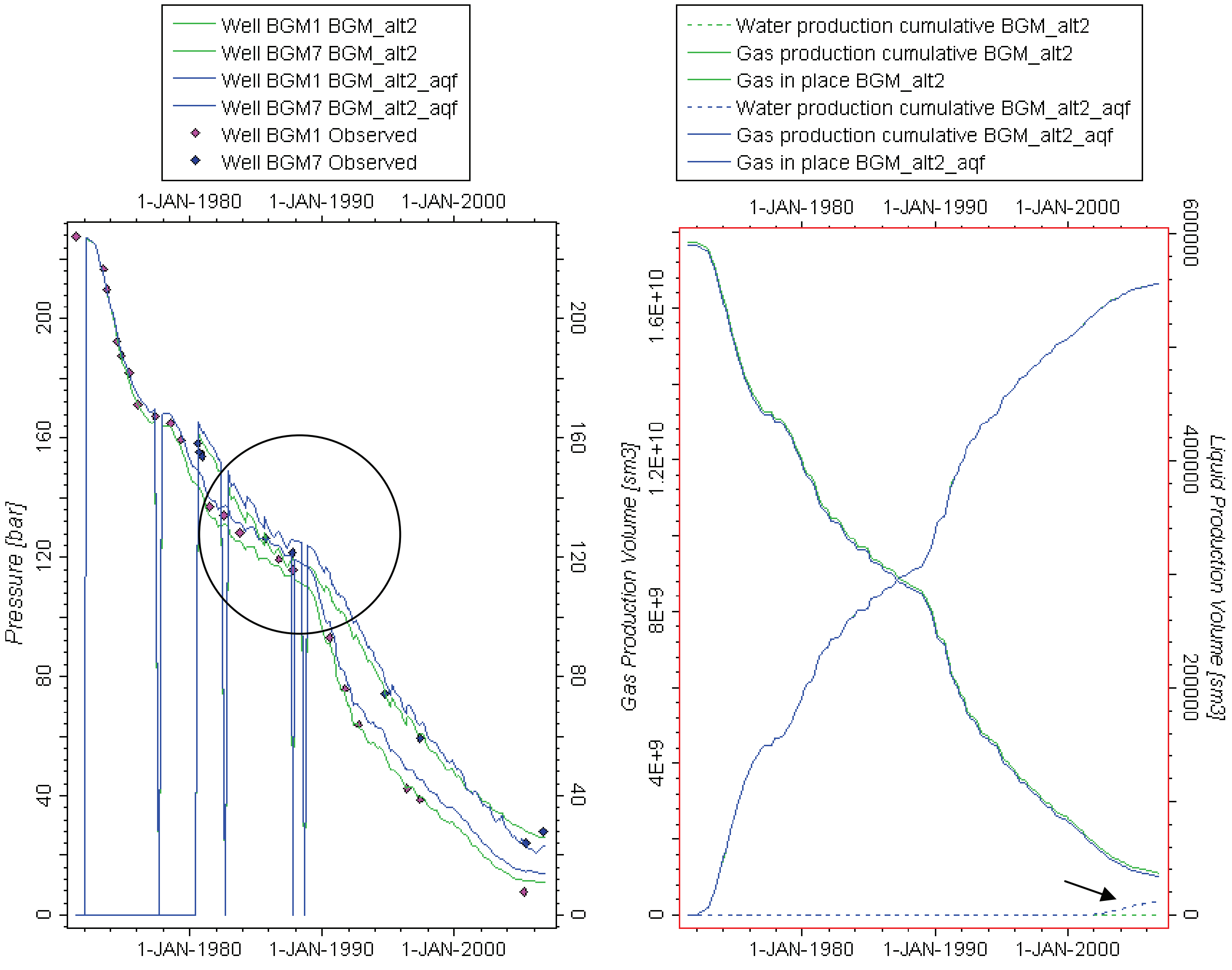

Figure 5-70 Match plot for BGM run with aquifer (attached to the block W of BGM7). The aquifer run in blue is compared to a green base run (“alt2”: with E fault2 extension). Data plotted is the same as in Figure 5-69, as are the effects seen. Water production is significantly less, though.

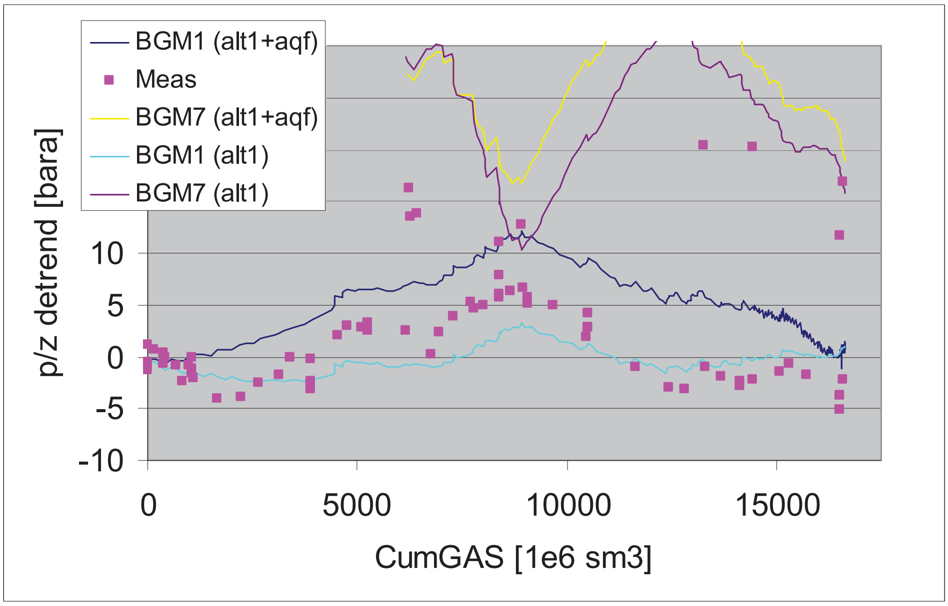

Figure 5-71 Zoomed in pressure match for W trending fault runs ("alt1") with and without aquifer. With this fault scenario, the aquifer directly supports BGM-main. Due to the compartment interaction, as well as the smaller aquifer size, the effect of the aquifer is less pronounced than in GRT.

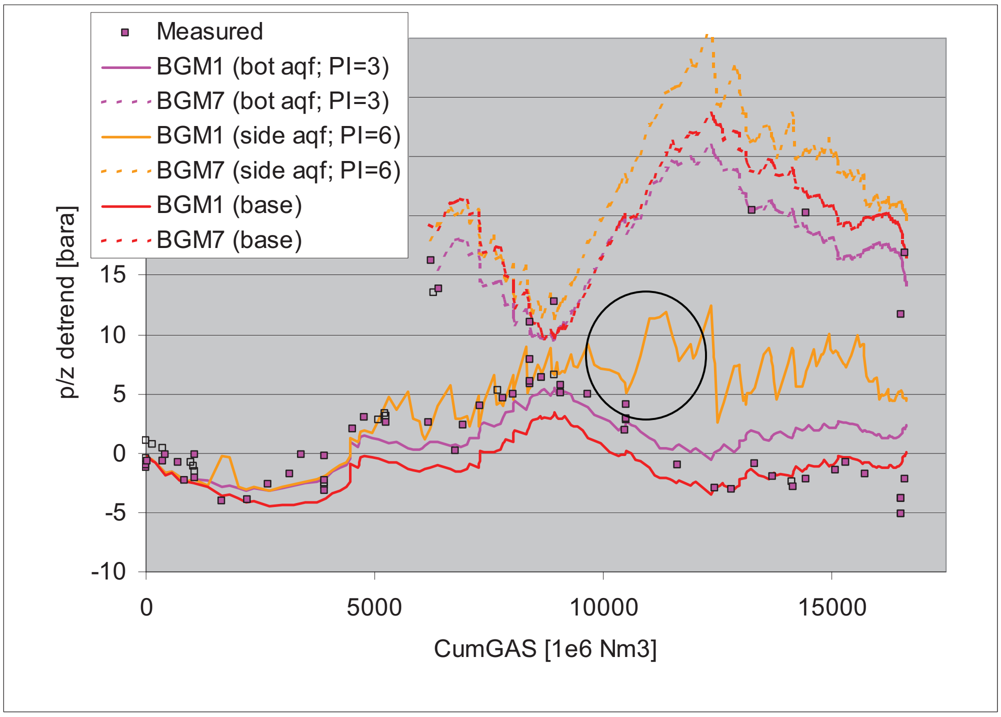

Figure 5-72 Zoomed in pressure match for base ("alt2": E extension of 'fault2'; 10 layers) vs. runs with bottom aquifer, with a PI of 3 (purple) and 6 (orange) vs. the base case (red). A bottom aquifer can be a bit stronger than an edge aquifer; in the PI=6 run a sizeable difference at the low-rate period develops (circle).

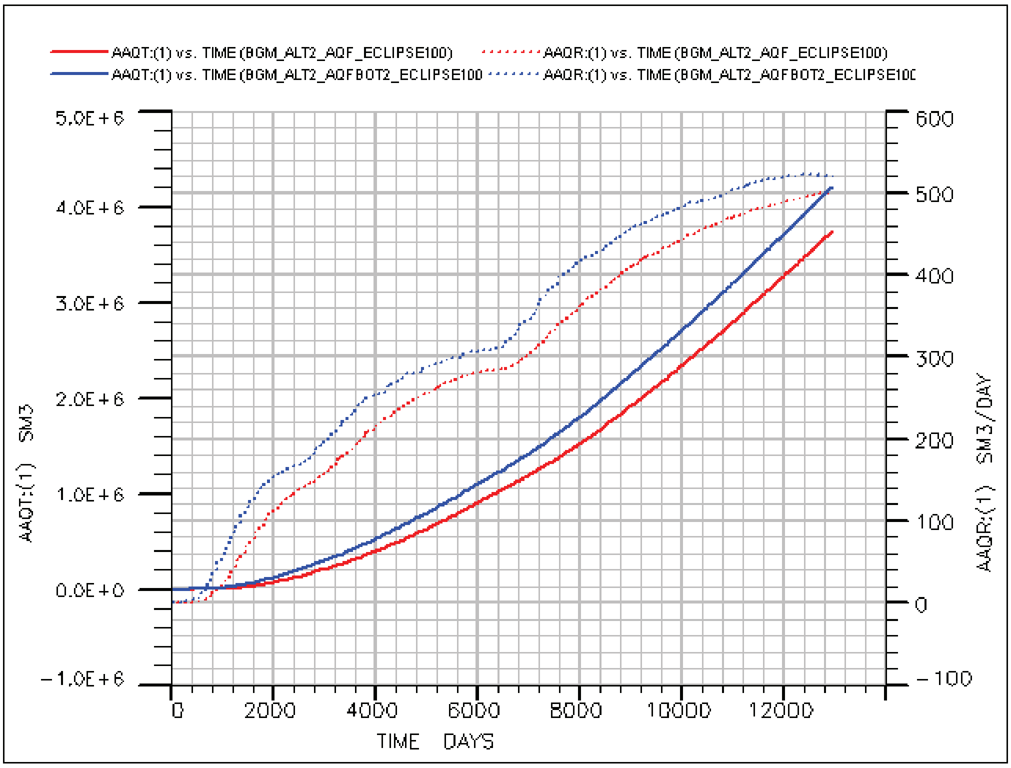

Figure 5-73 **Aquifer influx for edge (red) and bottom aquifer (blue). Dotted lines are rates, full lines cumulatives.**

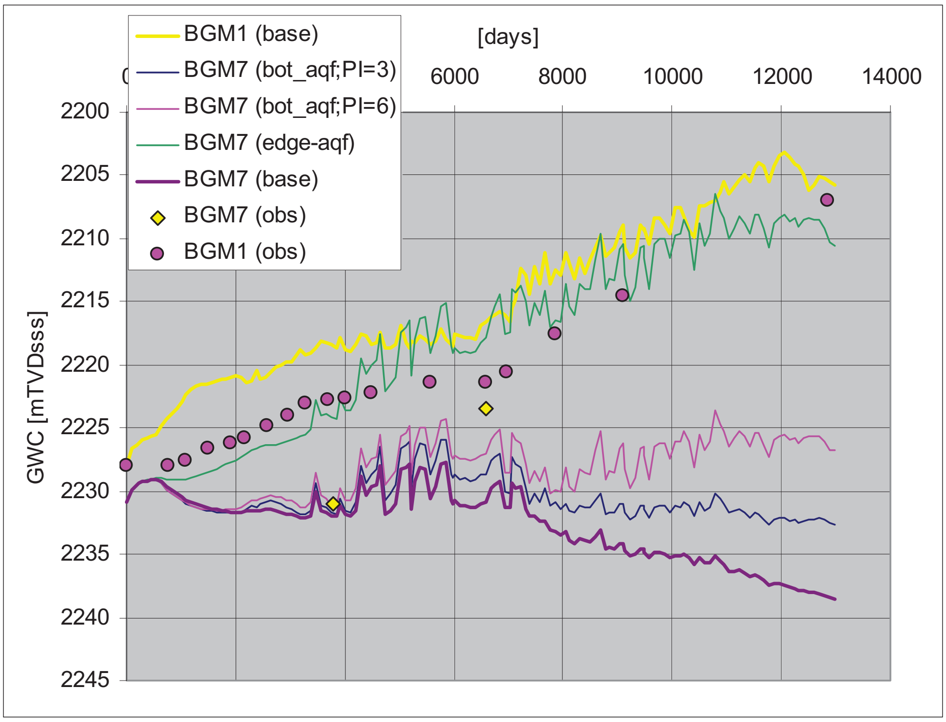

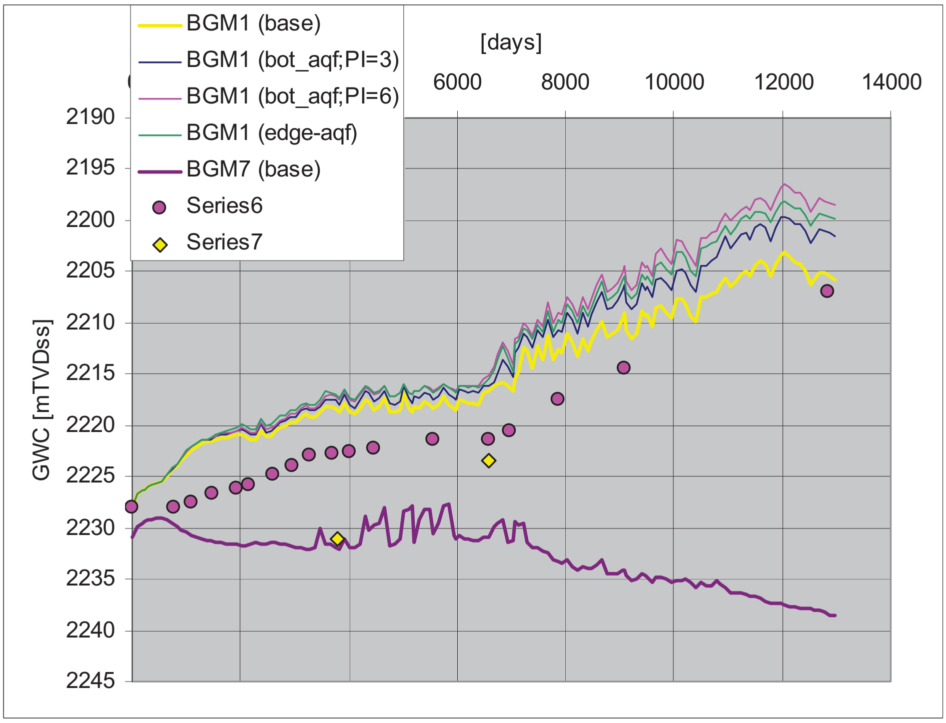

Figure 5-74 Contact rise in BGM1 and BGM7 for edge vs. bottom aquifer runs (both with E trending fault2 extension). The top plot focuses on BGM7, the lower one on BGM1. In contrast to the base run (Figure 5-42), the BGM7 contact goes up in W-edge-aquifer runs. For a run with a bottom aquifer the effect is less dramatic.

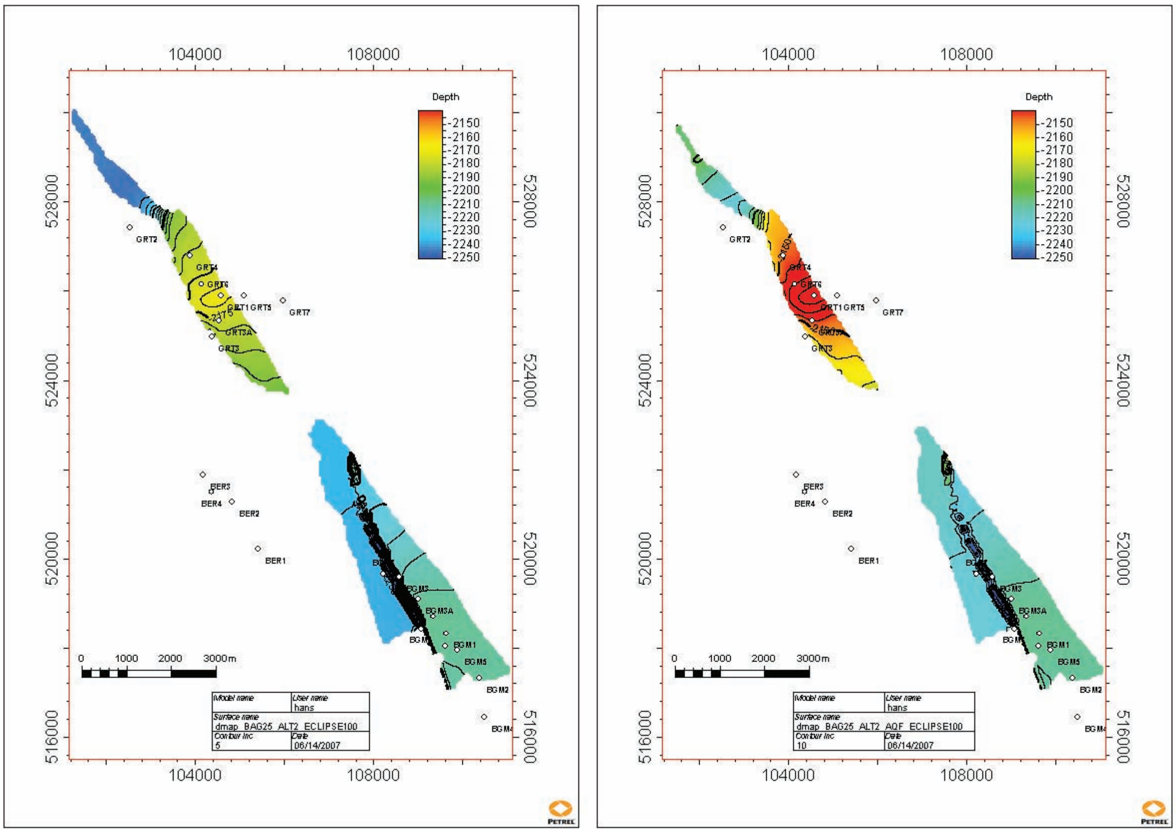

Figure 5-75 Contact map @ 2005 in 'cont-mid' BGM+GRT base case (left), vs. variation with an aquifer attached (right). In the latter BGM7 also exhibits a contact rise, and the contact rise in GRT is larger. [Note different color scale compared to Figure 5-45.]

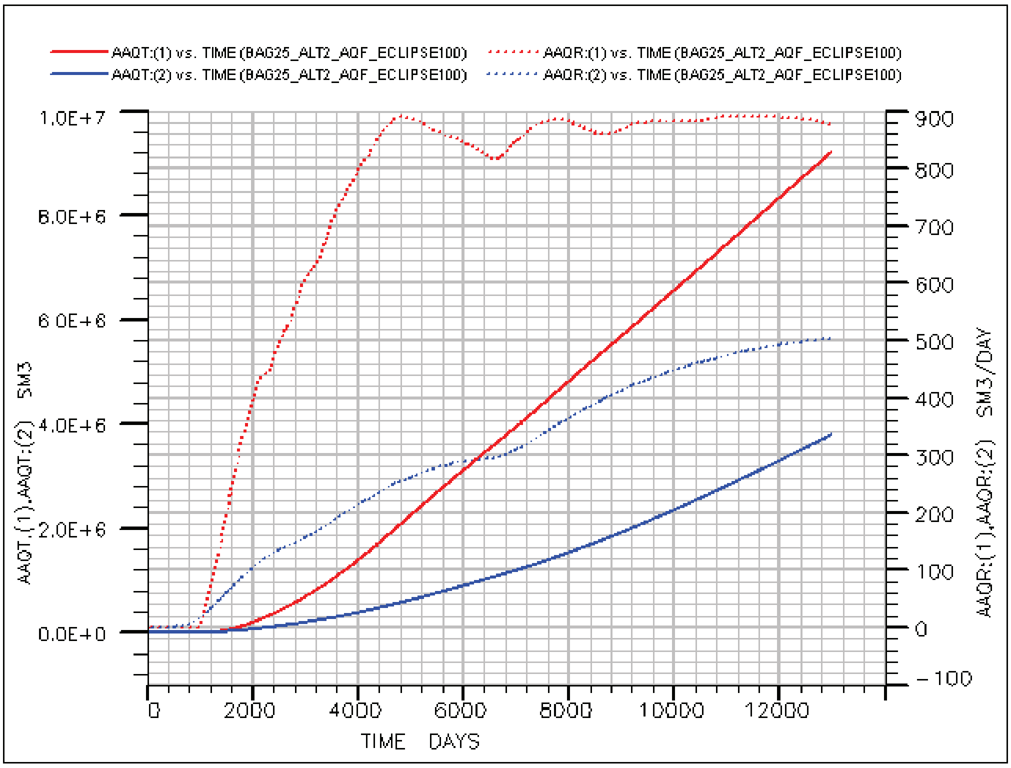

Figure 5-76 **Aquifer influx (cumulatives: full; rates: dotted) for GRT (red) and BGM (blue). Total influx is less than 1e7 m3. [25 layer model, BGM+GRT]**

5.3.9.5 Other sensitivities

5.3.9.5.1 Rock compressibility

Since the amount of connected water is small, the impact of rock compressibility is small as well. A sensitivity was run to confirm this behaviour of the model (Figure 5-77). Increasing the compressibility from 1e-5/bar to 1e-4/bar necessitated a small decrease in MULTPV (from 1.14 to 1.10) in order to maintain the pressure match, mainly in the middle part of the history. In the later part of the history match the reduced GIIP leads to a somewhat too rapid decrease in pressure. But, as the zoomed-in plot shows (Figure 5-77), the pressure match does not really constrain the compressibility in this range.

Nevertheless, the increase in compressibility is sufficient to affect the BGM7 contact: it no longer goes down at all (Figure 5-82). It should be noted that the BGM1 contact match is lost: the contact is now too. A further increase in permeability to counter this does not seem advisable.

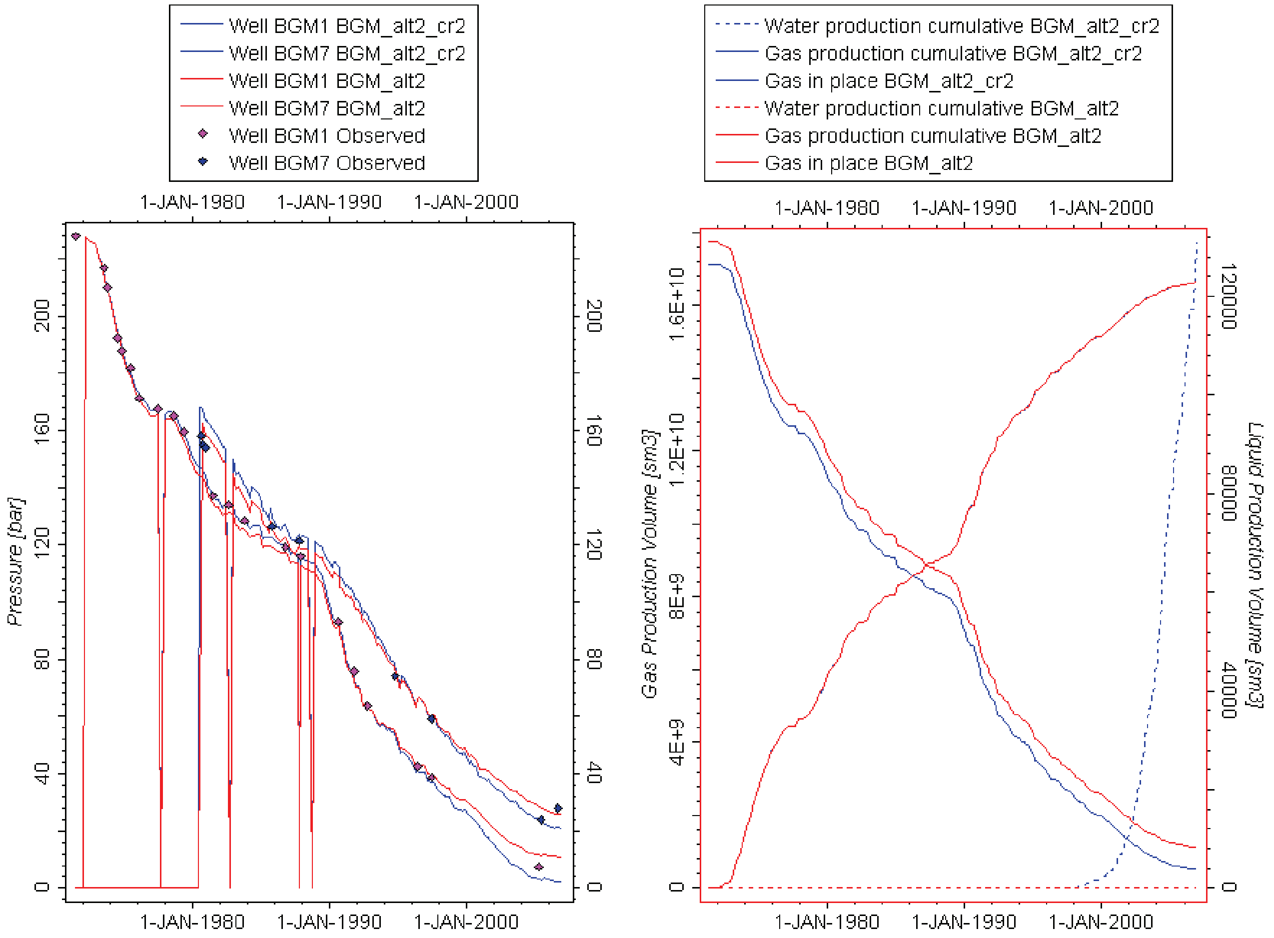

Figure 5-77 Pressures (left) and cumulatives (right) for a sensitivity with increased rock compressibility (blue, 'BGM_alt2_cr2') versus base case (red). The high compressibility run has enhanced GWC rise, and therefore exhibits water production.

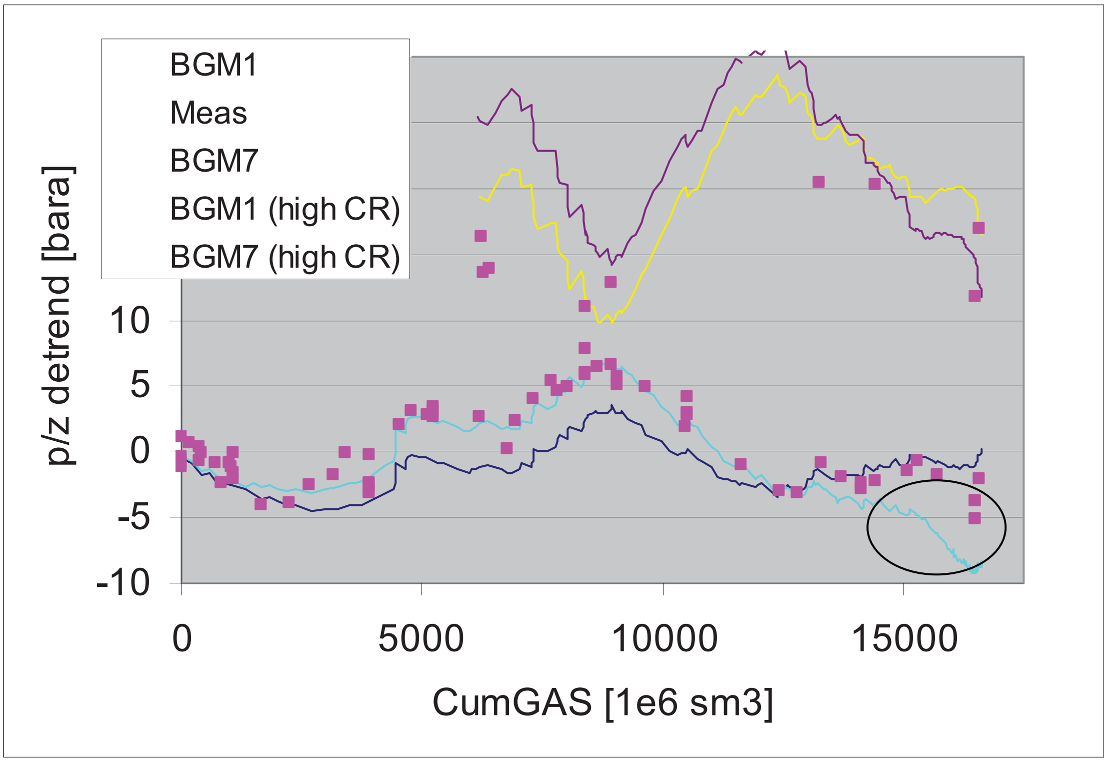

Figure 5-78 Zoomed-in BGM pressure match for high compressibility case. The GIIP decrease in the high-compressiblity run (to compensate for the pressure support due to the compressibility) leads to too-low gas volumes (thus rapid pressure decline) at the very end (circle).

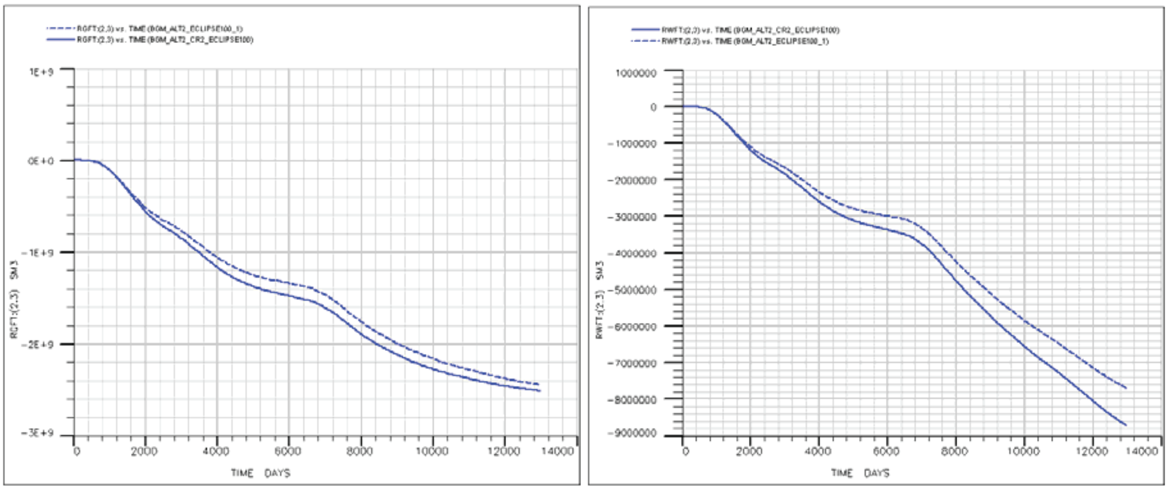

Figure 5-79 Gas flow cumulatives (‘RGFT’, left) & water flow cumulatives (‘RWFT’, right) from BGM-main to BGM7 as a function of time for cont_mid base run (dotted) and increased CR run (‘BGM_ALT2_CR2’, full). The sign convention is positive for BGM-main→BGM7, negative for the reverse. Note that volumes are at surface, leading to very different scales for the two figures (1e9 to –3e9 sm^3 left, 1e6 to –9e6 sm^3 right).

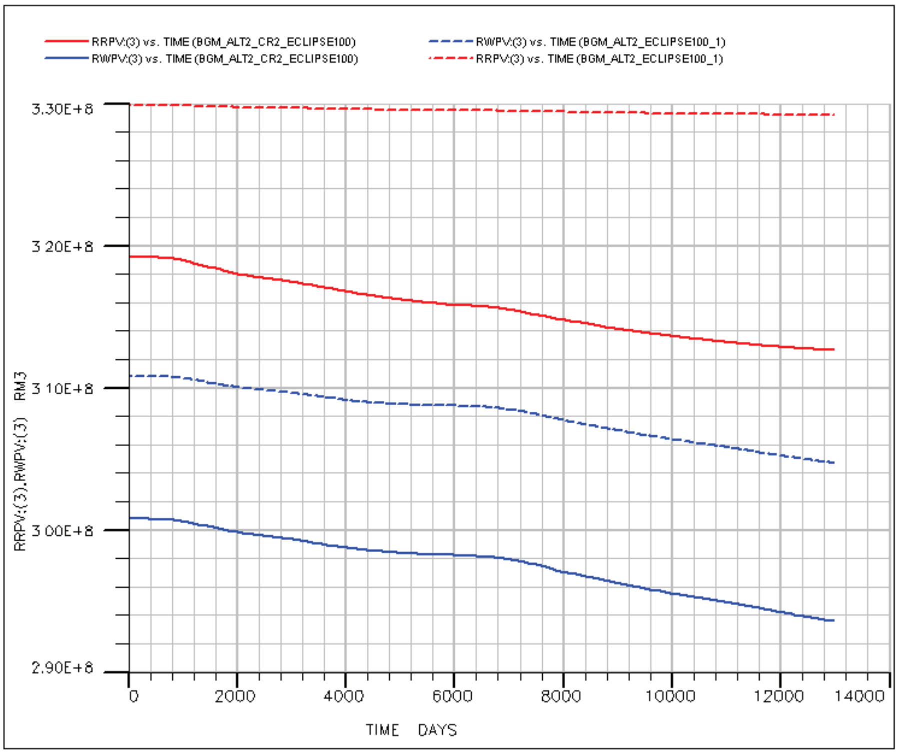

Figure 5-80 Pore volume (‘RRPV’) and water volume (‘RWPV’) in the BGM7 compartment as a function of time for cont_mid base run (dotted) and increased rock compressibility run (‘BGM_ALT2_CR2’, full). In the base run there is water efflux, while the pore volume stays more or less constant; hence the gas volume making up the difference has to increase. In the highly compressible run, the pore volume decreases in sync with the water efflux, so that the gas volume stays constant.

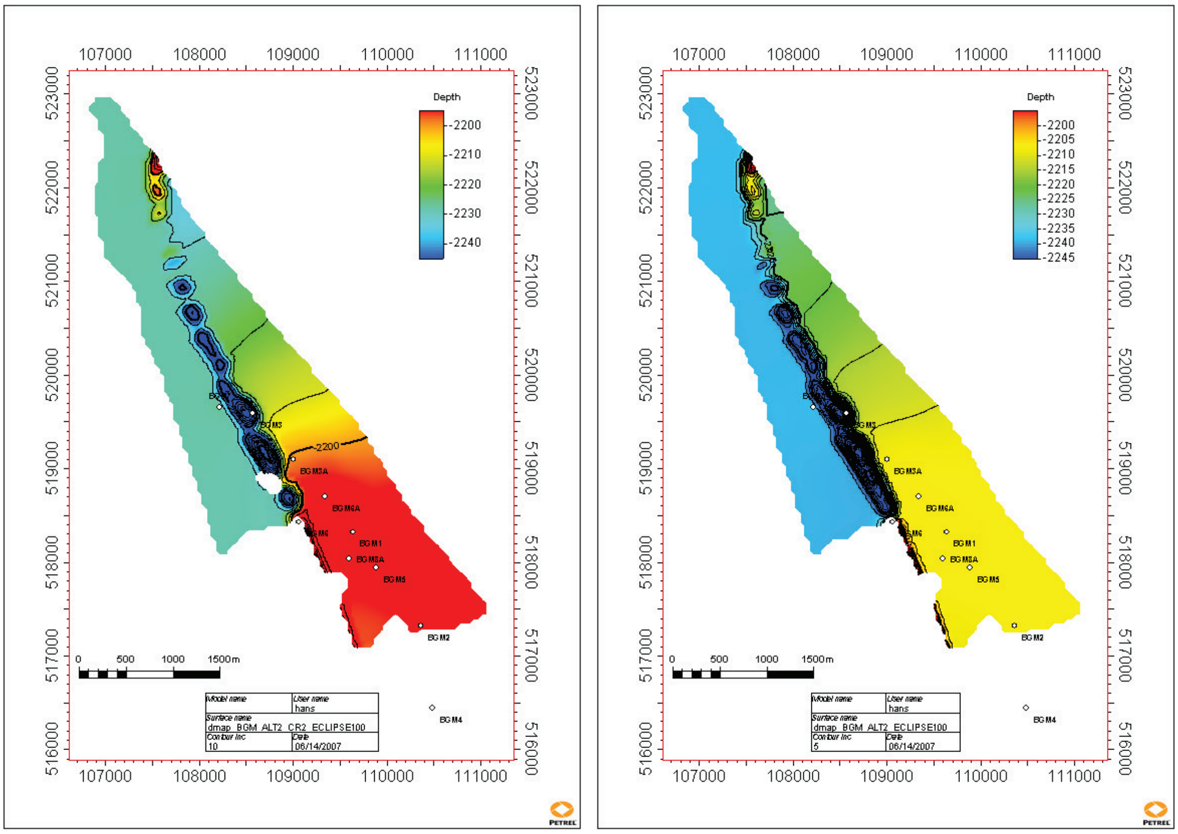

Figure 5-81 BGM base 'cont_mid' contact map @ 2005, vs. high rock compressibility sensitivity (left). [10 layer model]. The contact *gradient* across the main BGM block is seen to be very similar (from the contour spacing), whereas the contact levels are different.

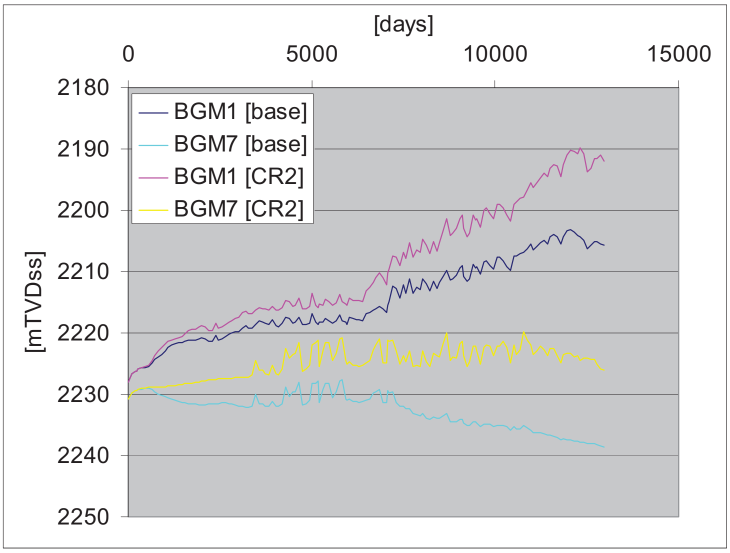

Figure 5-82 **Contact comparison of BGM base ('cont_mid', with "alt2"=E fault), vs. high rock compressibility sensitivity ('CR2', both runs on 10 layer model). The increased compressibility raises the GWC further, and stops the contact descent in the BGM7 compartment.**

5.3.9.5.2 Relperm

Since the fluids are almost always segregated, Corey exponents are expected to play a limited role. Similarly, S_{gr} does govern how much gas is trapped, but given the very low pressures to which the reservoir is depleted, the actual volume involved is relatively small. Indeed, the sensitivities (Table 5-21, Table 5-22) show very comparable results. The one exception to this is that increasing the S_{gr} increases the contact rise (Figure 5-87). However, given the SCAL work, the S_{gr} range is likely more limited than used here, so that the final conclusion remains that the relative permeabilities are not a key uncertainty in this field (other than via the volumetrics).

Table 5-21 **Relative permeability sensitivities**

Sensitivity		**Swc**	**Sgr**	**krw @ Sgr**	**krg @ Swc**	**Corey-W**	**Corey-G**
Base		0.22	0.19	0.56	0.92	2.50	4.00
RLP1		0.22	**0.29**	0.56	0.92	2.50	4.00
RLP2		0.22	0.19	0.56	0.92	**1.25**	**2.00**
RLP3		Depends on permeability category. See Table 5-22.					

Table 5-22 Coefficients & permeability classes in 'RLP3' sensitivity. Values are from the SCAL data (section 5.1.2). As far as S_{wc} is concerned, this data is not in perfect agreement with the well logs (chapter 3), which is where the base case S_{wc} is derived from.

Class #		K_from	K_to	Swc	Sgr	krw @ Sgr	krg @ Swc	Corey-W	Corey-G
1		1	10	0.42	0.24	0.1	0.90	2.50	4.00
2		10	100	0.30	0.21	0.1	0.92	2.50	4.00
3		100	1000	0.20	0.19	0.2	0.95	2.50	4.00
4		1000		0.12	0.17	0.33	0.98	2.50	4.00

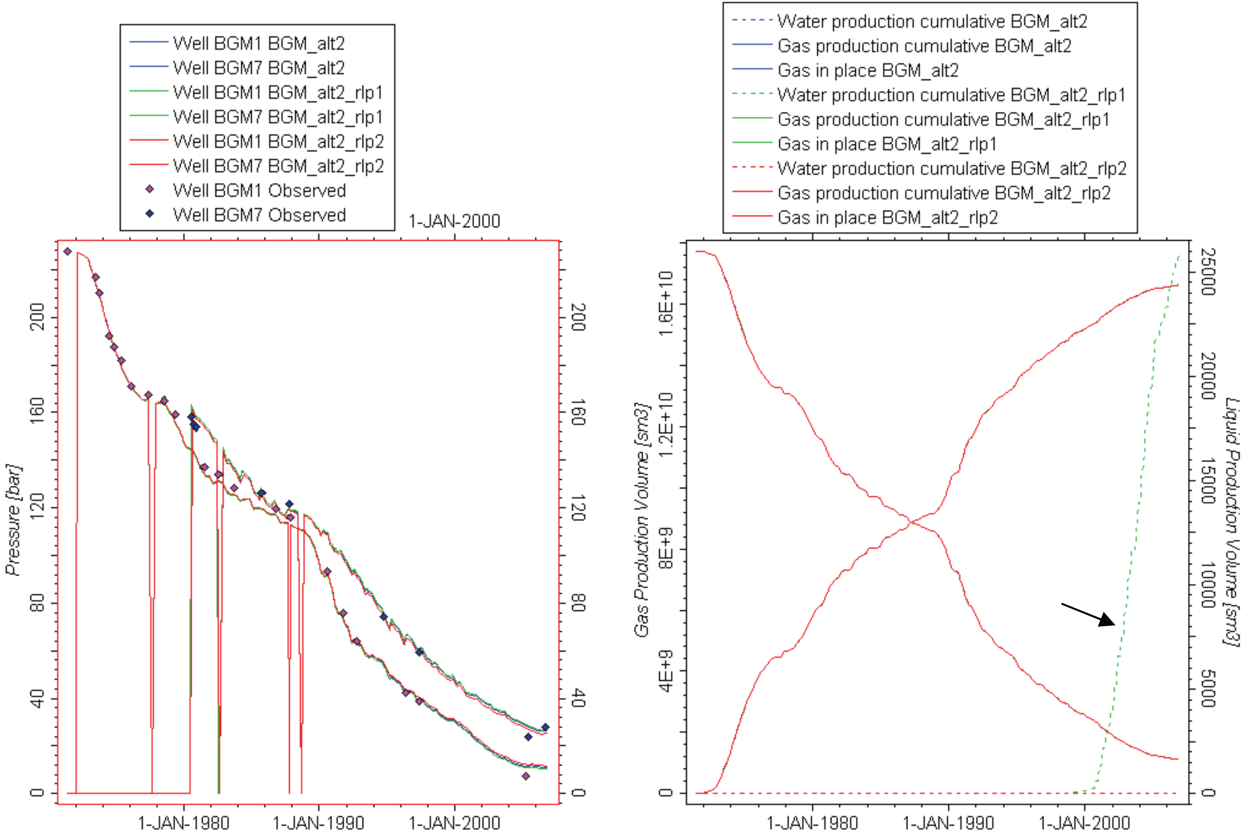

Figure 5-83 Pressures (left) and cumulatives (right) for BGM sensitivities with higher Sgr ('RLP1', 0.29; green) and lower Corey exponents ('RLP2', 2 and 1.25; red) compared to base case (blue). The only significant difference is the enhanced water production in the high-Sgr run due to increased GWC rise (marked by arrow; cf. Figure 5-87).

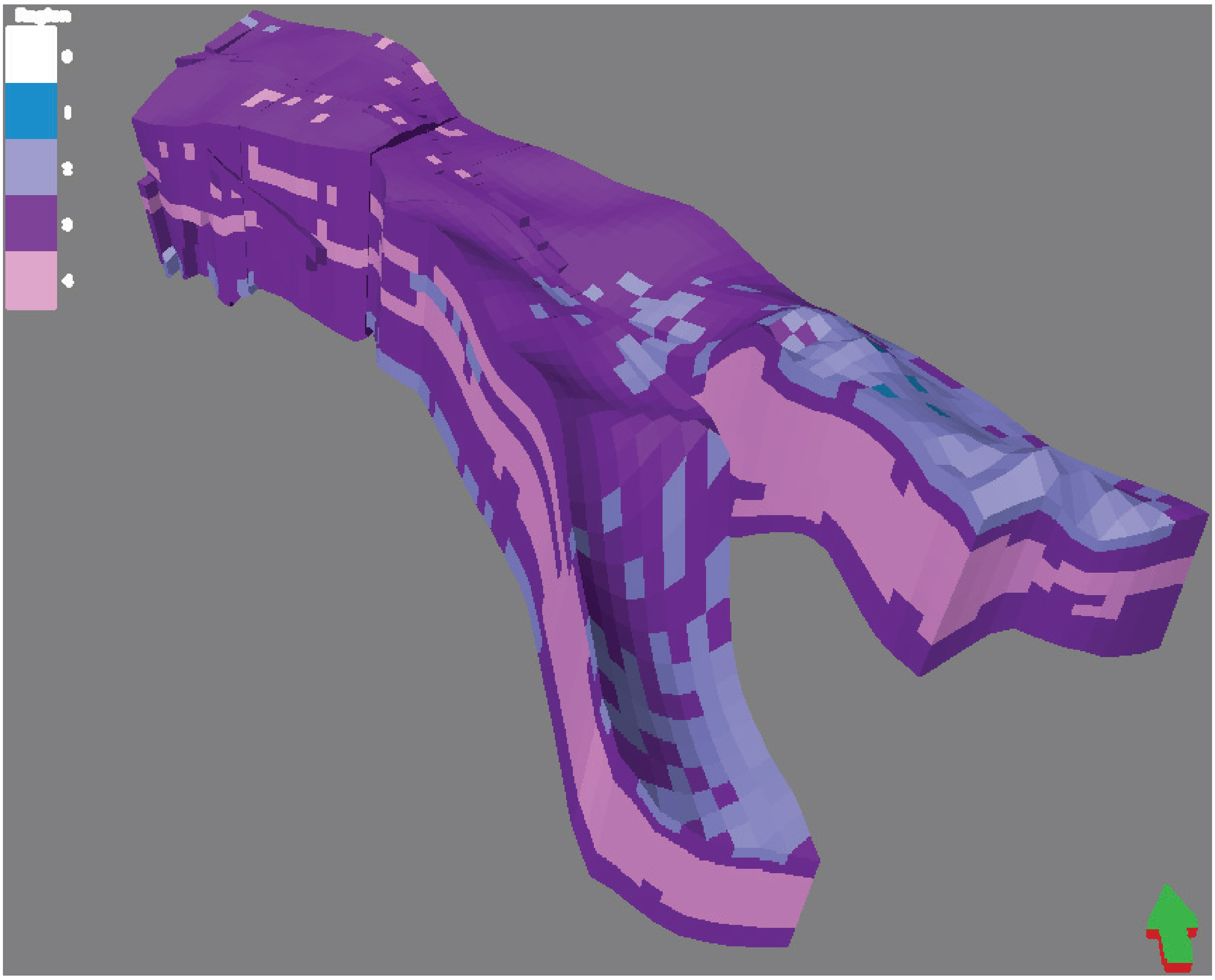

Figure 5-84 Plot of permeability categories for third rlp sensitivity. Categories are:

1	1-10 mD
2	10-100 mD
3	100-1000 mD
4	> 1000 mD

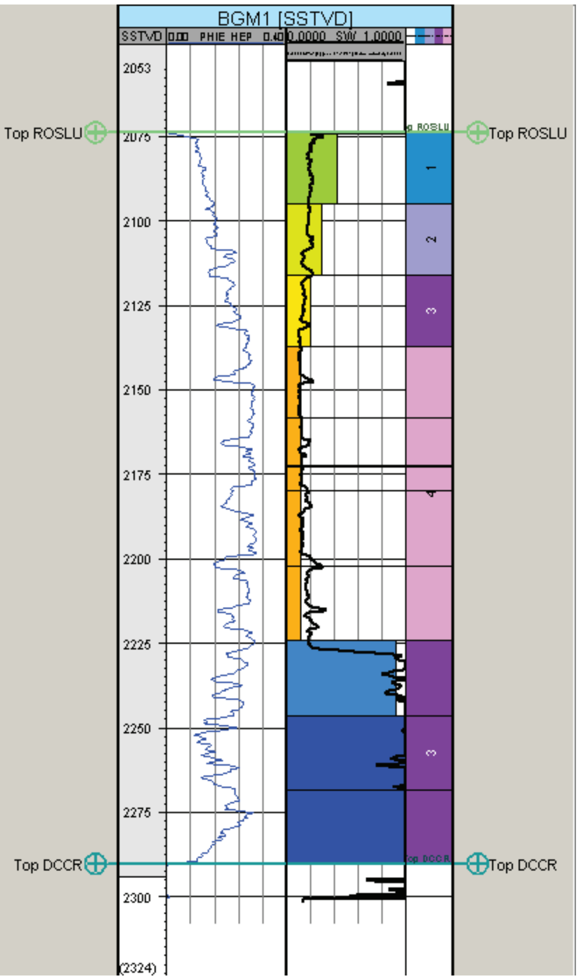

Figure 5-85 Permeability categories in third rlp scenario along BGM1 trajectory (right track in log plot) vs. porosity (left track) and saturation logs (middle track). The saturation variation is seen to exaggerate that seen in the logs.

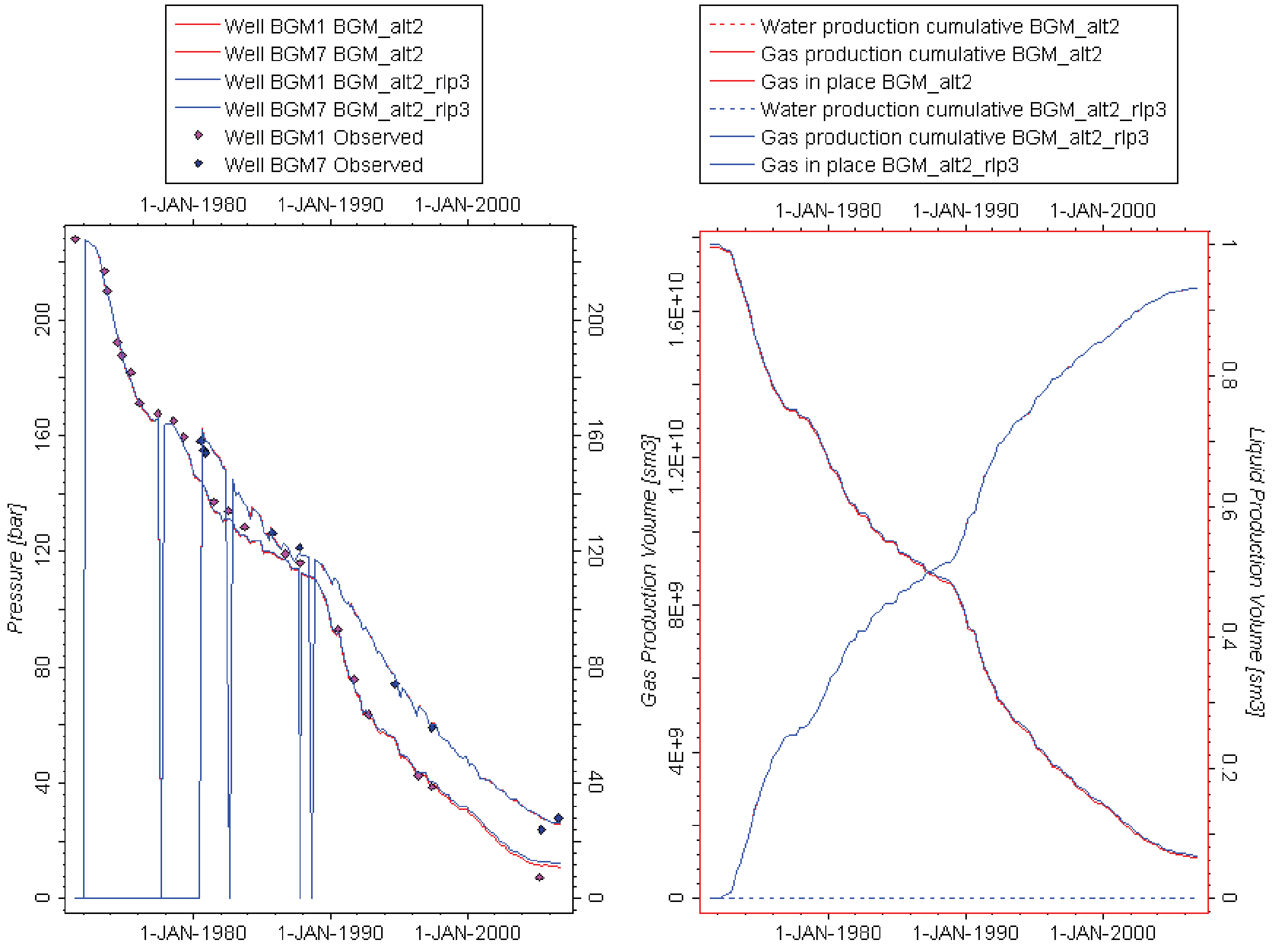

Figure 5-86 Pressure match (left) and cumulatives for 'RLP3' scenario (blue) vs. base case (red). The ‘RLP3’ case has a different pore volume multiplier (1.08 rather than 1.14). After this correction, the behaviour is almost identical.

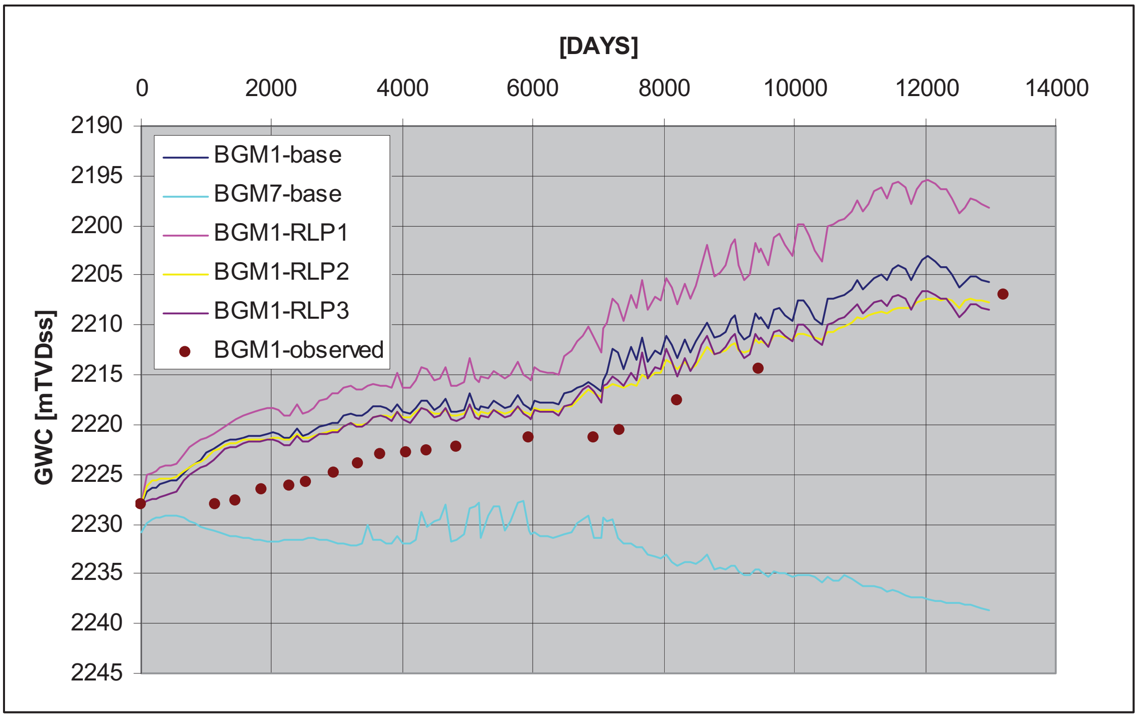

Figure 5-87 Impact of RLP sensitivities on BGM1 contact movement.

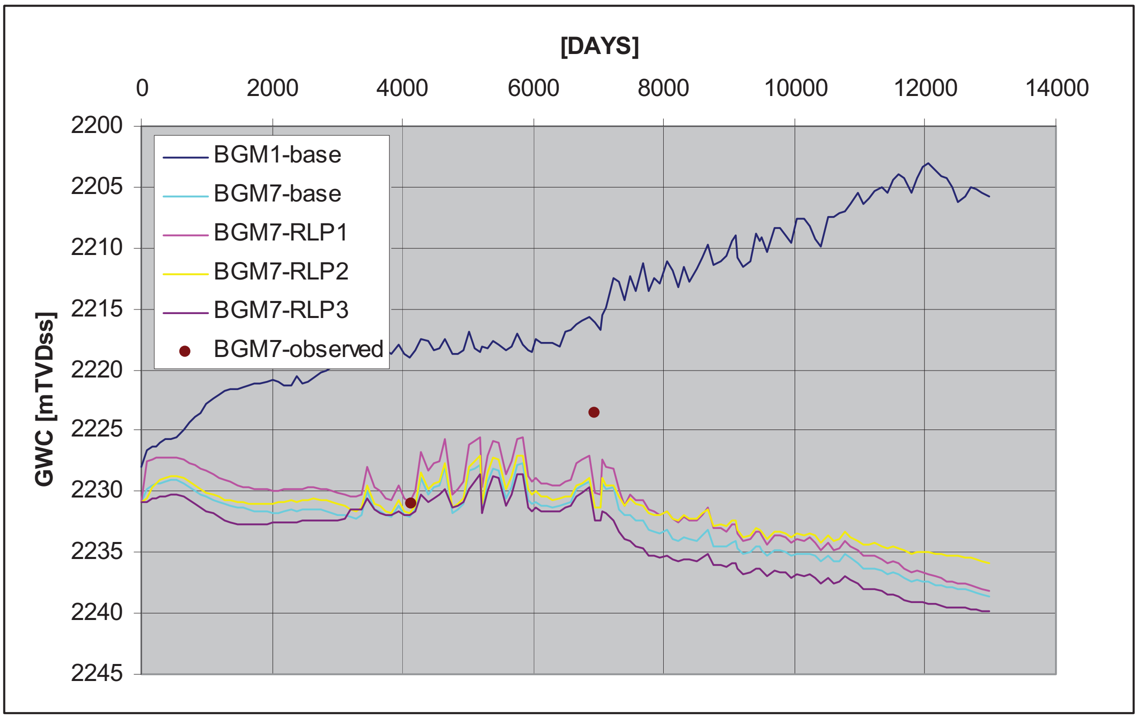

Figure 5-88 Impact of RLP sensitivities on BGM7 contact movement.

5.4 Well Test/Pressure Transient analysis.

A list of analyzed well tests for BGM1 and BGM6 can be found in Table 5-7 on page 34. Detailed analyses are reported in Appendix II.B. [The analysis was done with Kappa/Saphir, 4.02.03.]

The analysis was performed *after* most of the simulation work was done (due to data availability), hence the location of this section *after* the simulation section.

The main conclusions are the following:

- The 1990 BGM1 well test involves a large perforation interval across heterogeneous rock. That makes it more ambiguous.
- The well tests fit best with permeabilities of several hundreds of mD, with high k_v/k_h: radial flow is not visible.
- Skin/non-Darcy skin combinations that are needed to match the drawdrowns are sometimes exteme (low). In one case the program was not able to get a match at all (skin < -10). [Such a very low skin value corresponds to an effective wellbore radius of the order 1e4 times larger than the real wellbore.]
- There appear to be consistent phenomena (multi-phase?) causing dips in the pressure derivative at 0.01 and 0.1 hours. These are not matched, and they could hide other behaviour.

Thus the well test models support lower horizontal permeabilities, and higher vertical ones. This can, given plug permeabilities, and vertical permeabilities resulting from that on “normal” upscaling, only be explained by assuming that the length scale of the “poor streaks” is lower than 100m. However, it is not that case that the well tests analyses are a perfect fit (viz. the strongly negative skin); see e.g. Figure 5-89.

Barring the presence of fracs (not mentioned in the well history), the negative skin may point to the more complex (multi-layer?) nature of the Rotliegend. The analysis of this would be more involved (e.g. use well test simulation rather than analytical tools), and was not attempted.

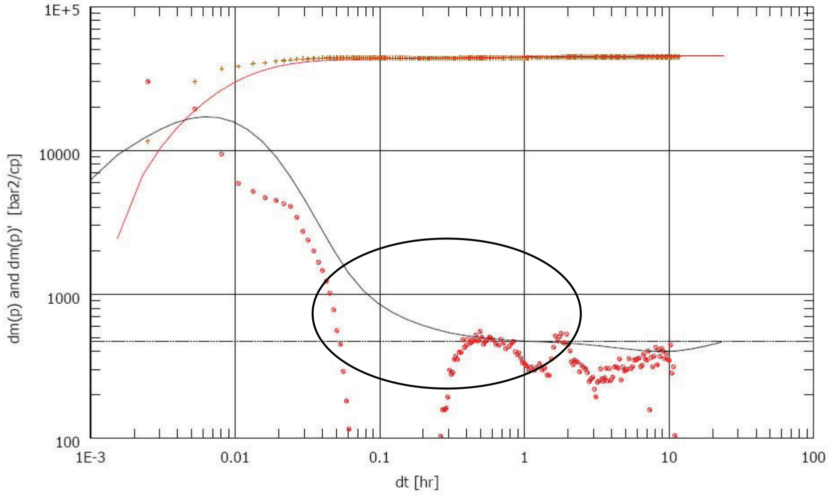

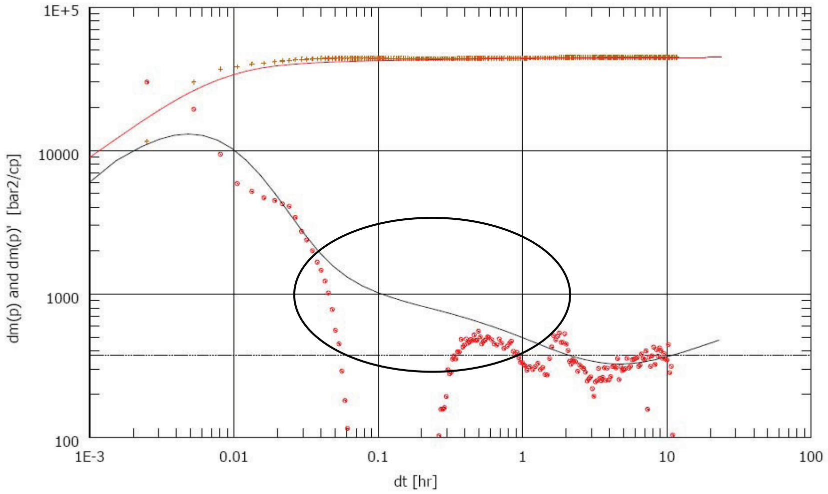

Figure 5-89 **Comparison of base analysis [top; k-320 mD; k_v/k_h=1] of the 1986 well test in BGM1, vs a low k_v/k_h analysis [bottom; k=600mD; k_v/k_h=0.1]. The spherical flow regimes in the modelled curve are indicated. Precisely in this time-frame, the measurements show complex non-modeled behaviour, precluding really definitive conclusions.**

6 Forecasting

6.1 Well Performance Modeling

For the forecasting model, we attempted to model the vertical lift inflow performance of a gas producer with the help of the software Prosper. The model used for this study was the 1979 well test of BGM-1 [19], which seems typical (see Table 7-2).

6.1.1 Input Data

To match the vertical lift performance of the well BGM-1, rates and stabilized pressures from a test on 7th April 1979 have been used [19]. The values are summarised in Table 6-6.

As evidenced by Figure 6-1, the drawdown in the well over the tested rates is about 3 bars. In the pressure drop, the quadratic term dominates the linear tem by a factor 6 for rates of the order 1e6 sm3/d. pressure loss across the tubing is about 30 bars. This means we need to model the pressure drops to an accuracy of the order of a few % to be able to predict rates sufficiently accurately.

The PVT data was input as Table 6-1.

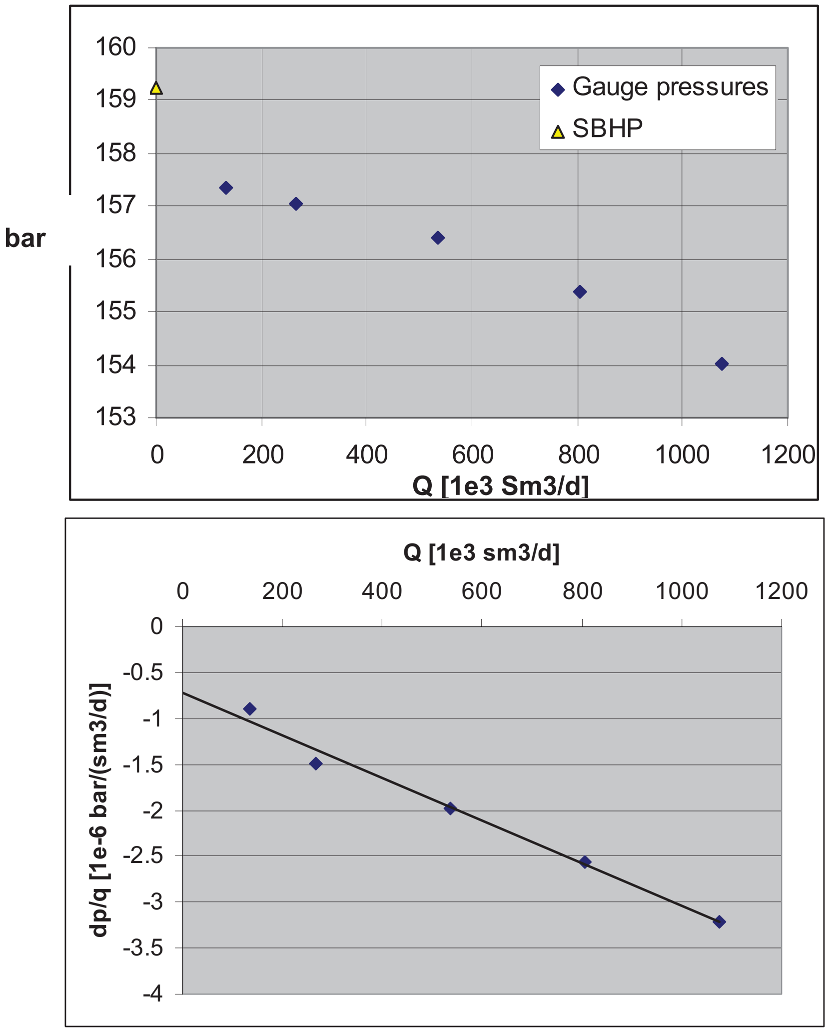

Figure 6-1 Graph of rate vs. pressure of the 1979 well test used. The top plot shows pressure vs. rate, the bottom plot shows pressure drop/rate vs. rate.

Table 6-1 **PVT inputs. Note the zero gas/condensate and gas/water ratios neededto get an approximate match (see text).**

Parameters	**Units**	**Value**	**Comments**
Gas Gravity	Sp.gravity	0.59	From PVT report
Separator Pressure	Bara	2.05	From previous Taqa Prosper model
Condensate to gas ratio	Sm^3/Sm^3	0	No evidence
Condensate Gravity	Kg/m^3	755	From previous Taqa Prosper model
Water to gas ratio	Sm^3/Sm^3	0	
Water Salinity	ppm	150000	From previous Taqa Prosper model [this is not correct, as no formation water is produced; bug gas/water ratio=0]
Mole Percent H_2S	%	0	From previous Taqa Prosper model
Mole Percent CO_2	%	0.7	From previous Taqa Prosper model
Mole Percent N_2	%	0.97	From previous Taqa Prosper model
Correlation gas Viscosity		Lee et al	

6.1.2 Inflow performance Relation

The reservoir model selected was Forchheimer (Table 6-2). The Darcy and non-Darcy coefficients were later adapted to match the observed rate/BHP dependency (section 6.1.4).

Table 6-2: Reservoir parameter for the inflow performance.

Parameters	**Units**	**Value**	**Comments**
Reservoir Pressure	Bara	157.46	Extrapolated from rate vs. gauge pressure; Note discrepancy with reported pressure at well test date [1] (April 1979)
Reservoir Temperature	Deg C	86.1	Initial temperature

6.1.3 Equipment data

A deviation survey of BGM-1 was used as provided by Taqa. The downhole equipments were copied from Taqa Bergermeer-1 well description from a Prosper model prepared by Taqa (Table 6-3).

The geothermal gradient is shown in Table 6-4. The Overall Heat Transfer Coefficient was set at 3, which is a common value for gas well. The average heat capacity was set as default.

Table 6-3: Downhole equipment.

Label	Type	Measured Depth (m)	Tubing Inside Diameter (m)	Tubing Inside Roughness (m)	Tubing Outside Diameter (m)	Tubing Outside Roughness (m)	Casing Inside Diameter (m)	Casing Inside Roughness (m)	Rate Multiplier
--------	-----------	--------	--------	---------	--------	---------	--------	---------	----------
	Xmas Tree	0							
4 1/2"	Tubing	7.1	0.10058	1.27E-05					1
5"	Tubing	83.9	0.10871	1.27E-05					1
3 1/2"	Tubing	92.8	0.075946	1.27E-06					1
	SSSV		0.071374						
3 1/2"	Tubing	107.2	0.075946	1.27E-06					1
5 1/2"	Tubing	2020.1	0.12421	1.27E-05					1
4 1/2"	Tubing	2057.1	0.10058	1.27E-06					1
	Restriction		0.05715						
4 1/2"	Tubing	2065.2	0.10058	1.27E-06					1
	Restriction		0.067056						
3 1/2"	Tubing	2075.3	0.075946	1.27E-06					1
7" liner	Casing	2080.8					0.15951	1.27E-06	1

Table 6-4: Geothermal gradient.

Formation Measured Depth (m)	Formation temperature (deg C)
0	15
2299	86

6.1.4 Calculations and results

The Darcy and non-Darcy Coefficients of the Forchheimer reservoir model were set as in Table 6-5, to match the IPR curve to the well test measurements.

To also match the vertical lift performance of the well BGM-1, 5 flow shave been inputted in Prosper.

Those 5 flows are from the well test carried out April 7th, 1979 [19]

The water gas ratio and condensate gas ratio were set at 0: with non-zero values we were not able to obtain a match (suggesting there are density/PVT issues that are not fully resolved). The values are summarised in Table 6-6:

The correlation used in the VLP is the Gray correlation. No corrections were applied to the correlation. The reason for this is that we were unable to match the low-rate behaviour of the BGM1 well; using the Prosper matching functionality lead to unrealistic Gray parameter correction values (0.99 for the first and 1.4 to 1.6 for the second). Since the high rate behaviour is more critical, and we could match that without corrections, we used those instead. What was clear was, that in order to obtain a match the WGR had to be, in essence, zero. The CGR had a lower impact, but again the low rate behaviour (gravity head) was better captured by setting it zero.

Base on the Gray correlation, the VLP/IPR Match is shown in Figure 6-3.

From this match, a VLP table was generated with 3 variables: the reservoir pressure (from 25 bara to 227 bara), Water gas ratio (from 0 to 1.e-5 Sm3/Sm3) and the WHP (from 21 bara to 200 bara).

The results are shown in Figure 6-4.

A similar (but obviously uncalibrated) table was generated for injection (based on the same PVT, reservoir and well assumptions).

Table 6-5: Reservoir parameter for the inflow performance.

Parameters	Units	Value	Comments
Water gas ratio	Sm^3/Sm^3	0	From VLP match
Condensate gas ratio	Sm^3/Sm^3	0	From VLP match
Non-Darcy Coefficient	$Bar^2/(Sm^3/day)^2$	1.5e-9	From IPR match
Darcy Coefficient	$Bar^2/(Sm^3/day)$	0.0003	From IPR match

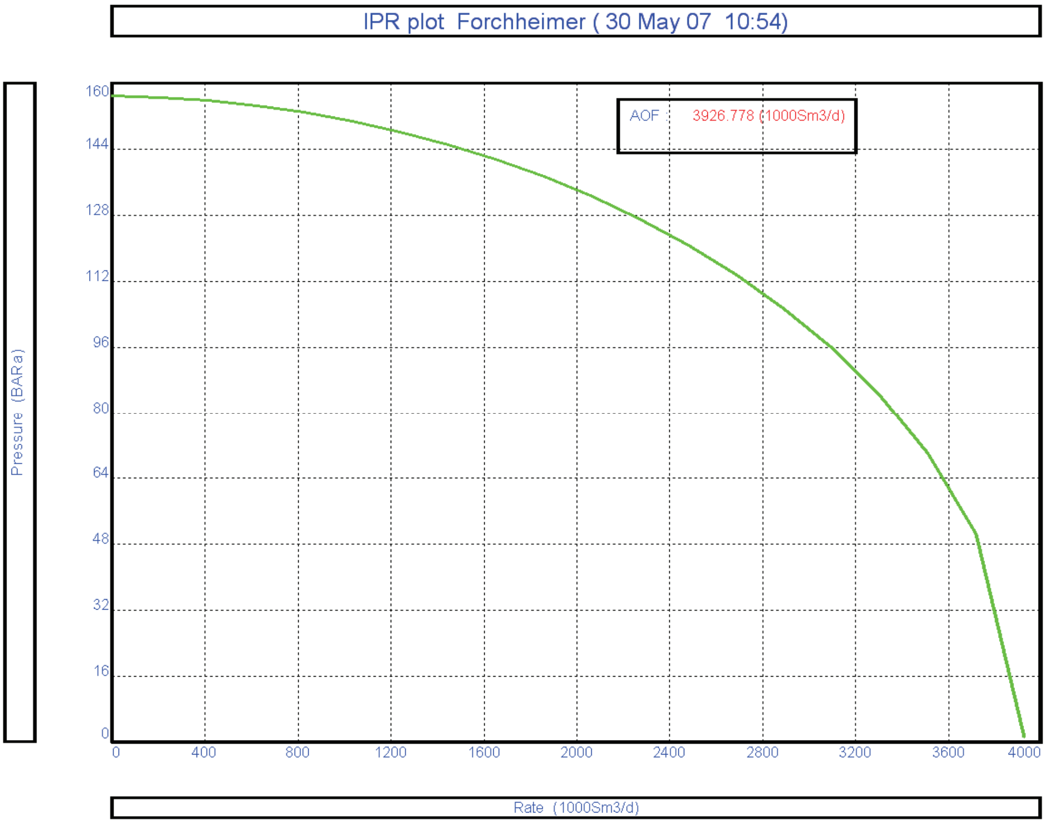

Figure 6-2: Inflow performance rate of the reservoir.

Table 6-6: Well test (see also Table 7-2).

Match Point Comment	Tubing Head Pressure (BARa)	Tubing Head Temperature (deg C)	Water Gas Ratio (Sm3/Sm3)	Condensate Gas Ratio (Sm3/Sm3)	Gas Rate (1000Sm3/d)	Gauge Depth (Measured) (m)	Gauge Pressure (BARa)
----------	---------	------------	----------	-----------	------------	-----------	---------
5th flow	123.7	62.70	0	0	1074.26	2069.50	154.01
4th flow	129.7	61.10	0	0	805.40	2069.50	155.40
3rd flow	133.6	57.78	0	0	536.10	2069.50	156.40
2nd flow	135.3	46.67	0	0	267.15	2069.50	157.06
1st flow	135.9	37.78	0	0	134.19	2069.50	157.34

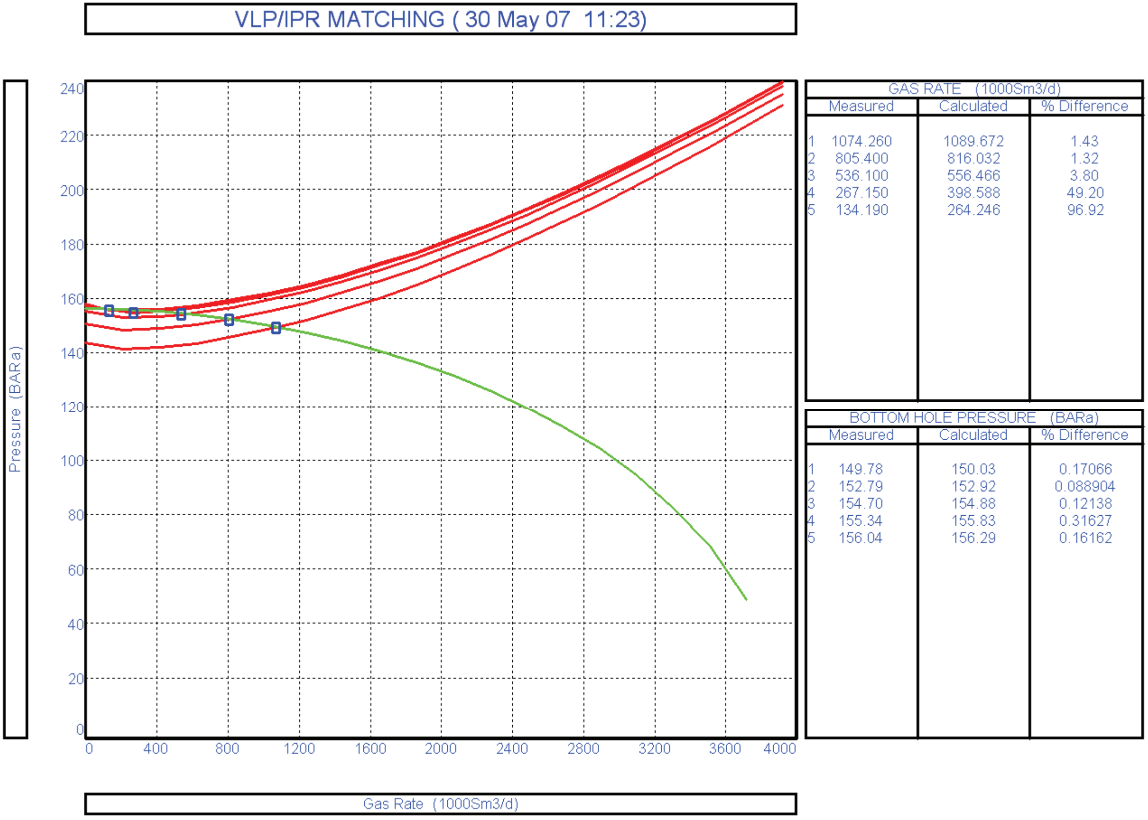

GAS RATE (1000Sm3/d)

	Measured	Calculated	% Difference
1	1074.260	1089.672	1.43
2	805.400	816.032	1.32
3	536.100	556.466	3.80
4	267.150	398.588	49.20
5	134.190	264.246	96.92

BOTTOM HOLE PRESSURE (BARa)

	Measured	Calculated	% Difference
1	149.78	150.03	0.17066
2	152.79	152.92	0.088904
3	154.70	154.88	0.12138
4	155.34	155.83	0.31627
5	156.04	156.29	0.16162

Figure 6-3: VLP/IPR match.

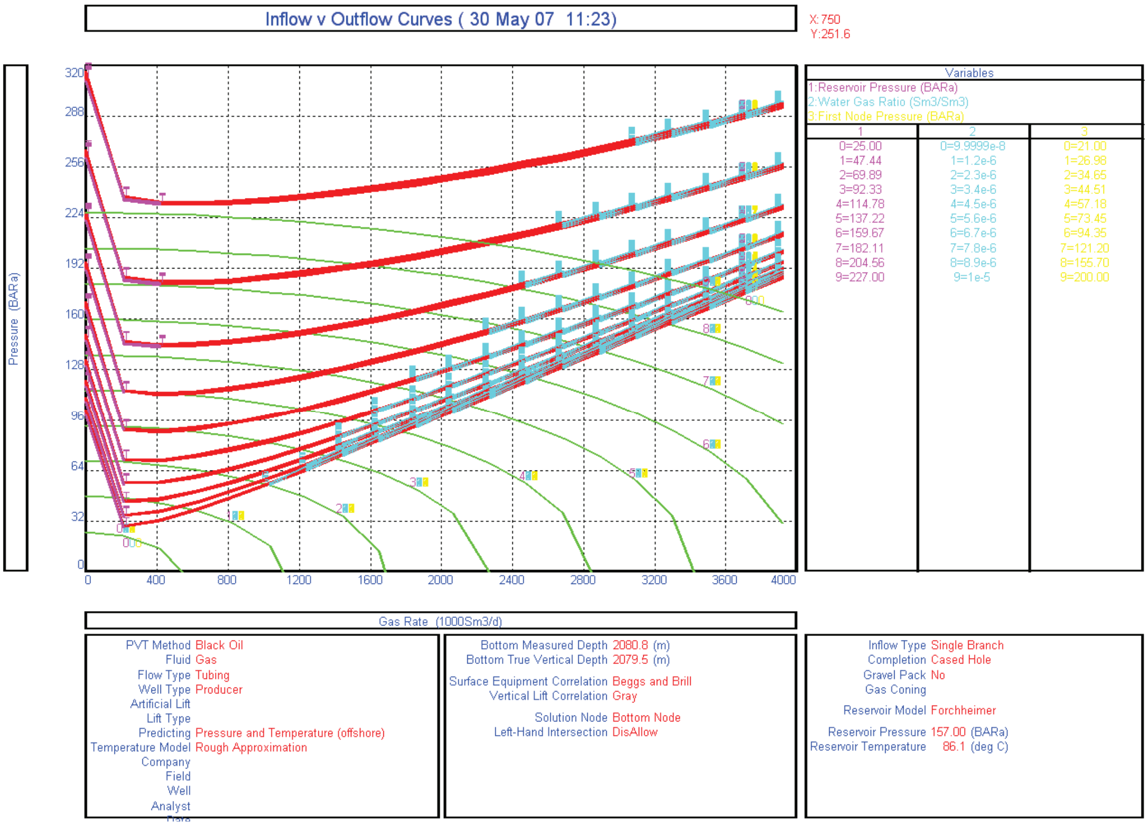

Inflow v Outflow Curves (30 May 07 11:23)

X:750
Y:251.6

Variables

1:Reservoir Pressure (BARa)
2:Water Gas Ratio (Sm3/Sm3)
3:First Node Pressure (BARa)

1	2	3
0=25.00	0=9.9999e-8	0=21.00
1=47.44	1=1.2e-6	1=26.98
2=69.89	2=2.3e-6	2=34.65
3=92.33	3=3.4e-6	3=44.51
4=114.78	4=4.5e-6	4=57.18
5=137.22	5=5.6e-6	5=73.45
6=159.67	6=6.7e-6	6=94.35
7=182.11	7=7.8e-6	7=121.20
8=204.56	8=8.9e-6	8=155.70
9=227.00	9=1e-5	9=200.00

PVT Method Black Oil
Fluid Gas
Flow Type Tubing
Well Type Producer
Artificial Lift
Lift Type
Predicting Pressure and Temperature (offshore)
Temperature Model Rough Approximation
Company
Field
Well
Analyst

Bottom Measured Depth 2080.8 (m)
Bottom True Vertical Depth 2079.5 (m)

Surface Equipment Correlation Beggs and Brill
Vertical Lift Correlation Gray

Solution Node Bottom Node
Left-Hand Intersection DisAllow

Inflow Type Single Branch
Completion Cased Hole
Gravel Pack No
Gas Coning

Reservoir Model Forchheimer

Reservoir Pressure 157.00 (BARa)
Reservoir Temperature 86.1 (deg C)

Figure 6-4: VLP graph

6.1.5 Application in the Eclipse Model

In order to match the Eclipse model to this data we need to do two things:

- Change the connection factors (~ skin) to match the inflow performance (linear) and the non-Darcy coefficient 'D' to match the rate dependent part.
- Add lift curves to match the outflow.

  In order to do this we needed to manually QC and edit the curves; Eclipse has certain restrictions on curve monoticity that Prosper does not automatically satisfy.

Examining the plots shown below, we can see that we have achieved a good match on the inflow performance with simple means (Table 6-9), and a reasonable match for the THP for rates of 6e5 Sm3/d and higher. (Note that the inflow matching needs to be done separately for different model realizations.)

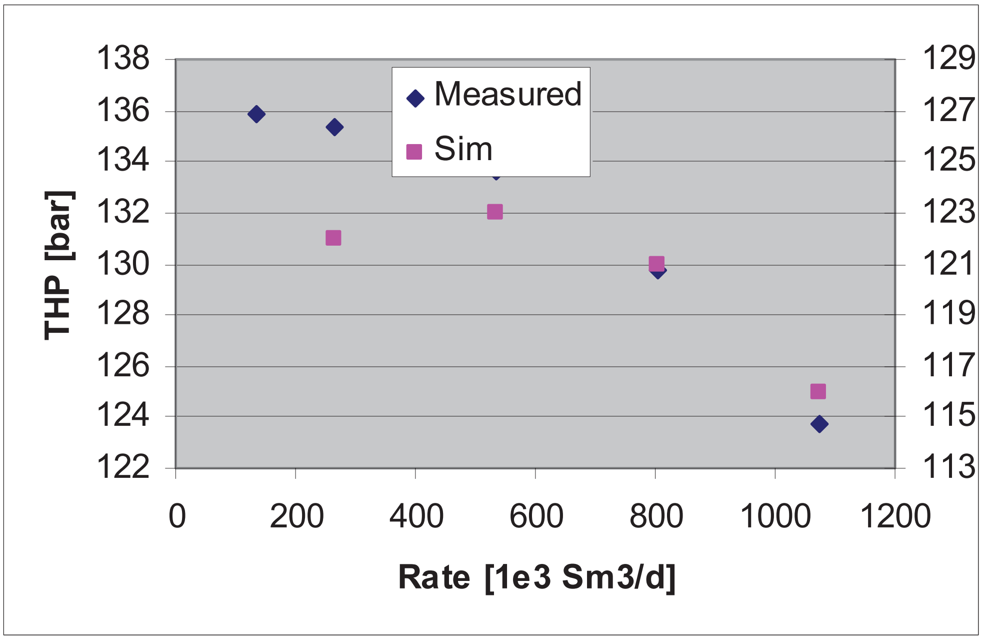

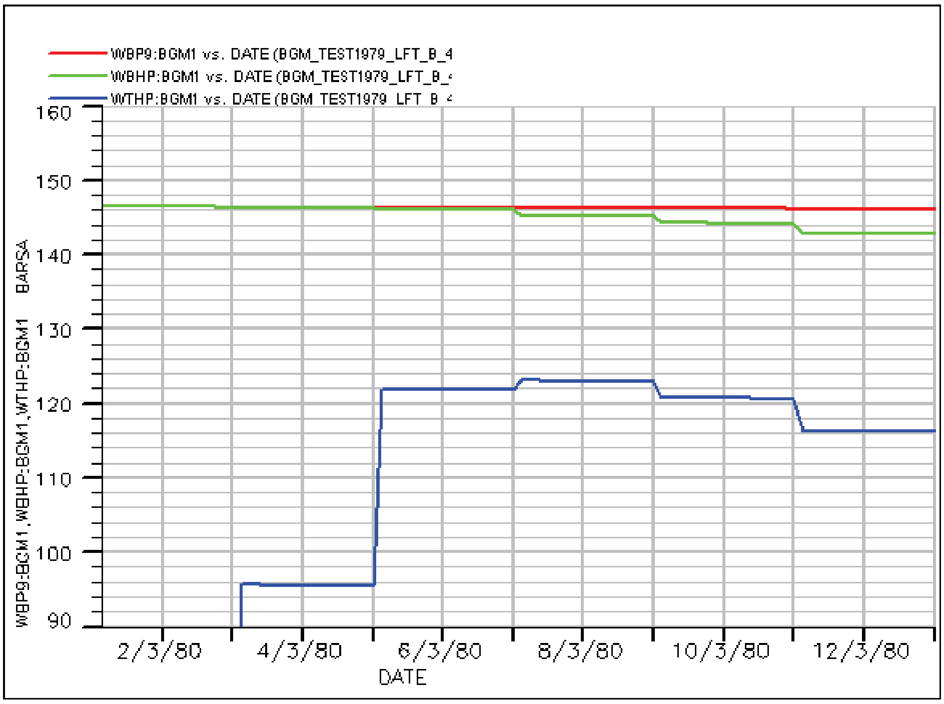

Table 6-7 THP match The top plot shows rate vs. pressure compared to measured, the bottom shows pressures vs. time over the “test” period. Note that the pressures in the top plot have different axis (left: measured; right: simulated) to compensate for the fact that the simulation is not done at precisely the right time. Above 6e5 sm3/d, the modelled pressure drop has an error of up to 3 bar. (The model underpredicts the drop.)

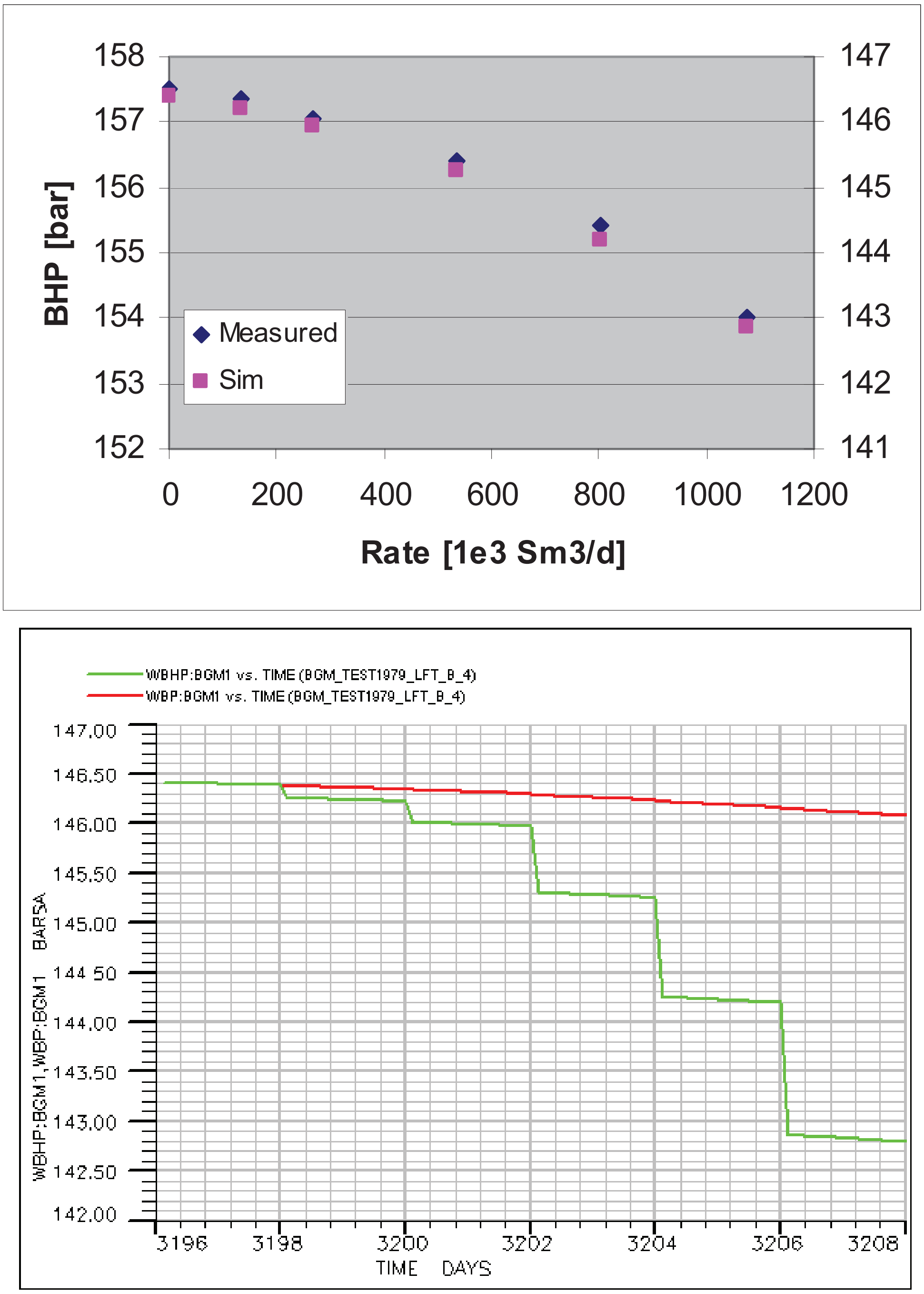

Table 6-8 BHP Match. The top plot shows rate vs. pressure compared to measured, the bottom shows pressures vs. time over the “test” period. The red curve is, for reference, a 9-block average pressure (closer to “static” pressure). Note that the pressures in the top plot have different axis (left: measured; right: simulated) to compensate for the fact that the simulation is not done at precisely the right time.

Table 6-9 **Adaptations needed to match the BGM1 inflow performance. Note the WPI multiplier has a non-extreme value.**

```
WDFAC
-- well well
-- name D-factor
'BGM*' 20e-6 /
/
-- The computed connection factor incorporates skin
-- set in Petrel RE, so we cannot specify skin values here.
-- Instead use a PI multiplier. Do note that this is applied
-- *after* the 'D' factor is computed.
WPIMULT
BGM1 1.2 /
/
```

6.1.6 Comments & Outlook

The computations in this section should rather be seen as a ‘proof of concept’, showing how the model can be adapted to match the well behaviour. Finalization of these parameters depends on a number of important parameters that have not been defined yet: PVT of the injected and produced gas (influences lift behaviour in particular), well design, completion design (e.g. sand control). Hence reasonably detailed UGS forecasts would necessarily be accompanied by further Prosper modelling. (In the light of this conclusion, it did not seem totally appropriate to further tune the model to address the remaining discrepancies in the outflow modelling, particularly in the low-rate range.)

6.2 Forecast Model Structure

A basic forecasting deck was set up in the form of an MS Excel spreadsheet. This spreadsheet can generate a series of restart decks, combining a series of HM runs with a given production injection scenario. The deck allows attachment of lift tables to injection and production, as well as the introduction of additional wells.

Water production rates are capped (at 150 sm3/d), as is injection BHP (250 bar) and production BHP (1 bar). These numbers can be easily adapted.

6.3 UGS behaviour & Spill Risk

A key target of the project was to assess the UGS behaviour (GWC in particular) and the risk of spilling gas to GRT. As can be gathered from the above, the contact behaviour can be explained from near-field water movements in response to the gas pressure distribution; contact with GRT is small. Hence it can be expected that the contact will recede, and that there will not be much spilling. To bracket this conclusion, several matches (including e.g. the not-so-good ‘open’ match discussed above) were taken forward into UGS.

A basic UGS profile was assumed, with repressurization using existing wells, then operation with 5 additional vertical wells. Injection/production periods were varied, as were rates and well locations. The rates (Table 6-10) are not meant to be realistically achievable with this number of wells (they are not), they are meant to examine the subsurface behaviour of the reservoir under large injection/production rates.

From the results of the sensitivities (as well as the discussions in the previous sections) we can make the following observations:

- The risk of spill to Groet is small, its main control is the transmissibility at the saddle (which is constrained by the Groet HM in particular; Figure 6-14). Significant spill should be detectable by means of pressure monitoring in GRT1 (Figure 6-15).
- Even with a weak aquifer (which, even though weak, is likely an overestimate, see section 5.3.9.4), the amount of hysteresis in the UGS phase is limited to less than 10 bars (Figure 6-10).
- Depending on the amounts injected in/produced from BGM7 in relation to the volume of this compartment, it will take time (years) to equilibrate this with the main compartment.
- The BGM7 compartment has (certainly given the uncertainty on its size) enhanced risk of water production.
- Well placement possibilities are constrained by the structure relief and permeability profile (Figure 5-11).

The contact movements are shown in Figure 6-12, Figure 6-13: the contact in the BGM-main near-well area is seen to go down in the injection phase, up in the production phase. In the north of the BGM-main block, the movements are the reverse. The largest movements occur in the BGM7 compartment. It should be noted that in that compartment there is less room to place the wells well above the GWC, but still in good permeability (Figure 5-50).

6.3.1 Comments & Outlook

A system has been set up that can run proposed well & UGS scenarios in combination with HM realizations efficiently. The runs carried out should be seen as a proof of concept, although some of the issues found are clearly of importance.

Once more specific/detailed UGS scenarios are defined, and appropriate (for well design, completion design and gas PVT) Prosper modelling is done, these can be combined with various HM realizations into

UGS forecast runs.

Table 6-10 Two sample UGS scenarios. The second, UGS2, was also applied to various HM realizations (Figure 6-14).

Name	# Extra wells in BGM-main/BGM7	Inj/Prod rate [1e6 sm3/d]	Inj/Prod period [months]	Input model
UGS1	5/0	2	6/6	'BGM_ALT2' BGM stand-alone Base, 'E' trending fault.
UGS2	5/0	6	2/2	'BGM_ALT2' BGM stand-alone Base, 'E' trending fault.
				'BGM_ALT2_AQF' BGM stand-alone Base, 'E' trending fault, weak aqf.

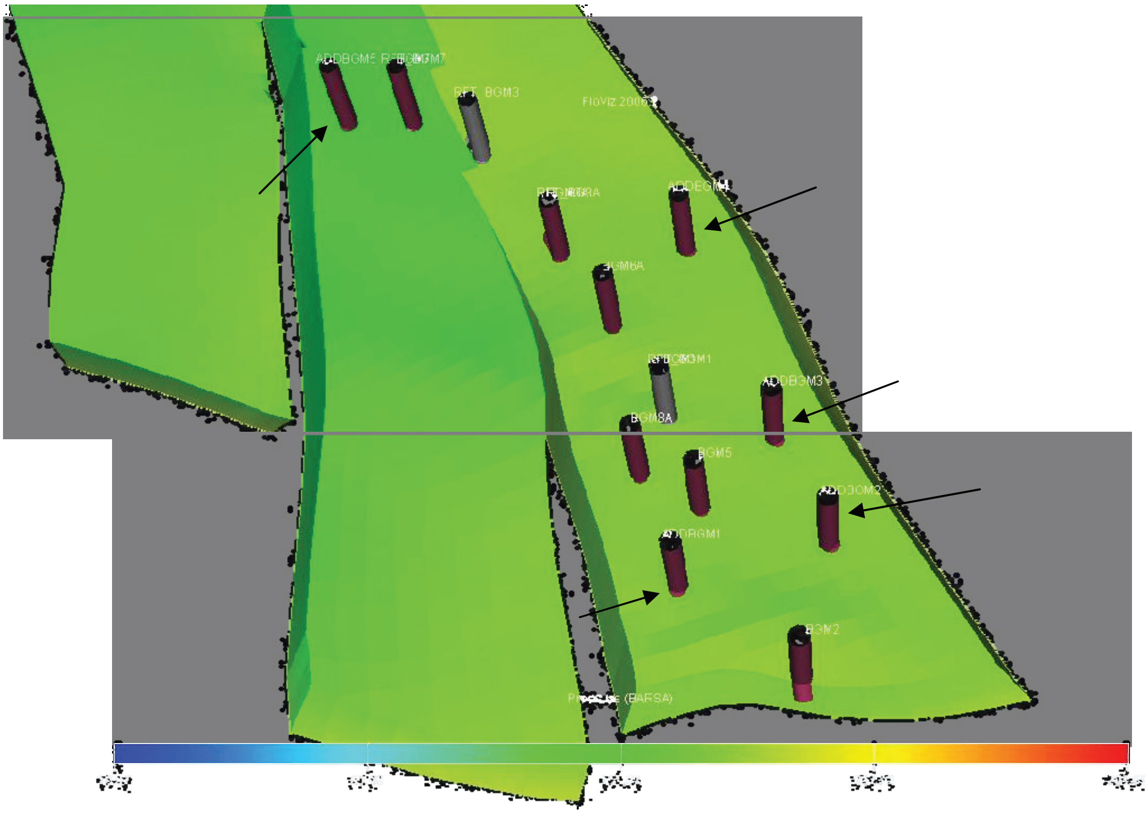

Figure 6-5 Location of the 5 notional extra UGS wells in proof-of-concept UGS runs. The well locations are not the result of detailed optimization considerations.

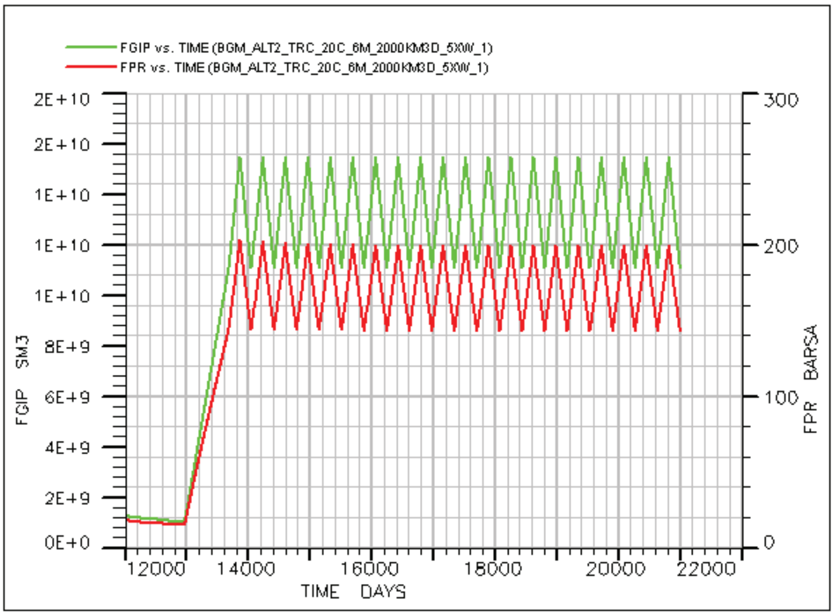

Figure 6-6 Field average pressure & GIP. The model is a base case stand-alone BGM model, with an E-trending fault (clearly visible in the right plot). Production/injection rates in this 'UGS1' run were 2e6 Sm3/day, for 6 months each.

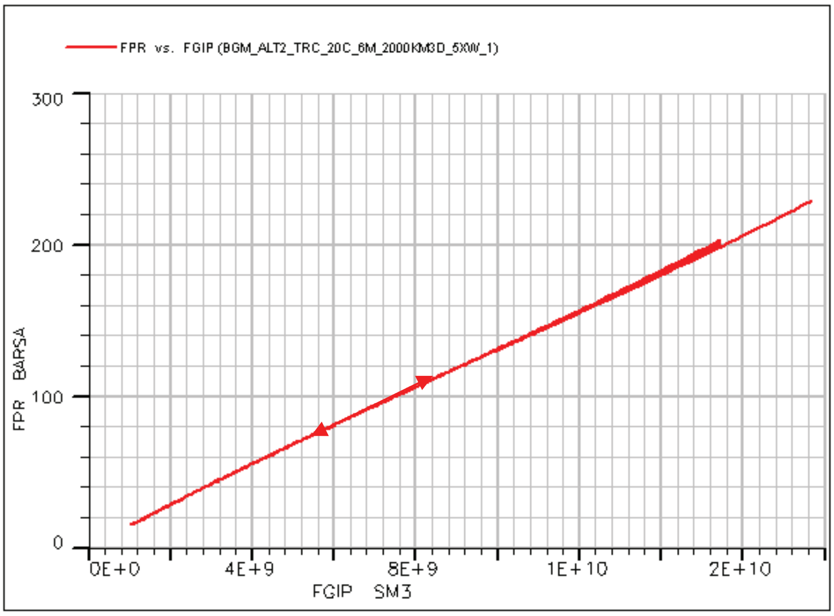

Figure 6-7 **Field** average pressure vs. GIP. The model is a base case stand-alone BGM model, with an E-trending fault. Production/injection rates in this 'UGS1' run were 2e6 Sm3/day, for 6 months each. Arrows indicate the direction of traversal: the GIP/pressure curves for production and UGS in essence coincide. Note that this is *not* the case for the pressures in either the BGM-main or BGM7 compartment taken separately (Figure 6-9).

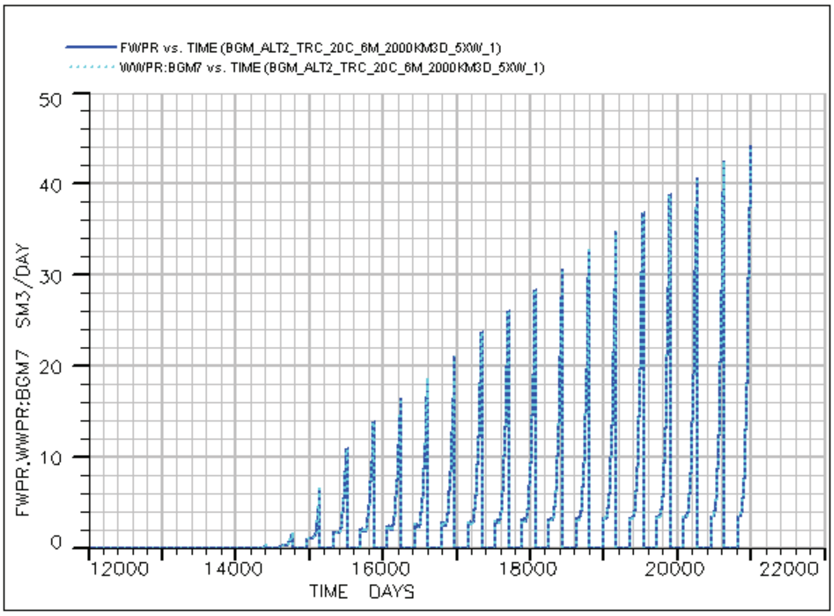

Figure 6-8 Field water production (from BGM7 alone). The model is a base case stand-alone BGM model, with an E-trending fault (clearly visible in the right plot). Production/injection rates in this 'UGS1' run were 2e6 Sm3/day, for 6 months each.

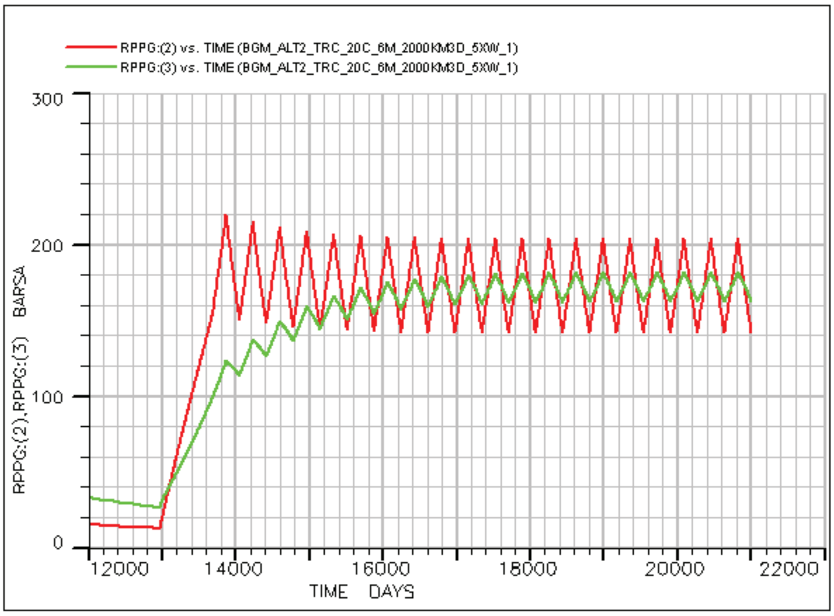

Figure 6-9 Pressure in BGM-main and BGM7 compartments. The model is a base case stand-alone BGM model, with an E-trending fault. Production/injection rates in this 'UGS1' run were 2e6 Sm3/day, for 6 months each. The BGM7 compartment had less injection compared to its volume (1 well only), so is underpressured at the end of the cushion gas injection. This takes about 10 cycles to equilibrate.

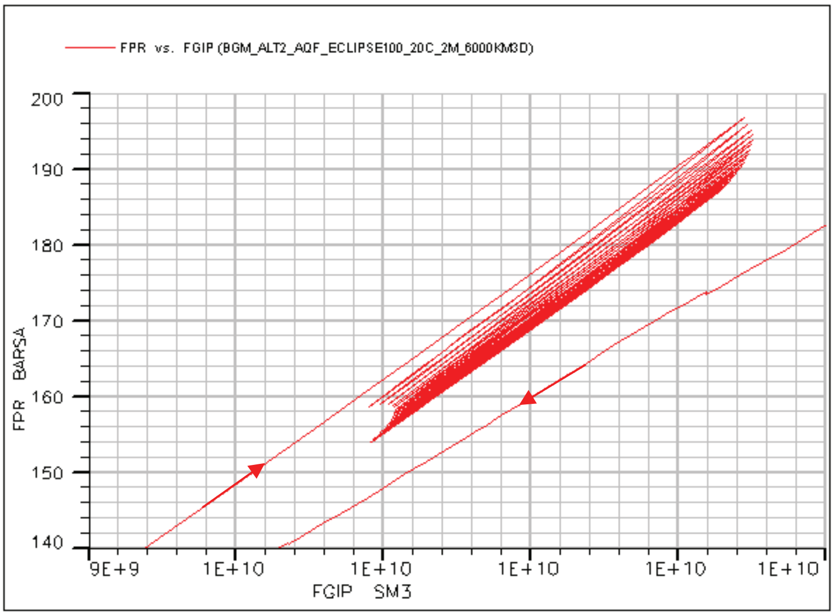

Figure 6-10 GIP vs. field average pressure in stand-alone BGM run with aquifer, rates at 6e6 sm3/d ('UGS2'). The scale is zoomed in w.r.t. Figure 6-7. Arrows indicate the direction of traversal: the lowest line indicates pressure/GIP behavior in the production phase. In the cushion gas injection the pressure follows a higher trend because of the aquifer water influx. As we go into the UGS cycles water gradually flows back into the aquifer as it is equilibrated to the new time-averaged field pressure.

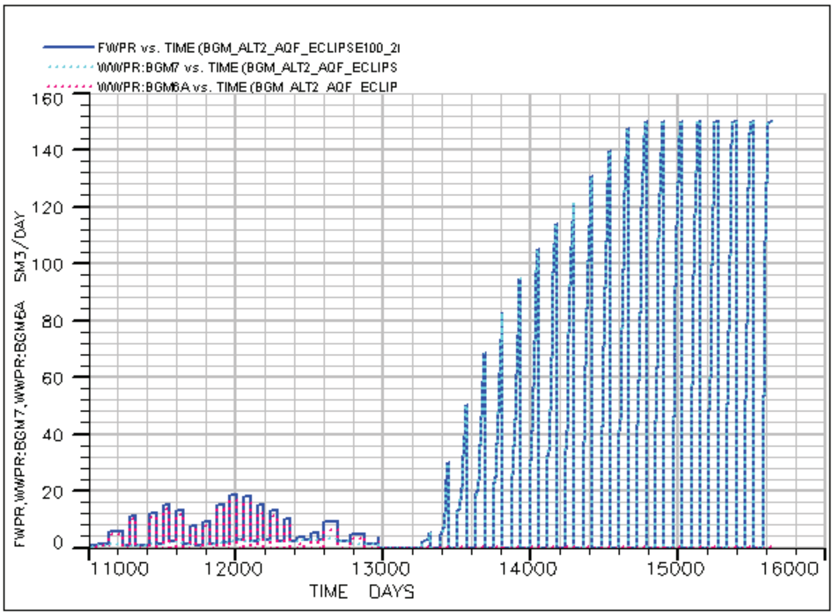

Figure 6-11 Water production in stand-alone BGM run with aquifer ('UGS2'). Initially BGM6A is water-prone, later again BGM7 is the culprit.

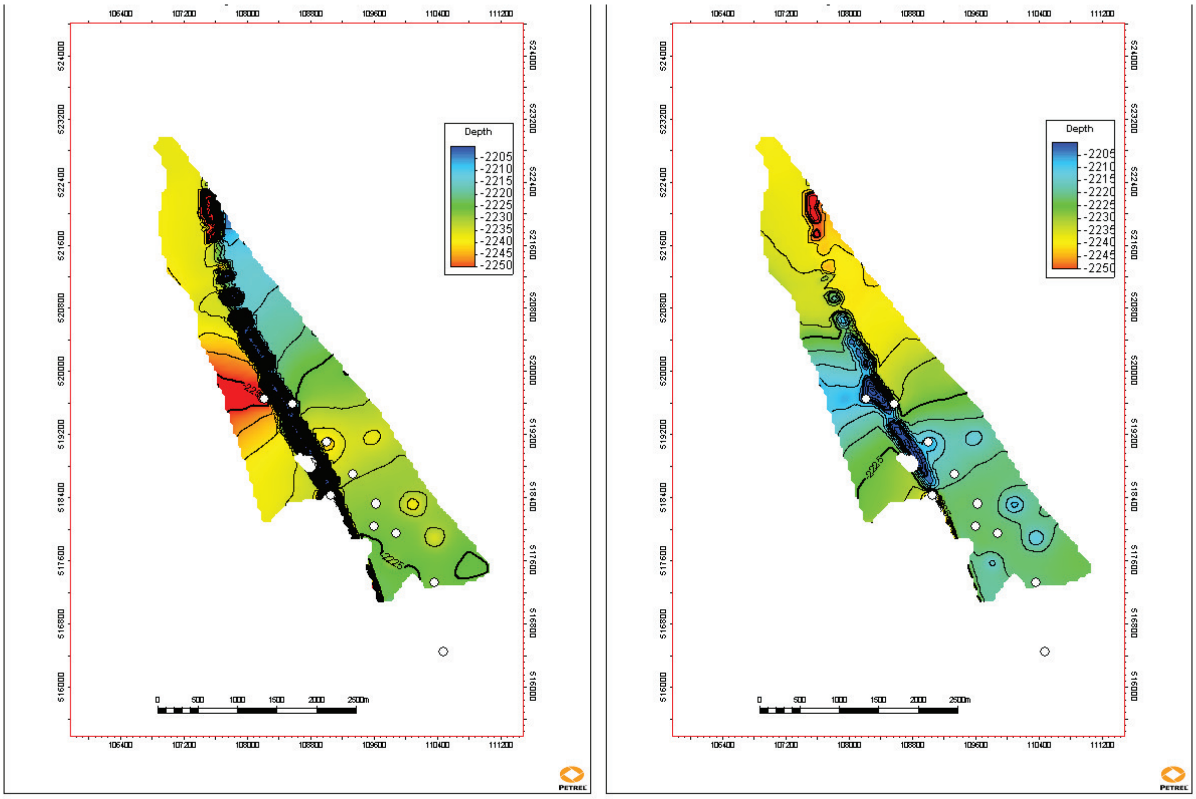

Figure 6-12 Contact map at the start and end of the last-but-one UGS cycle; left: after injection; right: after production. The color maps are the same, contours at 5m intervals.

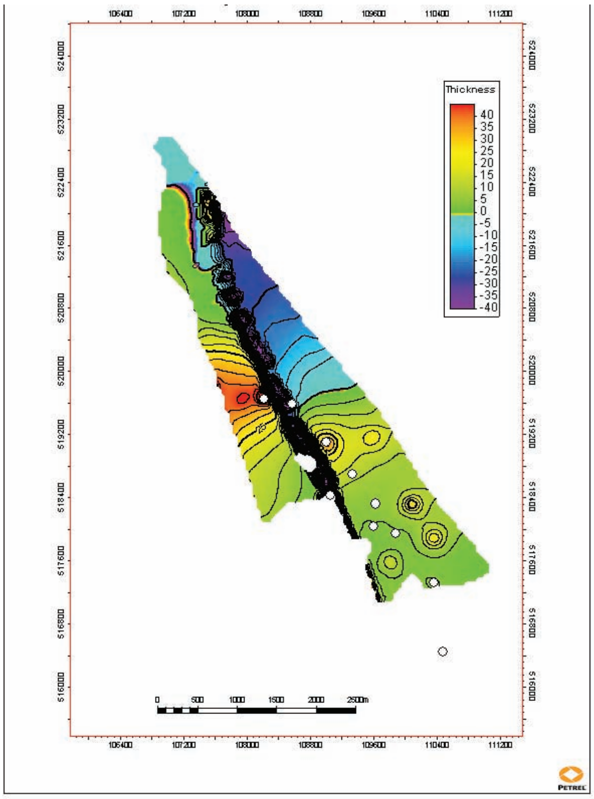

Figure 6-13 Difference between the contact maps of Figure 6-12 (at the start and end of the last-but-one UGS cycle). The color scale (red/green for positive; blue/purple for negative) emphasizes the fact that some areas move cyclically, some areas anti-cyclically.

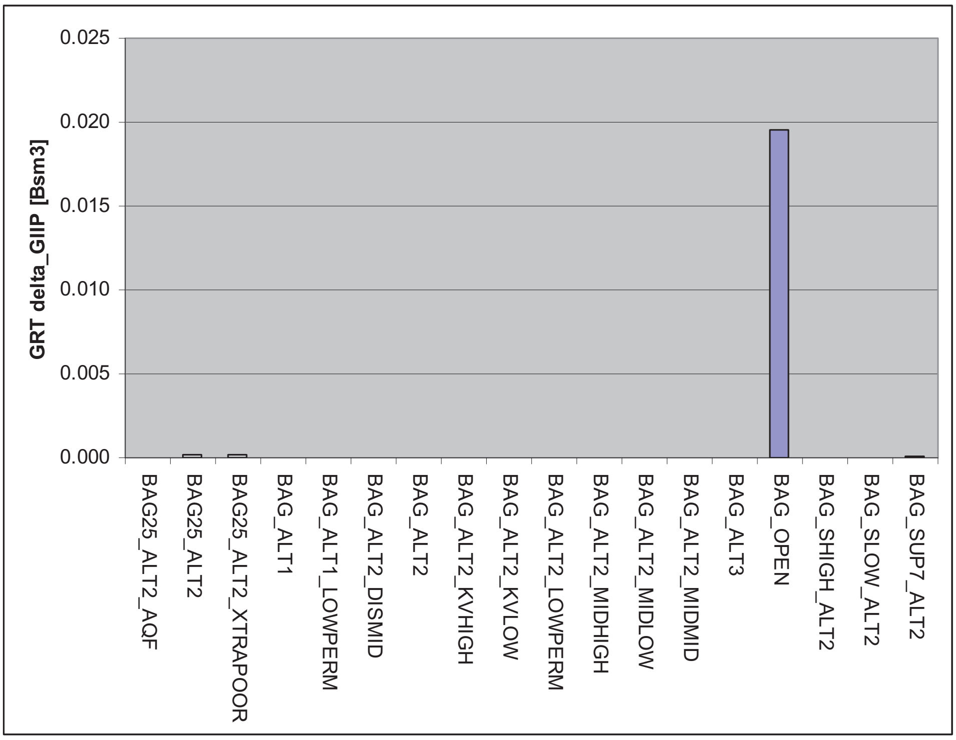

Figure 6-14 Amount of gas spilled over to GRT for various scenarios. Even on this small scale (25e6 sm3) the only significant scenario is the one with the (relatively) open fault at the spill point. This is (as discussed in section 5.3.9.3) a scenario that, given its pressure mismatch, overestimates the connectivity. The UGS scenario used was 'UGS2' (Table 6-10). See Table 7-3 (page 159)for a list & description of scenarios.

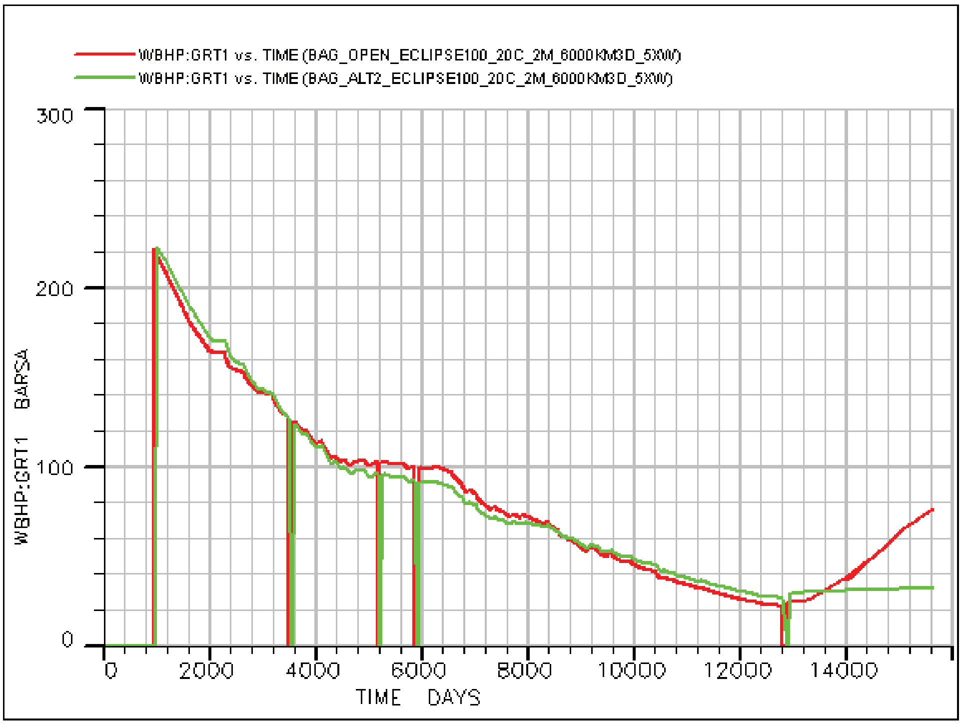

Figure 6-15. **GRT1 pressures in 'open' and 'base' models . Note that also in a situation where GRT is compartmentalized (see above) or it has a (small) aquifer, a degree of repressurization in GRT1 is to be expected.**

6.4 Tracer runs

Eclipse models can be quite easily equipped with passive tracers. These do not affect the PVT, but allow “tracking” of fluids. To test the concept, a BGM model was run into UGS forecast with a tracer injected in the first half of the cushion gas injection phase. The idea to test here is whether the first part of cushion gas is ever produced back (if not, this would allow the first part of the cushion gas to be of lesser quality). Results are shown in the plots below. The model conversion itself was easy (less than half an hour), so the concept should be readily adaptable for other purposes.

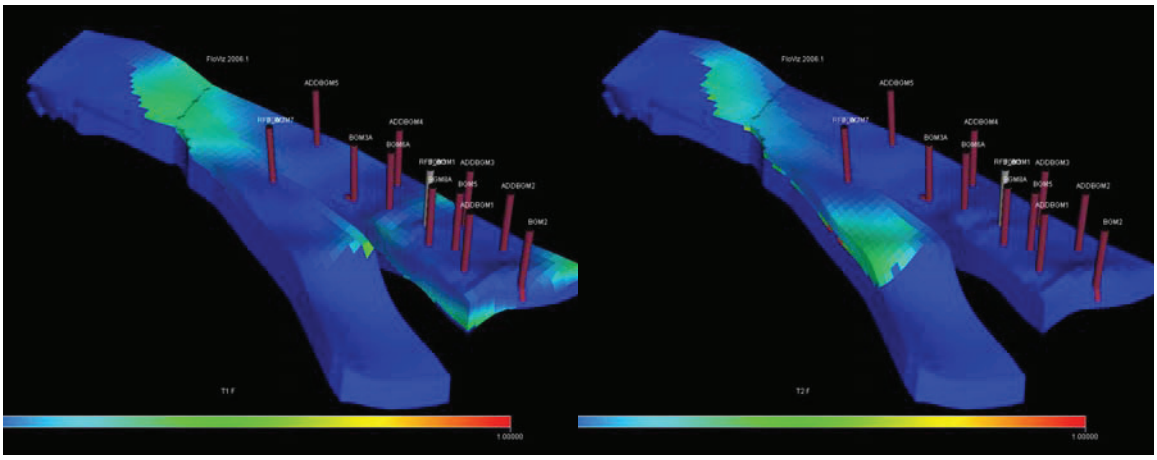

Figure 6-16 Tracer distribution at the end of 20 UGS cycles. The tracer was injected in the first half of the cushion gas period. The left plot shows the distribution of the tracer injected into the main compartment, the right shows the analog for the gas injected into the BGM7 compartment. The model is a base case stand-alone BGM model, with an E-trending fault (clearly visible in the right plot).

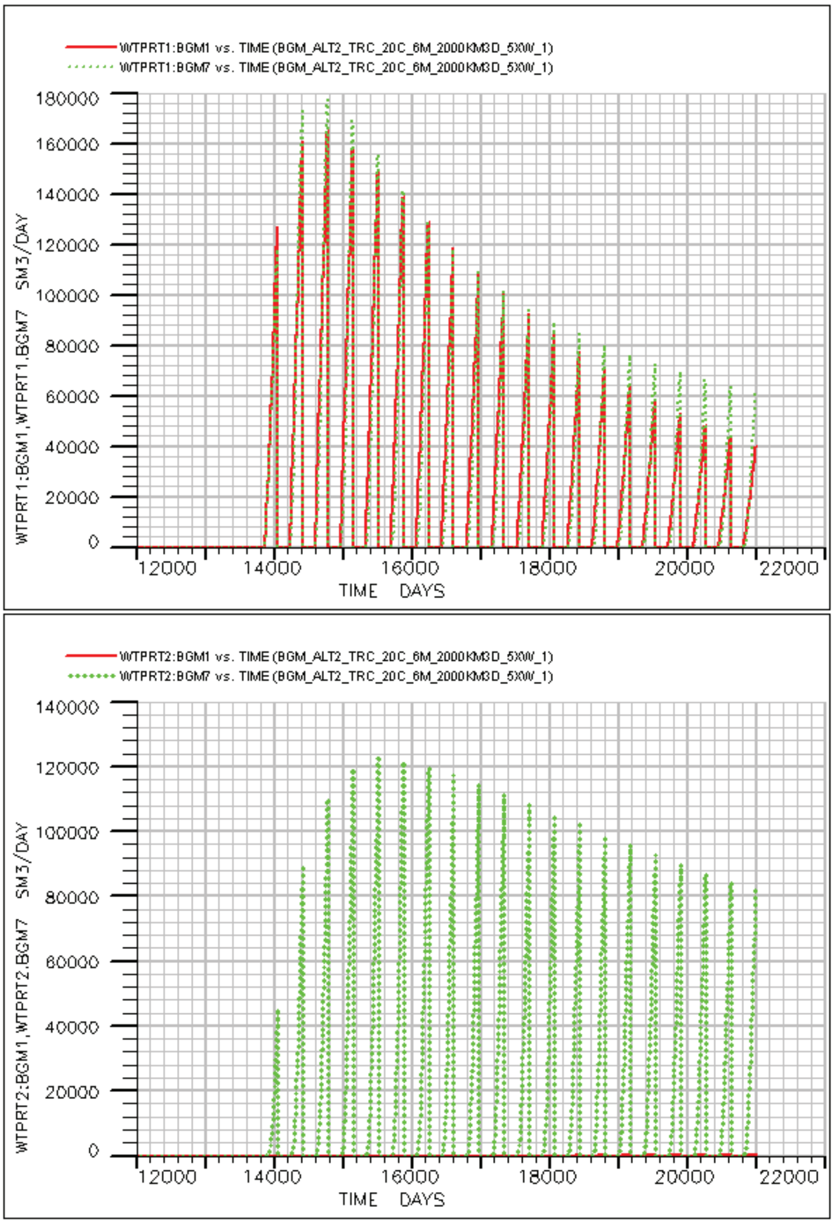

Figure 6-17 Tracer quantities produced in BGM1 (red) and BGM7 (green). The top plot shows the concentration of the tracer injected into the main compartment during the first half of cushion gas injection, the bottom shows that injected into the BGM7 compartment. Production/injection rates in this run were 2e6 Sm3/day, which makes the concentration scales of the two plots 9% and 7%, respectively. The tracer concentration can be interpreted as the concentration of early cushion gas in the UGS production cycles.

7 Conclusions & Recommendations

- A history matched model has been constructed, that can be used in UGS forecasting.
    - Various subsurface realizations have been created. These include structural variations, static property variations, as well as aquifer and other scenarios.
    - It can be combined readily with UGS scenarios, after appropriate equipment modelling.
    - It can be equipped with passive tracers to track injected gas.
- The two main uncertainties, in relation to the UGS operation, are (in order of importance) firstly the BGM7 GIIP and secondly the permeability.
    - The Bergen and Groet fields can be very well production/pressure history-matched assuming no aquifer and no connectivity to other fields.
    - The Bergermeer field can be well production/pressure history-matched assuming no aquifer and no connectivity to other fields.
    - A weak aquifer attached to the BGM7 compartment is possible. It can be tested by a GWC measurement in BGM7: with an aquifer this contact will go up almost as fast as BGM1, without an aquifer this will likely be less; the BGM7 contact may even have gone down.
    - Connectivity BGM→GRT must be assumed to be small, if present at all; increasing it to significant level will lead to a mismatch in GRT.
    - There is some discrepancy between the optimal Bergermeer compartment volumes from material balance computations, and those from more detailed reservoir structure analysis, even if alternate paths for the fault separating the two Bergermeer compartments are taken into account. The former points to a larger volume for the subsidiary compartment (BGM7) than the latter.
    - GWC rises like in Bergermeer and Groet can be explained without the presence of an aquifer by movements of the water within their respective blocks. Both in GRT and BGM the GWC is not flat, it is tilted.
    - The well tests, in combination with the contact rise match, fix the horizontal and vertical permeability to some extent: horizontal permeabilities (in wells that produce from the centre Rotliegend) are of the order 500 mD, with k_v/k_h between 0.1 and 1. Some uncertainty on the overall permeability level remains, since the well test analyses show some oddities, as well as on its areal & vertical distribution. This latter uncertainty affects well placement in the UGS phase.
    - Assuming a continuity of the heterogeneities seen in the well logs of several hundreds of metres, leads to a fairly low (<0.1) k_v/k_h ratio. The permeability then needed to explain the Bergermeer contact rise appears higher than that estimated from well tests. Lower permeabilities in combination with high k_v/k_h ratios can also give a reasonable match. This

implies that the heterogeneities are small-scale.

- Given these conclusions, the BGM field is expected behave in a fairly uncomplicated way in a UGS phase:
    - The GWC-rise will be reversed by injection;
    - Contacts, may show significant swings, leading to water production risks, which could affect well placement;
    - No large hysteresis is expected to take place in pressure/inventory behaviour.

References

[1] *Petrophysical Evaluation of the Bunter, Zechstein and Rotliegende Formations; Onshore Bergen Concession, Netherlands*; I Stockden, BP; October 2004

[2] *BERGERMEER NO.1 (BUNTER SANDSTONE AND ROTLIEGENDES) CORE ANALYSIS RESULTS*; 1969(?), Received from Taqa.

[3] *Log Interpretation Principles/Applications*, Schlumberger, 1989

[4] *Theory, Measurement, and Interpretation of Well Logs*, Z. Bassiouni, SPE, 1994

[5] *Chart Book*, Schlumberger, 1989

[6] *Rock Physics Handbook*, Mavko, Mukerji and Dvorkin, Cambridge University Press, 1998

[7] Geluk M. (2005) Permian and Triassic basins in the Netherlands: Stratigrapy, Tectonics and paleogeography. In Geluk M. (ed) Stratigraphy and Tectonics of Permo-Triassic Basins in the Netherlands and Surrounding Areas. Nederlandse Aardolie Maatschapppij (NAM) B.V. Ch.4: p. 61-72.

[8] Glennie K.W. (1998) Lower Permian – Rotliegend. In Glennie K.W. (ed) Introduction to the Petroleum Geology of the North sea. 4th edition, Blackwell Scient. Publ., Oxford, p. 137-173.

[9] Slatt R.M. (2006) Eolian (windblow) deposits & reservoir. In Slatt R.M. (ed) Stratigraphic Reservoir Characterization for Petroleum Geologists, Geophysicists and Engineers. Elsevier B.V. Ch 7: p. 249-274.

[10] Tobin R.C., Petrographic Evaluation of Rotliegendes Reservoir Sandstones, Amoco #1 Bergermeer, Onshore Netherlands

[11] “Operational Lithostratigraphy of the Netherlands”, version 1.1, NAM Assen Exploration

[12] “Fundamentals of gas reservoir engineering” by J. Hagoort, Elsevier, page 34.

[13] Hall, KR and Yarborough L, “A new equation of state for z-factor calculations”, Gas technology, SPE reprint series no 13, vol 1, 1977.

[14] Thodos

[15] Special Core Analysis Study; Bergermeer No. 1 and 2 Wells; Core Labs; 1971 [SCAL 70187]

[16] *GWC rise Bergermeer field*; Note, Taqa

[17] *Feasibility of peak shaving using concession gas reservoirs*; Hagoort & Associates BV, January 1994

[18] *Feasibility of gas storage in the Bergermeer reservoir*; Hagoort & Associates BV, May 1988

[19] Expro Operation report – Amoco Netherlands Petroleum Company, Bergermeer 1, BHP and BHT surveys during well test, 4th April – 7th April 1979.

Appendix II.A Contact extraction details

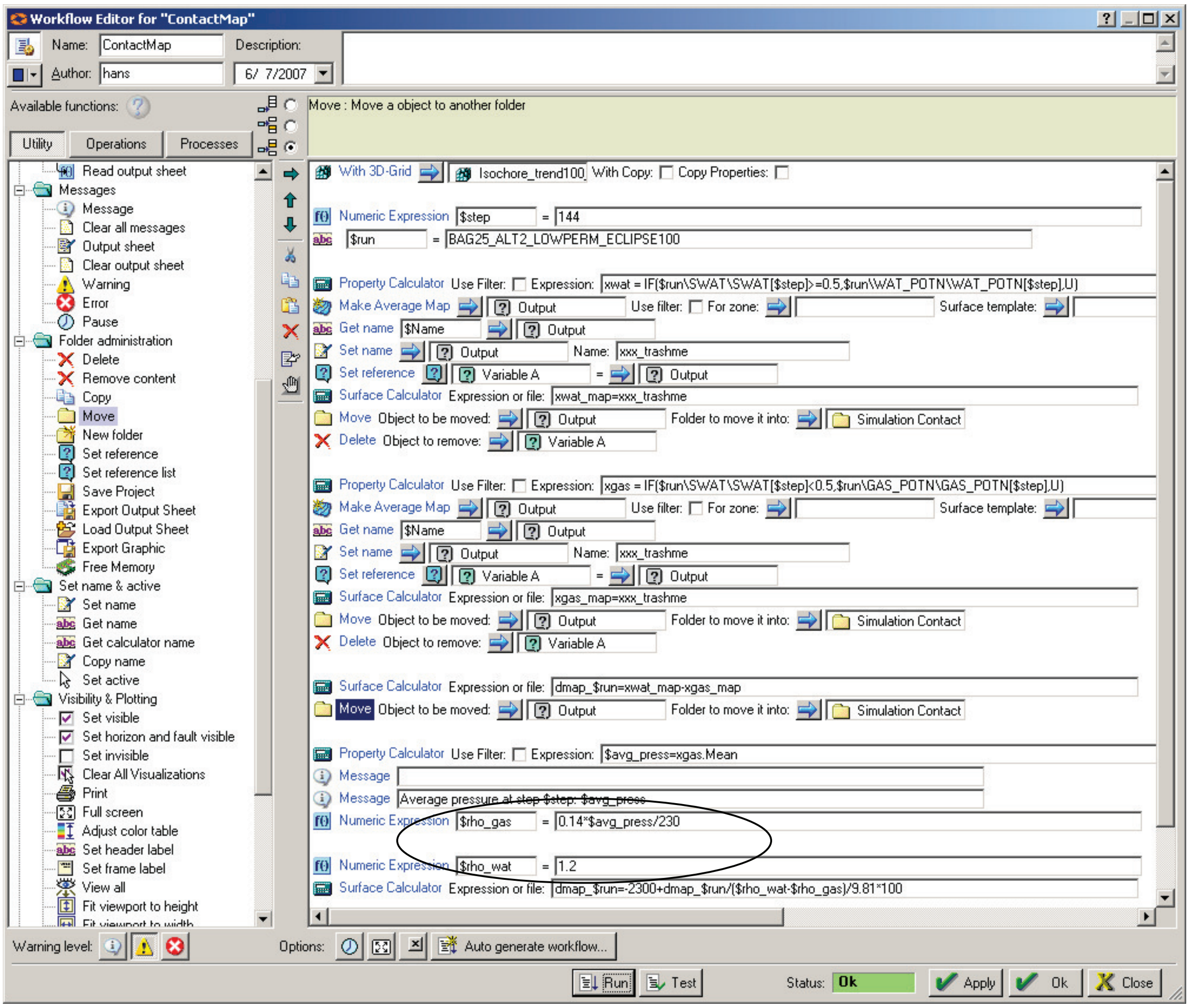

Name: ContactMap
Description:
Author: hans
6/ 7/2007

Move : Move a object to another folder

```
With 3D-Grid  Isochore_trend100  With Copy: ☐ Copy Properties: ☐

Numeric Expression  $step = 144
$run = BAG25_ALT2_LOWPERM_ECLIPSE100

Property Calculator  Use Filter: ☐ Expression: xwat = IF($run\SWAT\SWAT[$step]>=0.5,$run\WAT_POTN\WAT_POTN[$step],U)
Make Average Map  Output  Use filter: ☐ For zone:   Surface template:
Get name  $Name  Output
Set name  Output  Name: xxx_trashme
Set reference  Variable A = Output
Surface Calculator  Expression or file: xwat_map=xxx_trashme
Move  Object to be moved: Output  Folder to move it into: Simulation Contact
Delete  Object to remove: Variable A

Property Calculator  Use Filter: ☐ Expression: xgas = IF($run\SWAT\SWAT[$step]<0.5,$run\GAS_POTN\GAS_POTN[$step],U)
Make Average Map  Output  Use filter: ☐ For zone:   Surface template:
Get name  $Name  Output
Set name  Output  Name: xxx_trashme
Set reference  Variable A = Output
Surface Calculator  Expression or file: xgas_map=xxx_trashme
Move  Object to be moved: Output  Folder to move it into: Simulation Contact
Delete  Object to remove: Variable A

Surface Calculator  Expression or file: dmap_$run=xwat_map-xgas_map
Move  Object to be moved: Output  Folder to move it into: Simulation Contact

Property Calculator  Use Filter: ☐ Expression: $avg_press=xgas.Mean
Message
Message  Average pressure at step $step: $avg_press
Numeric Expression  $rho_gas = 0.14*$avg_press/230

Numeric Expression  $rho_wat = 1.2
Surface Calculator  Expression or file: dmap_$run=-2300+dmap_$run/($rho_wat-$rho_gas)/9.81*100
```

Status: Ok

Figure 7-1 Workflow for contact map extraction. Note the densities near the bottom: for gas we assume density proportional to pressure, for water a constant 1.2. The use of average potential maps implies that we neglect vertical non-gravity pressure gradients.

Table 7-1 **Listing of Linux shell script to convert the RFT's extracted from the simulation to contact values. Density assumptions (highlighted inb bold) are analogous to those in Figure 7-1.**

```
#!/bin/sh


uname=$1;

bname=`basename "$uname" .RFT`

dname=`dirname "$uname"`

cpath=`pwd`/"$dname"


# script cannot handle spaces in path. copy to /tmp, do the thing there

cp "$uname" /tmp

cd /tmp


echo "U

$bname

1

8

RFT

Y" | @convert


fname="$bname".FRFT


# then copy it back

cp $fname "$cpath"

rm -f "$bname".RFT

rm -f "$bname".FRFT

#echo "aaa " "$cpath"


# move to subdir (if any) where RFT file is

cd "$cpath"

cname="$bname"_rft.csv


echo
```

```
echo


# Write header to csv file

echo "Run: " $bname > "$cname"

echo "Date: "`date` >> "$cname"


# Then convert the FRFT to csv

cat "$fname" | awk '

BEGIN {

   header_done = 0;

   nwell = 0;

   delete w;

   swc = 0.2;

   g  = 9.81;

   tt = -1;

}


function sort(array, idx, n, tmp, i, j) {

   for (j=1; j<=n; j++) {

      idx[j] = j;

   }

   for (i=2;i<=n; i++) {

      for (j=i; 0+array[idx[j-1]]>0+array[idx[j]]; j--) {

         tmp = idx[j];

         idx[j] = idx[j-1];

         idx[j-1] = tmp;

      }

   }

}


function ProcessWell() {

   if (ww == "") { return }

   delete d;

   delete p;

   delete sw;

   delete sg;
```

```
delete f;

if (w[ww] == 0) {
   nwell++;
   w[ww] = nwell;
}
iwell = w[ww];

n = split(depth, d);
split(pressure, p);
split(swat, sw);
split(sgas, sg);

# Blocks may not be sorted (depends on how the
# well intersects the grid)
sort(d, depthorder, n);

# Simplistic assumptions on density
rg = 0.28*p[1]/229;
rw = 1.2;

# Loop in depth order
#for (j=1; j<=n; j++) {
#   print j ">"depthorder[j]"="0+d[depthorder[j]];
#}
for (j=1; j<=n; j++) {
   i = depthorder[j];
   if (sw[i]-swc > sg[i]) {
      f[i] = "water"
   } else {
      f[i] = "gas"
   }
}
if (f[2] == "gas") {
   rg = (p[1]-p[2])/(d[1]-d[2])/g*100;
##   print "***" rg;
```

```
   ##} else {

   ##   print "+++" rg;

   }


   lf="gas";

   ld=0+d[1];

   for (j=1; j<=n; j++) {

      i = depthorder[j];

      #print ww " " i " " 0+p[i] " " f[i];

      if (f[i] != lf) {

         dgwc[ww]=(d[i]+ld)/2;

         if (i>1) {

            dgwc[ww] = ((p[i]-p[i-1])*1e2 + (d[i-1]*rg-d[i]*rw)*g)/(rg*g-rw*g);

            #dgwc[ww] = ((p[i+1]-p[i-2])*1e2 + (d[i-2]*rg-d[i+1]*rw)*g)/(rg*g-rw*g);

         }

         #if (dgwc[ww] < 0+ld) { dgwc[ww] = 0+ld; }

         #if (dgwc[ww] > 0+d[i]) { dgwc[ww] = 0+d[i]; }

      }

      lf = f[i];

      ld = d[i];

   }

}


function PrintHeader() {

   txt = "TIME";

   for (i in w) {

      txt = txt ", " i;

   }

   print txt;

}


function ProcessVector() {

   ProcessWell();

   ClearWell();


   if (header_done == 0) {
```

```
      PrintHeader();
      header_done = 1;
   }

   txt = tt;
   for (i in w) {
      txt = txt ", " dgwc[i];
   }
   print txt;
}

function ClearWell() {
   depth="";
   pressure="";
   swat="";
   sgas="";
   ww="";
}

function ClearVector() {
   ClearWell();
   delete dgwc;
}

/^ *.TIME/ {
   # If we moved to a new time, dump the data gathered for
   # the previous time (if there is one)
   getline;
   if (tt < 0+$1) {
      if (tt >= 0)  { ProcessVector(); }
      ClearVector();
   }
   tt=0+$1;
   getline;
}
/^ *.DATE/ {
```

```
   getline;
   dd=0+$1;
   mm=0+$2;
   yy=0+$3;
   getline;
}
/^ *.WELLETC/ {
   ProcessWell();
   ClearWell();
   getline;
   # Hmmm...Need to get rid of single quote...
   #gsub("","`");
   ww=$4;
   getline;
}
/^ *.[A-Z]/ {
   vec=$1;
}
/^ *.[0-9,.]/ {
   if (match(vec,"DEPTH")) {
      depth=depth $0;
   } else if (match(vec,"PRESSURE")) {
      pressure=pressure $0;
   } else if (match(vec,"SWAT")) {
      swat=swat $0;
   } else if (match(vec,"SGAS")) {
      sgas=sgas $0;
   }
}



END {
   # End with some empty lines. This is convenient in Excel,
   # when overpasting, because it will delete data from
   # an earlier run with more steps.
   for (i=1; i<=40; i+=1) {
```

```
      print "";

   }

}' >> "$cname"


echo $cname " written. "

echo
```

Appendix II.B Well Test/Pressure Transient Analysis Details

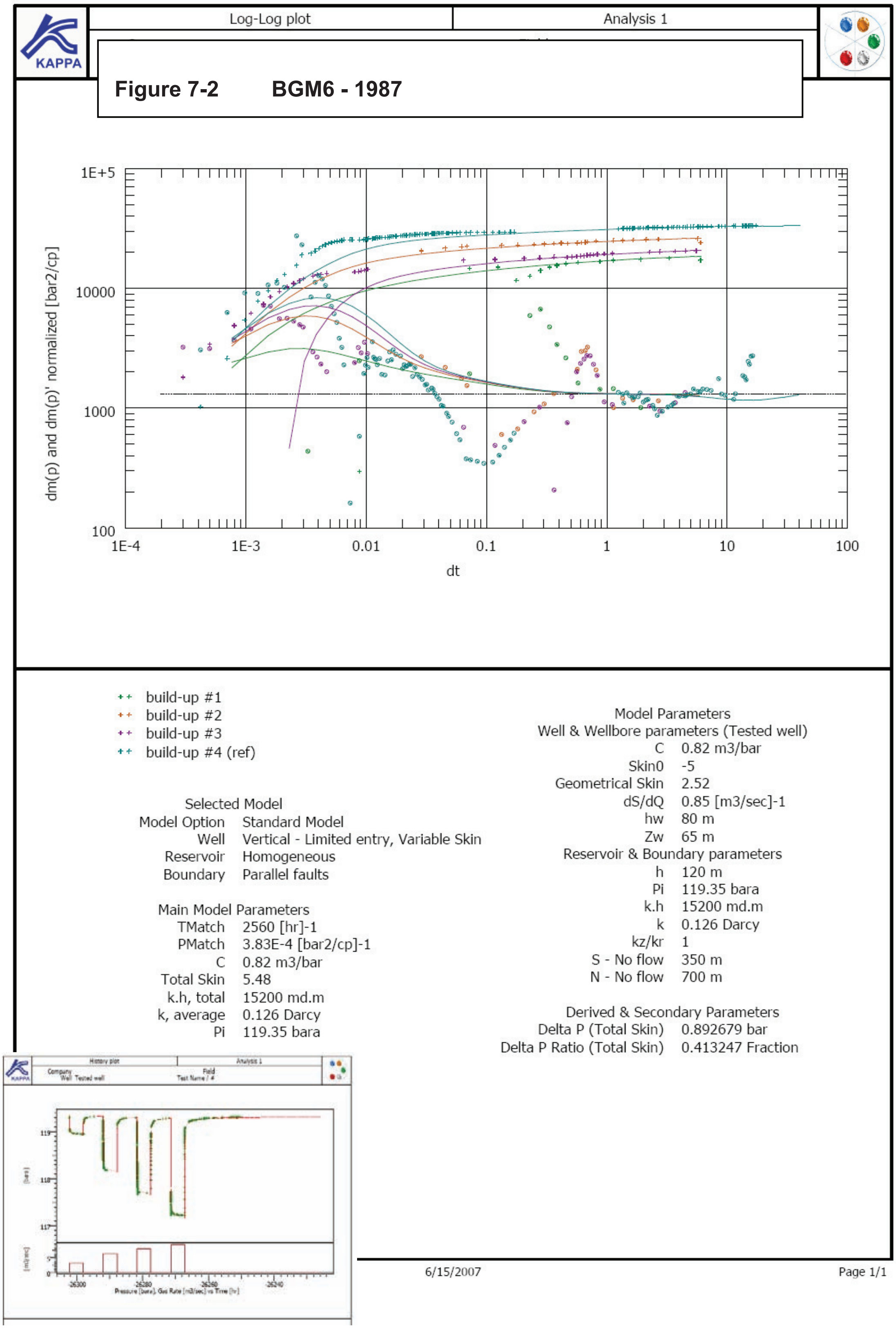

Figure 7-2 BGM6 - 1987

Selected Model

Model Option	Standard Model
Well	Vertical - Limited entry, Variable Skin
Reservoir	Homogeneous
Boundary	Parallel faults

Main Model Parameters

TMatch	2560 [hr]-1
PMatch	3.83E-4 [bar2/cp]-1
C	0.82 m3/bar
Total Skin	5.48
k.h, total	15200 md.m
k, average	0.126 Darcy
Pi	119.35 bara

Model Parameters

Well & Wellbore parameters (Tested well)

C	0.82 m3/bar
Skin0	-5
Geometrical Skin	2.52
dS/dQ	0.85 [m3/sec]-1
hw	80 m
Zw	65 m

Reservoir & Boundary parameters

h	120 m
Pi	119.35 bara
k.h	15200 md.m
k	0.126 Darcy
kz/kr	1
S - No flow	350 m
N - No flow	700 m

Derived & Secondary Parameters

Delta P (Total Skin)	0.892679 bar
Delta P Ratio (Total Skin)	0.413247 Fraction

6/15/2007

Page 1/1

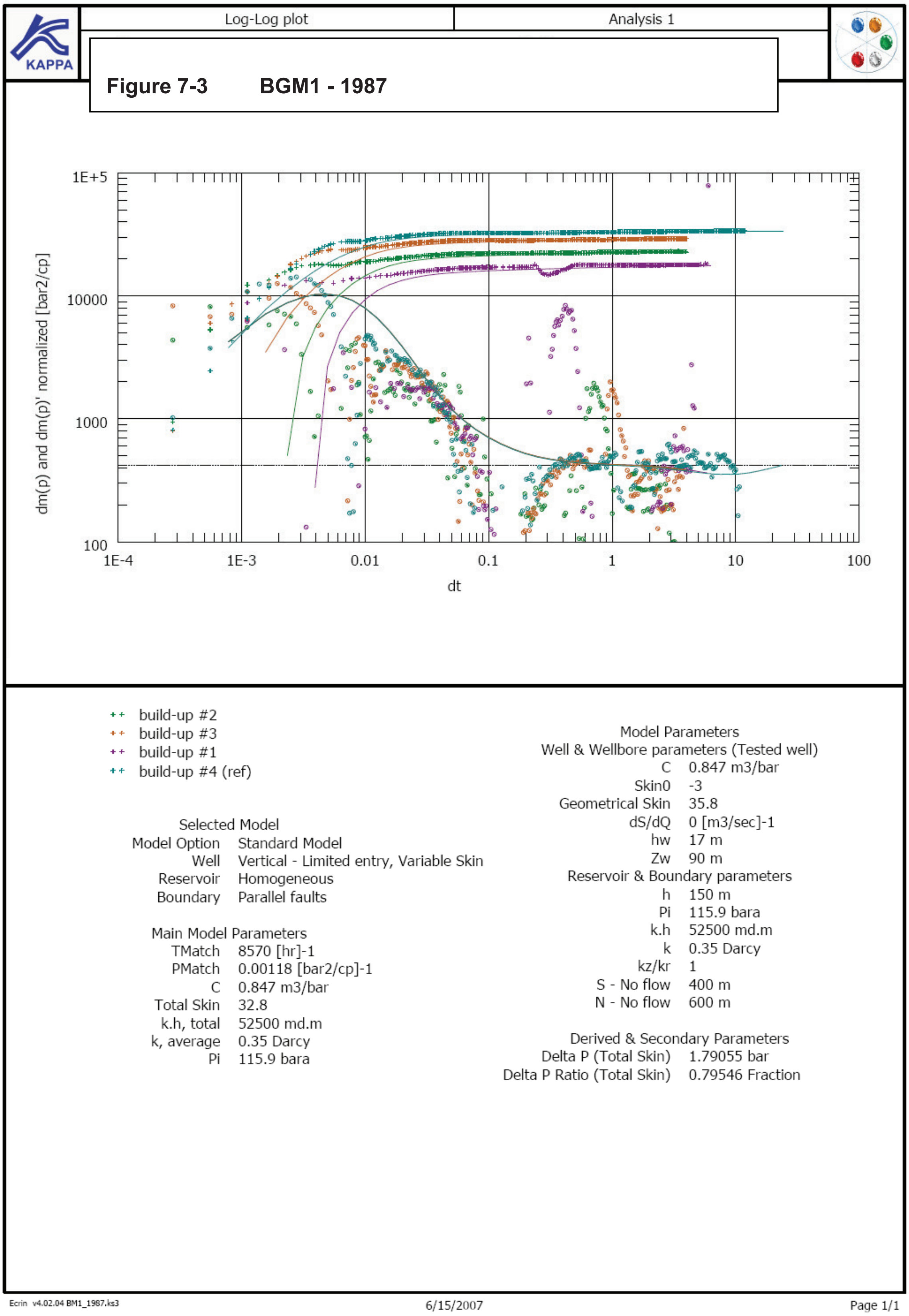

Figure 7-3 BGM1 - 1987

- ++ build-up #2
- ++ build-up #3
- ++ build-up #1
- ++ build-up #4 (ref)

Selected Model

Model Option	Standard Model
Well	Vertical - Limited entry, Variable Skin
Reservoir	Homogeneous
Boundary	Parallel faults

Main Model Parameters

TMatch	8570 [hr]-1
PMatch	0.00118 [bar2/cp]-1
C	0.847 m3/bar
Total Skin	32.8
k.h, total	52500 md.m
k, average	0.35 Darcy
Pi	115.9 bara

Model Parameters

Well & Wellbore parameters (Tested well)

C	0.847 m3/bar
Skin0	-3
Geometrical Skin	35.8
dS/dQ	0 [m3/sec]-1
hw	17 m
Zw	90 m

Reservoir & Boundary parameters

h	150 m
Pi	115.9 bara
k.h	52500 md.m
k	0.35 Darcy
kz/kr	1
S - No flow	400 m
N - No flow	600 m

Derived & Secondary Parameters

Delta P (Total Skin)	1.79055 bar
Delta P Ratio (Total Skin)	0.79546 Fraction

[bara]

[m3/sec]

Ecrin v4.02.04 BM1_1987.ks3 6/15/2007 Page 1/1

Log-Log plot	Analysis 18

Figure 7-4 BGM1 - 1986

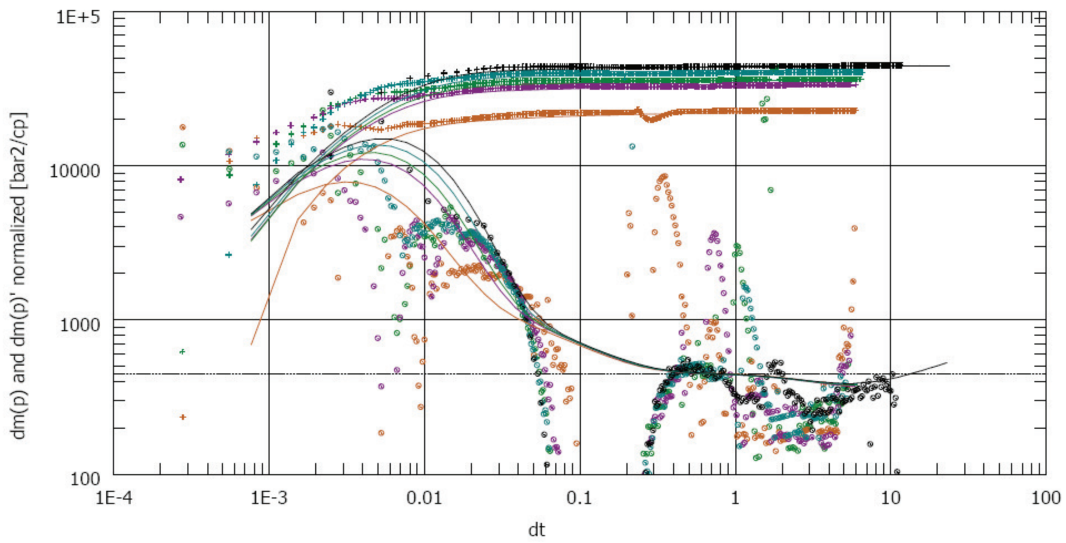

++ build-up #3
++ build-up #1
++ build-up #2
++ build-up #4
++ build-up #5 (ref)

Selected Model	
Model Option	Standard Model
Well	Vertical - Limited entry, Variable Skin
Reservoir	Homogeneous
Boundary	Parallel faults

Main Model Parameters	
TMatch	8950 [hr]-1
PMatch	0.00111 [bar2/cp]-1
C	0.773 m3/bar
Total Skin	43.1
k.h, total	50000 md.m
k, average	0.5 Darcy
Pi	119.35 bara

Model Parameters	
Well & Wellbore parameters (Tested well)	
C	0.773 m3/bar
Skin0	-8
Geometrical Skin	21.8
dS/dQ	2.75 [m3/sec]-1
hw	17 m
Zw	80 m
Reservoir & Boundary parameters	
h	100 m
Pi	119.35 bara
k.h	50000 md.m
k	0.5 Darcy
kz/kr	1
S - No flow	400 m
N - No flow	600 m

Derived & Secondary Parameters	
Delta P (Total Skin)	2.45461 bar
Delta P Ratio (Total Skin)	0.836253 Fraction

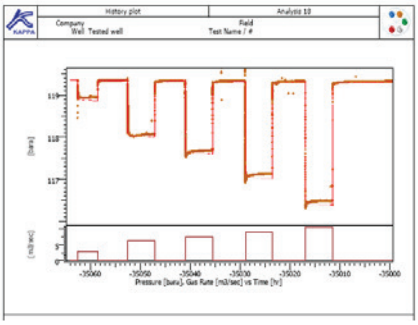
History plot | Analysis 10
Company
Well Tested well
Field
Test Name / #

6/15/2007 Page 1/1

Log-Log plot | Analysis 1

Figure 7-5 BGM1 - 1990

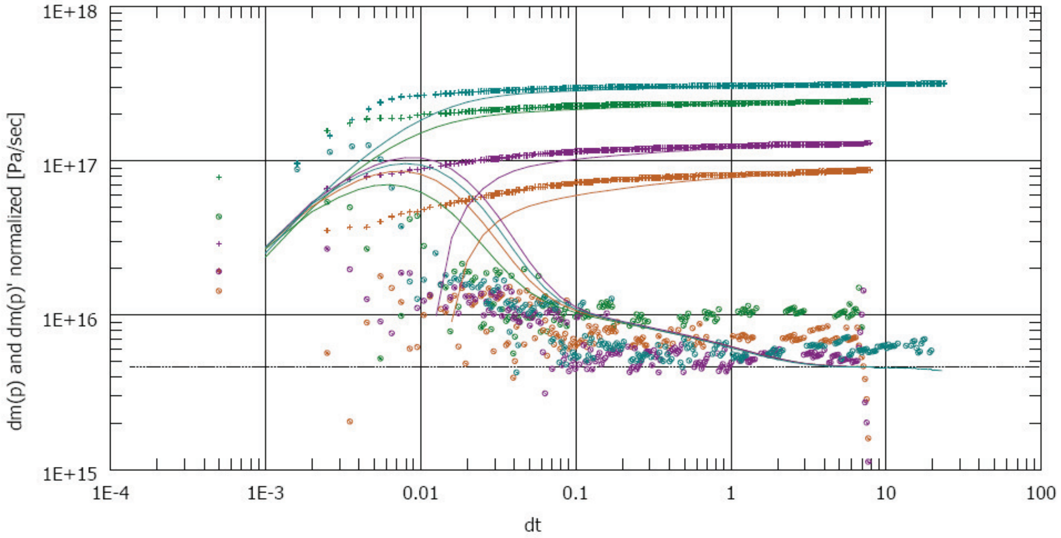

++ build-up #1
++ build-up #2
++ build-up #3
++ build-up #4 (ref)

Selected Model

Model Option	Standard Model
Well	Vertical - Limited entry, Variable Skin
Reservoir	Homogeneous
Boundary	Parallel faults

Main Model Parameters

TMatch	3730 [hr]-1
PMatch	1.08E-16 [Pa/sec]-1
C	1.74E-5 m3/Pa
Total Skin	26.8
k.h, total	4.34E-11 m3
k, average	2.96E-13 m2
Pi	93.5296 bara

Model Parameters

Well & Wellbore parameters (BGM1)

C	1.74E-5 m3/Pa
Skin0	0.5
Geometrical Skin	8.69
dS/dQ	1.75 [m3/sec]-1
hw	57 m
Zw	110 m

Reservoir & Boundary parameters

h	147 m
Pi	93.5296 bara
k.h	4.34E-11 m3
k	2.96E-13 m2
kz/kr	1
S - No flow	613 m
N - No flow	886 m

Derived & Secondary Parameters

Delta P (Total Skin)	1.8713 bar
Delta P Ratio (Total Skin)	0.768376 Fraction

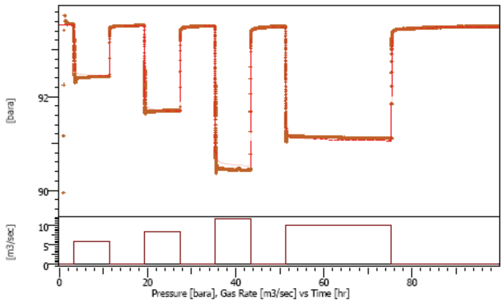

6/15/2007

Table 7-2 Selection of inflow performance well test data (BH pressure/rate).

Well	Date	Q	P
		sm3/d	bar
BGM1	1986	2.74E+05	118.97
		5.80E+05	118.07
		6.90E+05	117.72
		8.33E+05	117.17
		9.70E+05	116.52
		0.00E+00	119.38
BGM1	1987	2.42E+05	115.62
		4.98E+05	115.10
		7.26E+05	114.41
		9.12E+05	113.72
		0.00E+00	115.93
BGM1	1990	5.29E+05	92.40
		7.60E+05	91.70
		1.05E+06	90.45
		9.14E+05	91.10
		0.00E+00	93.60
BGM1	1976	2.64E+05	165.66
		5.18E+05	165.17
		7.80E+05	164.32
		0.00E+00	165.83
BGM1	Jun-97	1.88E+05	38.07
		2.43E+05	37.91
		3.45E+05	37.61
		3.45E+05	37.59
		0.00E+00	38.44

Well	Date	Q	P
BGM6	1987	2.73E+05	118.97
		5.63E+05	118.21
		6.92E+05	117.72
		8.13E+05	117.24
		0.00E+00	119.38
BGM2	1988	2.66E+05	112.83
Periods not long enough		4.25E+05	112.28
		6.44E+05	111.38
		7.42E+05	110.83
		0.00E+00	113.59
BGM3	1988	1.07E+05	105.52
		1.75E+05	94.83
		2.88E+05	75.86
		2.38E+05	87.24
		0.00E+00	114.48
BGM8	1999	1.90E+05	30.22
		2.60E+05	29.99
		3.48E+05	29.66
		4.55E+05	29.28
		4.55E+05	29.22
		0.00E+00	30.63

BGM1	May-96	8.91E+04	41.46
		1.34E+05	41.20
		2.05E+05	40.73
		3.03E+05	40.32
		3.03E+05	40.32
		0.00E+00	41.73
BGM1	Sep-73	2.75E+05	208.76
		5.49E+05	208.34
		8.36E+05	208.07
		1.11E+06	207.31
		0.00E+00	208.83
BGM1	April-1979	1.34E+05	157.34
		2.67E+05	157.06
		5.36E+05	156.40
		8.05E+05	155.40
		1.07E+06	154.01

Appendix II.C Data of main simulation runs

Table 7-3 List of main runs, with brief descriptions.

Run Name	Description
BAG25_ALT2_AFP	BGM+GRT, 25 layers; alternate MULTPV's to make BGM7 compartment big
BAG25_ALT2_AQF	BGM+GRT, 25 layers, aquifers to BGM as well as GRT
BAG25_ALT2_DISMIDHIGHKV_BEL	BGM+GRT, 25 layers; adhoc high-kv scenario based on 'discont_mid', with enforced 'bell' permeability profile
BAG25_ALT2_DISMIDHIGHKV	BGM+GRT, 25 layers; adhoc high-kv scenario based on 'discont_mid'
BAG25_ALT2	BGM+GRT, 25 layers
BAG25_ALT2_XTRAPOOR	BGM+GRT, 25 layers; exaggerated 'poor' streaks (they are given 10x lower perms and higher Swc)
BAG25_ALT4	BGM+GRT, 25 layers; extreme E extension of 'fault2'
BAG_ALT1	BGM+GRT, 10 layers; 'W extension of 'fault2'
BAG_ALT1_LOWPERM	BGM+GRT, 10 layers; 'W extension of 'fault2', low permeability
BAG_ALT2_DISMID	BGM+GRT, 10 layers; 'discont_mid' scenario
BAG_ALT2	BGM+GRT, 10 layers
BAG_ALT2_KVHIGH	BGM+GRT, 10 layers; 'discont_mid', higher kv
BAG_ALT2_KVLOW	BGM+GRT, 10 layers; 'discont_mid', lower kv
BAG_ALT2_LOWPERM	BGM+GRT, 10 layers; low permeability
BAG_ALT2_MIDHIGH	BGM+GRT, 10 layers; 'mid_high' scenario
BAG_ALT2_MIDLOW	BGM+GRT, 10 layers; 'mid_low' scenario
BAG_ALT2_MIDMID	BGM+GRT, 10 layers; 'mid_mid' scenario
BAG_ALT3	BGM+GRT, 10 layers, N (centre) extension of 'fault2'
BAGFINE_ALT2	BGM+GRT, 150 layers
BAG_OPEN	BGM+GRT, 10 layers; more open to GRT (i.e. higher fault multiplier of the fault at the spillpoint)
BAG_SHIGH_ALT2	BGM+GRT, 10 layers; high structural case
BAG_SLOW_ALT2	BGM+GRT, 10 layers; low structural case
BAG_SUP7_ALT2	BGM+GRT, 10 layers; high structure in the BGM7 block alone
BGM_ALT1_AQF	BGM, 10 layers, W extension of fault 2, aquifer

BGM_ALT1	BGM, 10 layers, W extension of fault 2
BGM_ALT2_AQF	BGM, 10 layers, aquifer
BGM_ALT2_CR2	BGM, 10 layers, high compressibility
BGM_ALT2	BGM, 10 layers
BGM_ALT2_RLP1	BGM, 10 layers, RLP variation: high Sgr
BGM_ALT2_RLP2	BGM, 10 layers, RLP variation: low(er) Corey coefficients
GRT	GRT, 10 layers
GRT25_3	GRT, 25 layers, faulted
BER	BER, 10 layers
BER25_4	BER, 10 layers, faulted

Table 7-4 Main parameters for the various simulation runs.

Short descriptions can be found in Table 7-3.

Run Name	Grid	PHIE (scenario)	NTG	MULTPV BGM-main	MULTPV BGM7	MULTX-BGM	MULTZ-BGM	MULTPV BER	MULTX-BER	MULTZ-BER	MULTPVGRT	MULTX-GRT	MULTZ-GRT
BAG25_ALT2_AFP	upscale25	continous_midR	0.995	0.92	3.00	2.00	1.00	1.05	1.00	0.50	0.95	0.25	0.13
BAG25_ALT2_AQF	upscale25	continous_midR	0.995	1.14	1.14	2.00	1.00	1.05	1.00	0.50	0.95	0.25	0.13
BAG25_ALT2_DISMIDHIGHKV_BEL	upscale25	discontinous_midR	0.995	1.19	1.19	0.25	0.25	1.05	0.25	0.25	0.83	0.13	0.13
BAG25_ALT2_DISMIDHIGHKV	upscale25	discontinous_midR	0.995	1.19	1.19	1.00	1.00	1.05	1.00	1.00	0.83	0.50	0.50
BAG25_ALT2	upscale25	continous_midR	0.995	1.14	1.14	2.00	1.00	1.05	1.00	0.50	0.95	0.25	0.13
BAG25_ALT2_XTRAPOOR	upscale25	continous_midR	0.995	1.14	1.14	2.00	1.00	1.05	1.00	0.50	0.95	0.25	0.13
BAG25_ALT4	upscale25	continous_midR	0.995	1.14	1.14	2.00	1.00	1.05	1.00	0.50	0.95	0.25	0.13
BAG_ALT1	upscale10	continous_midR	0.995	1.14	1.14	2.00	1.00	1.05	1.00	0.50	0.95	0.25	0.13
BAG_ALT1_LOWPERM	upscale10	continous_midR	0.995	1.14	1.14	0.50	0.50	1.05	0.50	0.50	0.95	0.50	0.50
BAG_ALT2_DISMID	upscale10	discontinous_midR	0.995	1.22	1.22	2.00	1.00	1.05	1.00	0.50	0.83	0.25	0.13
BAG_ALT2	upscale10	continous_midR	0.995	1.14	1.14	2.00	1.00	1.05	1.00	0.50	0.95	0.25	0.13
BAG_ALT2_KVHIGH	upscale10	continous_midR	0.995	1.14	1.14	1.00	1.00	1.05	1.00	1.00	0.95	1.00	1.00
BAG_ALT2_KVLOW	upscale10	continous_midR	0.995	1.14	1.14	2.00	0.05	1.05	2.00	0.05	0.95	2.00	0.05
BAG_ALT2_LOWPERM	upscale10	continous_midR	0.995	1.14	1.14	0.50	0.50	1.05	0.50	0.50	0.95	0.50	0.50
BAG_ALT2_MIDHIGH	upscale10	mid_highR	0.995	1.22	1.22	2.00	1.00	1.05	1.00	0.50	0.83	0.25	0.13
BAG_ALT2_MIDLOW	upscale10	mid_lowR	0.995	1.22	1.22	2.00	1.00	1.05	1.00	0.50	0.83	0.25	0.13

BAG_ALT2_MIDMID	upscale10	mid_midR	0.995	1.22	1.22	2.00	1.00	1.05	1.00	0.50	0.83	0.25	0.13
BAG_ALT3	upscale10	continous_midR	0.995	1.14	1.14	2.00	1.00	1.05	1.00	0.50	0.95	0.25	0.13
BAGFINE_ALT2			0.995	1.14	1.14	2.00	1.00	1.05	1.00	0.50	0.95	0.25	0.13
BAG_OPEN	upscale10	continous_midR	0.995	1.14	1.14	2.00	1.00	1.05	1.00	0.50	0.95	0.25	0.13
BAG_SHIGH_ALT2	HighCase 10L	continous_midR	0.995	0.91	0.91	2.00	1.00	1.05	1.00	0.50	0.92	0.25	0.13
BAG_SLOW_ALT2	LowCase 10L	continuous_midR	0.995	1.65	1.65	2.00	1.00	1.05	1.00	0.50	1.05	0.25	0.13
BAG_SUP7_ALT2	10L_up7	continous_midR	0.995	1.08	1.08	2.00	1.00	1.00	1.00	0.50	0.90	0.25	0.13
BGM_ALT1_AQF	upscale10	continous_midR	0.995	1.14	1.14	2.00	1.00	1.05	1.00	0.50	0.95	0.25	0.13
BGM_ALT1	upscale10	continous_midR	0.995	1.14	1.14	2.00	1.00	1.05	1.00	0.50	0.95	0.25	0.13
BGM_ALT2_AQF	upscale10	continous_midR	0.995	1.14	1.14	2.00	1.00	1.05	1.00	0.50	0.95	0.25	0.13
BGM_ALT2_CR2	upscale10	continous_midR	1.000	1.10	1.10	2.00	1.00	1.10	1.00	0.50	1.10	0.25	0.13
BGM_ALT2	upscale10	continous_midR	1.000	1.14	1.14	2.00	1.00	1.05	1.00	0.50	0.95	0.25	0.13
BGM_ALT2_RLP1	upscale10	continous_midR	1.000	1.14	1.14	2.00	1.00	1.05	1.00	0.50	0.95	0.25	0.13
BGM_ALT2_RLP2	upscale10	continous_midR	1.000	1.14	1.14	2.00	1.00	1.05	1.00	0.50	0.95	0.25	0.13
GRT	upscale10	continous_midR	0.995	1.14	1.14	2.00	1.00	1.05	1.00	0.50	0.95	0.25	0.13
GRT25_3	upscale25	continous_midR	0.995	1.14	1.14	2.00	1.00	1.05	1.00	0.50	0.95	0.25	0.13
BER	upscale10	continous_midR	0.995	1.14	1.14	2.00	1.00	1.05	1.00	0.50	0.95	0.25	0.13
BER25_4	upscale25	continous_midR	0.995	0.94	0.94	2.00	1.00	0.94	1.00	0.50	0.94	0.25	0.13

Table 7-5 **Volumetrics for the various simulation runs.**

Short descriptions can be found in Table 7-3.

Run Name	GIIP BGM-main	GIIP BGM7	GIIP BGM	GIIP GRT	GIIP BER	GIIP other (BER1)
BAG25_ALT2_AFP	11.59	6.72	18.31	7.27		
BAG25_ALT2_AQF	13.91	3.71	17.62	7.27		
BAG25_ALT2_DISMIDHIGHKV_BEL	13.61	4.00	17.61	7.30		
BAG25_ALT2_DISMIDHIGHKV	13.61	4.00	17.61	7.30		
BAG25_ALT2	13.91	3.71	17.62	7.27		
BAG25_ALT2_XTRAPOOR	13.82	3.68	17.50	7.22		
BAG25_ALT4	11.63	5.99	17.62	7.27		
BAG_ALT1	15.63	2.03	17.66	7.29		
BAG_ALT1_LOWPERM	15.63	2.03	17.66	7.29		

BAG_ALT2_DISMID	13.96	4.10	18.06	7.31		
BAG_ALT2	14.97	2.69	17.66	7.29		
BAG_ALT2_KVHIGH	13.91	3.75	17.66	7.29		
BAG_ALT2_KVLOW	13.91	3.75	17.66	7.29		
BAG_ALT2_LOWPERM	14.97	2.69	17.66	7.29		
BAG_ALT2_MIDHIGH	14.25	4.00	18.25	7.14		
BAG_ALT2_MIDLOW	14.25	4.00	18.25	7.14		
BAG_ALT2_MIDMID	14.23	3.94	18.17	6.68		
BAG_ALT3	14.97	2.69	17.66	7.29		
BAGFINE_ALT2	13.94	3.70	17.64	7.24		
BAG_OPEN	15.63	2.03	17.66	7.29		
BAG_SHIGH_ALT2	15.51	3.08	18.58	7.45		
BAG_SLOW_ALT2	15.05	2.51	17.56	7.27		
BAG_SUP7_ALT2	13.22	4.56	17.78	6.91		
BGM_ALT1_AQF	15.63	2.03	17.66	0.00		
BGM_ALT1	15.63	2.03	17.66	0.00		
BGM_ALT2_AQF	13.91	3.75	17.66	0.00		
BGM_ALT2_CR2	13.51	3.64	17.15	0.00		
BGM_ALT2	13.98	3.77	17.75	0.00		
BGM_ALT2_RLP1	13.98	3.77	17.75	0.00		
BGM_ALT2_RLP2	13.98	3.77	17.75	0.00		
GRT				7.29		
GRT25_3				7.64		
BER				0.00	7.87	
BER25_4				0.00	7.04	0.96

s for the various simulation runs. Reference values are in Table 7-7. Values shown are simulated –
egative value in a GWC column means that the simulation has a too-shallow contact. The ‘Error
weighted sum of the absolute values of the errors, above a certain threshold.
t certain runs were intended to investigate the effect of a particular parameter (e.g.
or to provide ‘worst-case’ scenarios for the forecast (e.g. ‘BAG25_ALT2_AQF’), so that there less
ended.
n be found in Table 7-3.

	p_bgm7_1981	p_bgm1_1989	p_bgm7_1988	p_bgm1_2001	p_bgm7_1997	p_grt1_1976	p_grt1_1990	p_grt1_2005	p_ber4_1990	p_ber4_2005	gwc_bgm1_1981	gwc_bgm1_2005	gwc_bgm7_1981	gwc_bgm7_1989	gwc_grt6_1999	gwpt_bgm	gwpt_grt	ggpt_bgm	ggpt_grt;
	[bar]	[bar]	[bar]	[bar]	[bar]	[bar]	[bar]	[bar]	[bar]	[bar]	[m]	[m]	[m]	[m]	[m]	[m3]	[m3]	[sm3]	[sm3]
2.3	0.9	3.0	-1.7	2.2	-3.2	-0.6	-5.5	2.1	0.0	0.0	-6.8	-21.0	0.3	8.3	18.0	1.1E+05	2.4E+04	-1.7E+07	-3.8E+07
0.8	9.7	4.0	1.8	3.6	5.5	0.0	3.8	8.6	0.0	0.0	-2.2	3.0	-4.2	1.1	-10.4	-1.0E+03	2.2E+05	-1.7E+07	-5.8E+07
-4.8	19.8	-2.7	6.8	-7.5	16.8	0.2	-4.5	4.5	0.0	0.0	-2.4	-18.3	-4.3	6.9	31.7	5.7E+04	1.4E+04	-2.8E+07	-2.5E+07
-0.3	5.5	0.9	-2.8	1.1	0.5	0.4	-4.1	4.1	0.0	0.0	-1.0	6.4	-4.4	3.0	38.1	-1.0E+03	5.9E+03	-1.7E+07	-6.5E+05
0.3	6.0	0.7	-2.8	0.5	1.7	-0.4	-5.2	2.4	0.0	0.0	-1.8	3.5	-1.3	7.1	17.4	-1.0E+03	2.7E+04	-1.7E+07	-3.9E+07
0.0	5.5	-0.1	-3.6	-1.2	0.5	-0.6	-6.3	0.7	0.0	0.0	-2.0	2.5	-1.3	7.1	13.4	-1.0E+03	2.9E+04	-1.7E+07	-4.3E+07
-2.1	2.5	-0.2	-3.1	-3.0	-2.4	-0.5	-5.4	2.2	0.0	0.0	-4.8	-9.9	-1.3	7.5	17.7	-9.9E+02	2.5E+04	-1.7E+07	-3.8E+07
2.7	15.4	1.5	-0.4	2.4	7.1	-0.8	-6.3	0.7	0.0	0.0	-5.1	-1.5	3.7	12.5	5.9	-1.0E+03	7.1E+04	-1.7E+07	-4.0E+07

1.8	16.2	1.2	0.4	0.2	8.9	0.2	-5.0	3.0	0.0	0.0	-7.1	-14.9	4.3	13.8	21.9	1.9E+05	3.2E+04	-1.7E+07	-1.6E+07
2.1	7.8	4.3	-0.3	7.4	4.7	2.1	-2.6	4.7	0.0	0.0	-3.1	6.7	-6.2	3.0	23.1	-1.0E+03	1.6E+04	-3.0E+07	-3.1E+07
1.0	7.8	1.5	-1.9	0.8	3.9	1.5	-3.7	1.7	0.0	0.0	-4.5	-1.8	-2.1	7.2	11.2	-1.0E+03	8.6E+04	-3.0E+07	-5.6E+07
3.2	2.4	2.2	-3.9	2.6	-2.5	2.5	-1.9	4.3	0.0	0.0	-5.6	-5.6	-1.8	7.6	28.0	6.6E+03	1.4E+04	-3.0E+07	-1.4E+07
3.5	1.8	1.7	-4.7	2.5	-3.0	2.4	-0.6	4.5	0.0	0.0	-5.8	-6.3	-1.4	7.9	28.0	4.0E+03	2.1E+03	-3.0E+07	-4.7E+06
0.0	9.6	1.3	-0.5	-1.3	7.0	2.3	-2.9	3.8	0.0	0.0	-6.6	-15.3	-0.9	7.9	20.4	1.1E+05	3.9E+04	-3.0E+07	-3.0E+07
2.4	9.6	5.1	1.2	8.7	8.0	0.5	-7.0	-1.7	0.0	0.0	-4.2	3.1	-4.2	5.4	7.2	-1.0E+03	5.2E+04	-3.0E+07	-6.1E+07
2.1	10.5	5.0	1.4	8.7	8.6	1.2	-5.9	-0.8	0.0	0.0	-3.2	5.5	-4.6	4.8	20.3	-1.0E+03	2.2E+04	-3.0E+07	-4.1E+07
2.3	9.1	4.6	0.2	8.0	6.0	-1.4	-16.6	-19.7	0.0	0.0	-3.4	4.6	-4.0	5.6	13.8	-1.0E+03	6.5E+04	-3.0E+07	-7.9E+07
3.4	6.3	2.8	-3.2	3.8	0.6	2.8	1.7	11.2	0.0	0.0	-4.7	-0.2	-0.9	7.6	15.3	-1.0E+03	4.0E+04	-3.0E+07	-2.7E+07
-0.1	7.2	0.7	-2.2	0.4	2.9	-0.6	-6.0	1.0	0.0	0.0	-0.3	5.5	-1.6	7.0	19.1	-1.0E+03	1.9E+04	-1.7E+07	-3.5E+07
6.4	16.3	-2.8	-3.3	3.5	5.8	-8.7	1.4	-2.8	0.0	0.0	-4.6	-7.7	3.7	13.5	22.4	1.3E+04	1.2E+05	-1.7E+07	-4.9E+07
3.8	7.4	7.0	1.5	13.2	6.7	1.6	-0.7	8.1	0.0	0.0	-3.5	5.3	-3.9	5.4	17.3	-1.0E+03	5.3E+04	-3.0E+07	-5.2E+07
2.2	12.2	0.8	-0.2	-2.3	7.5	2.0	-2.0	3.6	0.0	0.0	-7.1	-19.9	3.6	13.6	25.0	2.3E+05	5.3E+04	-3.0E+07	-5.4E+07
-0.8	9.2	1.1	-0.4	-0.4	6.4	-0.4	-11.3	-12.0	0.0	0.0	-2.6	-1.2	0.7	9.4	3.5	-1.0E+03	5.5E+04	-3.0E+07	-7.2E+07
7.6	13.9	9.1	4.4	5.4	10.2				0.0	0.0	-8.0	-28.7	6.8	0.0	0.0	0.0E+00	0.0E+00	0.0E+00	0.0E+00
2.6	15.1	1.4	-1.2	2.5	7.2				0.0	0.0	-4.5	1.3	3.9	0.0	0.0	0.0E+00	0.0E+00	0.0E+00	0.0E+00
3.8	10.5	8.4	4.7	6.4	7.9				0.0	0.0	-5.4	-6.1	-8.2	0.0	0.0	0.0E+00	0.0E+00	0.0E+00	0.0E+00
2.6	12.3	4.5	2.3	-2.9	4.1				0.0	0.0	-6.7	-14.1	-6.4	0.0	0.0	0.0E+00	0.0E+00	0.0E+00	0.0E+00
0.9	7.2	1.5	-1.8	1.7	4.1				0.0	0.0	-4.3	-0.8	-1.0	0.0	0.0	0.0E+00	0.0E+00	0.0E+00	0.0E+00
0.9	7.4	1.4	-1.6	1.2	4.5				0.0	0.0	-6.8	-8.7	-3.0	0.0	0.0	0.0E+00	0.0E+00	0.0E+00	0.0E+00
1.2	6.3	1.7	-2.3	2.3	2.9				0.0	0.0	-3.3	2.4	-1.5	0.0	0.0	0.0E+00	0.0E+00	0.0E+00	0.0E+00

0.0	0.0	0.0	0.0	0.0	0.0	1.5	-5.1	1.3	0.0	0.0	0.0	0.0	0.0	0.0	6.7	0.0E+00	0.0E+00	0.0E+00	0.0E+00
0.0	0.0	0.0	0.0	0.0	0.0	-5.3	-7.5	-5.7	0.0	0.0	0.0	0.0	0.0	0.0	-24.6	0.0E+00	0.0E+00	0.0E+00	0.0E+00
0.0	0.0	0.0	0.0	0.0	0.0				5.0	4.8	0.0	0.0	0.0	0.0	0.0	0.0E+00	0.0E+00	0.0E+00	0.0E+00
0.0	0.0	0.0	0.0	0.0	0.0				0.1	3.2	0.0	0.0	0.0	0.0	0.0	0.0E+00	0.0E+00	0.0E+00	0.0E+00

Table 7-7 **Historic values used in Table 7-6. Note that the water production values (‘gwpt’) are notional, and non-zero to give some tolerance.**

Name	Historical	
p_bgm1_1976	172	[bar]
p_bgm7_1981	153	[bar]
p_bgm1_1989	109	[bar]
p_bgm7_1988	121	[bar]
p_bgm1_2001	25	[bar]
p_bgm7_1997	61	[bar]
p_grt1_1976	187	[bar]
p_grt1_1990	87	[bar]
p_grt1_2005	28	[bar]
p_ber4_1990	95	[bar]
p_ber4_2005	15	[bar]
gwc_bgm1_1981	2223	[m]
gwc_bgm1_2005	2205	[m]
gwc_bgm7_1981	2231	[m]
gwc_bgm7_1989	2223.5	[m]
gwc_grt6_1999	2161	[m]
gwpt_bgm	1000	[m3]
gwpt_grt	1000	[m3]
ggpt_bgm	1.65E+10	[sm3]
ggpt_grt;	6.43E+09	[sm3]
fwpt	2000	[m3]

Table 7-8 Fault multipliers for base run (BAG_ALT2) and low perm/high kv run (BAG25_ALT2_DISMIDHIGHKV). As horizontal permeability decreases, the fault multipliers BGM_main ←→ BGM7 need to be increased to keep the pressure match.

```
MULTFLT
'FAULT2A'  0.0002 /
'FAULT2BA' 0.0002 /
'FAULTATS' 0.0002 /
  /
```

```
MULTFLT
'FAULT2A'  0.0005 /
'FAULT2BA'  0.0005 /
'FAULTATS' 0.0002 /
  /
```